



Norwegian University of
Science and Technology

3D Analysis of Artificial Seabed for a Floating Bridge with Tunnel across Sognefjorden

Tryg-Arne Alnes Løkkeborg

Mechanical Engineering

Submission date: June 2016

Supervisor: Bjørn Haugen, IPM

Norwegian University of Science and Technology
Department of Engineering Design and Materials

MASTEROPPGAVE VÅR 2016

FOR

STUD.TECHN. TRYG-ARNE ALNES LØKKEBORG

3D analyse av kunstig sjøbunn for flytebro og tunnel for Sognefjorden

3D analysis of artificial seabed for a floating bridge with tunnel across Sognefjorden.

I forbindelse med bygging av kombinert flytebro og tunell over Sognefjorden, som en del av «Ferjefri E39»-prosjektet, er det av interesse å etablere tekniske løsninger for en såkalt kunstig sjøbunn over fjorden, som den øvrige konstruksjonen er tenkt å være forankret i.

DeapOcean og Reintertsen har kommet med flere konsept for dette. Et konsept av særlig interesse består av to rør som strekkes på tvers av fjorden, for så å strammes inn mot hverandre i en bueform basert på et «Skolissekonsept».

Todimensjonal analyse av dette konseptet ble utført av Bjørn Harald Snersrud i hans masteroppgave våren 2015. Enkelte 3-D analyser ble utført i løpet av prosjektoppgaven til Tryg-Arne. Basert på de foreløpige resultatene så ønsker en blant annet å foreta ytterligere studier. Følgende punkt og oppgaver ønskes belyst:

- Automatisere de utførte enkeltstående 3D analysene ved hjelp av Python-skripting
- Studere elastisk kontra stiv modell av oppstrammingswire.
- Parameterstudie i forhold til påvirkning fra havstrømsbelastning på rørene.
- Parameterstudie i forhold til vind og strømning på monteringslektene.
- Parameterstudie i forhold til oppdrift av rørene.

De overstående analysene forutsettes utført som kvasi-statiske analyser der demping i første rekke gir numerisk stabilitet. Dersom tiden tillater det, så kan det være aktuelt å utføre mer fysisk riktige dynamiske analyser, og da eventuelt med bølgebelastning.

Formelle krav:

Senest 3 uker etter oppgavestart skal et A3 ark som illustrerer arbeidet leveres inn. En mal for dette arket finnes på instituttets hjemmeside under menyen masteroppgave (<https://www.ntnu.no/web/ipm/masteroppgave-ved-ipm>). Arket skal også oppdateres en uke før innlevering av masteroppgaven.

Risikovurdering av forsøksvirksomhet skal alltid gjennomføres. Eksperimentelt arbeid definert i problemstilling skal planlegges og risikovurderes innen 3 uker etter utlevering av oppgavetekst. Konkrete forsøksvirksomhet som ikke omfattes av generell risikovurdering skal spesielt vurderes før eksperimentelt arbeid utføres. Risikovurderinger skal signeres av veileder og kopier skal inngå som vedlegg til oppgaven.

Besvarelsen skal ha med signert oppgavetekst, og redigeres mest mulig som en forskningsrapport med et sammendrag på norsk og engelsk, konklusjon, litteraturliste, innholdsfortegnelse, etc. Ved utarbeidelse av teksten skal kandidaten legge vekt på å gjøre teksten oversiktlig og velskrevet. Med henblikk på lesning av besvarelsen er det viktig at de nødvendige henvisninger for korresponderende steder i tekst, tabeller og figurer anføres på begge steder. Ved bedømmelse legges det stor vekt på at resultater er grundig bearbeidet, at de oppstilles tabellarisk og/eller grafisk på en oversiktlig måte og diskuteres utførlig.

Besvarelsen skal leveres i elektronisk format via DAIM, NTNUs system for Digital arkivering og innlevering av masteroppgaver.

Kontaktperson:

Ved instituttet: Bjørn Haugen

Fra industrien: Jorge Bermudez, Reinertsen og Martin Hasle, DeepOcean.



Torgeir Welo
Instituttleder



Bjørn Haugen
Faglærer



NTNU
Norges teknisk-
naturvitenskapelige universitet
Institutt for produktutvikling
og materialer

Preface

You have now started to read my Master's thesis, written at Norwegian University of Science and Technology, NTNU, Department of Engineering Design and Materials, IPM, in Trondheim during the spring semester of 2016. The thesis is written as a part of the study programme Mechanical Engineering (Produktutvikling og produksjon), PuP. Earlier I have written a project thesis about the same topic as in this thesis.

The thesis is written in cooperation with ÅF Reinertsen and DeepOcean, where my contact persons were Jorge Bermudez and Marit Reiso from ÅF Reinertsen and Martin Hasle from DeepOcean. ÅF Reinertsen is the main developer behind the bridge/tunnel concept, while DeepOcean has developed the shoe-lacing principle and working with marine operations. During this semester I have met the companies regularly to present results and get new input regarding the topics in the thesis.

I want to thank the companies, especially Martin, Jorge and Marit, for the cooperation and giving me the opportunity to write about such an interesting and current topic. They have always given me good answers and taken an interest in my work.

I also want to thank my supervisor at NTNU, Bjørn Haugen. He is always available for a question or a discussion and always gives supplementary and good answers. He has guided me very well through this project.

Finally, I want to thank Bjørn Harald Snersrud. He has written the Master's thesis I have continued from and is the developer of ASAT. He has friendly replied to my e-mails and given me an easier start of the work.

This was an interesting project for me. I have work with a relevant issue, which have motivated me. I have also covered a wide span of topics from my education. Finally I want to tell that this Master's thesis is written without drinking a single cup of coffee.

As far as possible the report is written as a semi-technical report. I.e., I have assumed that the reader knows roughly as much as I did when I started with my project thesis.

Tryg-Arne A. Løkkeborg

Tryg-Arne Alnes Løkkeborg
Trondheim, June 2016

Abstract

This report deals with different aspect of the artificial seabed, which is a support structure for a combined floating bridge and submerged tunnel and is developed by ÅF Reinertsen. To pre-tension the artificial seabed, the shoe-lacing principle is introduced. To simulate this process, the Artificial Seabed Analysis Tool, ASAT, was developed, which is a Python code utilizing Abaqus. This project is a part of a concept for crossing of Sognefjorden in conjunction with the project “Ferry-free E39”.

The objectives for this thesis is to extend ASAT to include water current and an elastic wire and perform parameter study of the influence of external forces acting on the artificial seabed during the installation.

In this Master’s thesis is a new version of the analysis tool ASAT developed. Compared to the old version, the new version includes the opportunity to include water current and an elastic wire. The old version didn’t include any external forces and the wire was rigid. Still, it’s possible to run ASAT equivalent with the old version, so no options are lost. The new version is tested, and gives the same results as the old version. A new numerical optimum for ASAT is also established, which are to be used together with the new options. If ASAT is run similar to the old version, the old numerical optimum still applies.

The external forces were not calculated before. The drag force due to water current is calculated to 425 N/m and the buoyancy is 143 N/m.

There are run analyses of the bundle with water current, buoyancy and these two together. Taking material integrity, deformations and practical aspects, as logistics and cost, into account, one found a recommended configuration of tugboats and barges. By using three barges and three tugboats with 50-55 tonnes of towing force each, where the vessels are evenly distributed along the bundle, one found a suitable solution. With this configuration the material integrity is taken care of, while the number of tugboats and barges are kept low. To avoid that the bundle is lifted up by the vertical force from the tugboat, the stay should be at least 119 meters long.

Samandrag

Denne oppgåva handlar om forskjellige tema rundt Kunstig sjøbunn, ein støttestruktur for ein kombinasjon av flytebru og røyrbru over Sognefjorden. Konseptet er utvikla av ÅF Reinertsen og er eit prosjekt i forbindelse med “Fergefri E39”. For å forspenne den kunstige sjøbotnen har skolissepriinsippet blitt introdusert. I tilknytning til skolissepriinsippet har Artificial Seabed Analysis Tool, ASAT, tidlegare blitt utvikla. ASAT er ein Pythonkode, som brukar Abaqus for å køyre analysar.

Målsetjingane for denne oppgåva er å utvide ASAT med meir funksjonalitet, både å inkludere krefter frå havstraum og ein elastisk vaier. I tillegg skal det utførast parameterstudie av påvirkninga til eksterne krefter på den kunstig sjøbotnen under installasjon.

I løpet av denne oppgåva har ein ny versjon av ASAT blitt utvikla. Denne versjonen inkluderar både krefter frå havstraum og ein elastisk vaier. Til tross for oppgraderingane er det fortsatt mogeleg å køyre analysar tilsvarande den gamle utgåva. Den nye utgåva er testa, og gir resultat som er lik med den gamle utgåva. I tillegg er eit nytt numerisk optimum utarbeidd for den nye versjonen.

Eksterne krefter er berekna til å vere 425 N/m for havstraum og 143 N/m for oppdrift.

Det er køyrd parameterstudie av både havstraum og oppdrift, og desse to i lag. Ved å ta fleire omsyn i betraktning, har ein kome fram til ei tilfredsstillande løysing. Ved å bruke tre lekterar og tre slepebåtar med ei trekraft på 50-55 tonn kvar, der fartøya er plassert parvis med like stor avstand langs røyrbunten, har ein eit fullgodt oppsett. For å unngå at slepebåtane løftar opp røyrbunten, er det naudsynt med eit drag på minimum 119 meter mellom slepebåten og røyrbunten.

Table of Contents

Problem Text	i
Preface	iii
Abstract	v
Samandrag	vii
1 Introduction	1
2 Theory and Background	3
2.1 Ferry-free E39	3
2.2 ÅF Reinertsen's Concept	4
2.2.1 Artificial Seabed	5
2.2.2 Shoe-lacing Principle	7
2.3 The Artificial Seabed Analysis Tool	8
2.3.1 Why ASAT?	8
2.3.2 The Theory of ASAT	9
2.3.3 ASAT in Use	12
2.4 Loads on the Artificial Seabed	15
2.4.1 Water current	15
2.4.2 Buoyancy	18
2.5 Abaqus	18
2.5.1 Macro Manager	19
2.5.2 The Slipping Connector Element	19
3 Method	21
3.1 Upgrading of ASAT	21
3.1.1 Water Currents in ASAT	21
3.1.2 Elastic Wire	27
3.2 Testing of Wire Elasticity	28
3.3 Calculation of Loads	32
3.3.1 Water Current	33
3.3.2 Buoyancy	33
3.4 Simulations	34

3.4.1	Water Current	35
3.4.2	Buoyancy	36
3.4.3	Water Current and Buoyancy	37
3.4.4	Tugboat with Vertical Force Component	37
4	Results	41
4.1	New Version of ASAT	41
4.1.1	Comparison of New and Old Version	41
4.1.2	Example of Analysis in New Version of ASAT	43
4.2	New Numerical Optimum	44
4.3	Wire Elasticity	46
4.4	Water Currents	46
4.5	Buoyancy	48
4.6	Water Current and Buoyancy	49
4.7	Tugboat with Vertical Force Component	50
5	Discussion	53
5.1	New Version of ASAT	53
5.2	New Numerical Optimum	54
5.3	Wire Elasticity	56
5.4	Water Currents	56
5.5	Buoyancy	57
5.6	Water Current and Buoyancy	59
5.7	Tugboat with Vertical Force Component	60
5.8	A few final remarks	61
6	Conclusion	63
6.1	Recommended further work	64
	References	66
 Appendix 		
A	Python Script for Tugboats	69
B	Analyses with Elastic Wire	73
B.1	Elastic/Rigid Wire	73
B.2	Varied Winching Magnitude	75

C	Additional Plots and Figures	79
C.1	New Version of ASAT	79
C.1.1	Comparison – Old Version	79
C.1.2	Comparison – New Version	81
C.1.3	Example of New Version of ASAT	83
C.2	Numerical Optimum	86
C.3	Water current	86
C.4	Buoyancy	87
C.4.1	One barge	87
C.4.2	Two barges	89
C.5	Water Current and Buoyancy	90
C.6	Comparison with and without Buoyancy	91
C.7	Plots from Analyses	91
C.7.1	Water Current	92
C.7.2	Water Current and Buoyancy	97
D	Wire Elasticity	103
E	Input parameters to ASAT	107
F	Risk Evaluation	113

Chapter 1

Introduction

Earlier several theses are written about ÅF Reinertsen's bridge crossing concept for Sognefjorden. In this thesis especially the parts named artificial seabed and the shoe-lacing principle are covered. The thesis continues the work from two of the earlier theses, it is Bjørn Harald Snersrud's Master's thesis from the spring 2015 and Tryg-Arne Alnes Løkkeborg's project thesis from the autumn 2015. Snersrud developed the Artificial Seabed Analysis Tool, ASAT, in his thesis, which is an important part of this thesis too. However, this thesis is written so it is possible to just read this one and still understand its content.

ÅF Reinertsen has developed the combined bridge and submerged floating tunnel concept shown in Figure 2.1 for a project named 'Ferry free E39'. This project was initiated by the Norwegian government and aims to build the E39 highway without any ferry services and upgrade the roads. ÅF Reinertsen has based their dimensions on data from Sognefjorden. A lot of feasibility studies are performed, both by ÅF Reinertsen and several other companies, for the fjord crossing along E39 and still more possibilities are considered.

Mainly the mounting phase is covered in this thesis. The sensitivity of buoyancy and water currents for a free bundle is investigated and discussed. In addition are water current and the selection between an elastic and rigid wire included in ASAT. ASAT simulates the winching procedure of the shoe-lacing principle, which is a part of the mounting phase.

Based on the work performed in the project thesis from the autumn 2015 and suggestions from DeepOcean and ÅF Reinertsen a problem text for this Master's thesis is written. The objectives for this Master's thesis is:

- Include the manually performed analyses from the project thesis in the ASAT script
- Study elastic versus rigid wire (slipping elements) in ASAT

- Parameter study of water currents on the pipe bundles
- Parameter study of wind and current influence on mounting barges
- Parameter study of buoyancy of the bundles

The work is limited to look at global phenomena.

This thesis consists of six chapters, where this is the first. The next chapter is the theory and background chapter, where one finds theory and information about all topics covered in this thesis. Chapter 3 contains a description of all of the work performed during this period. The first part of this chapter deals with the development of ASAT, while the latter part is about calculations and simulations. All of the results are presented and objectively spoken of in chapter 4. The results are then discussed in chapter 5. Finally the conclusion is made up in chapter 6 together with some recommendations for further work.

When mentioning the coordinate axes, they are always according to the coordinate system shown in Figure 2.3. I.e. X-axis is across the fjord, Y-axis in longitudinal direction of the fjord and Z-axis is vertical. This isn't mentioned further in this thesis, so keep this in mind when continuing reading.

Chapter 2

Theory and Background

This chapter contains theory, derivations and background for the thesis. Some of the information is necessary to understand the thesis and some is on a good to know-level.

The first part of this chapter contains some general information about the ‘Ferry-free E39’ project, further is information about ÅF Reinertsen’s crossing concept, with the artificial seabed and shoe-lacing principle included. The next part is a thorough introduction to ASAT, with some theory and user guide. After this are all of the equations used in this thesis presented and finally some theory about Abaqus, especially about Python scripting and the slipping connector element, which is an important part of ASAT.

2.1 Ferry-free E39

In 2010 the Norwegian government initiated a project named ‘Ferry-free E39’, where the Norwegian Public Roads Administration (Statens vegvesen) should evaluate the feasibility of a ferry-free E39. In 2010 in National Transport Plan, NTP, for 2014-2023 has the Norwegian government decided to build a ferry-free E39. The ambition is to realise this project within 20 years[1].

In Norway E39 starts south of Trondheim in north and goes along the western part of Norway and ends up in Kristiansand in south. This is approximately a 1100 kilometres long stretch of road. One of the objectives for the Ferry-free E39 project is to replace all these ferry services with bridges or tunnels, or an alternative route. When the project started this road included eight fjord crossings by ferry.

‘Ferry-free E39’ is a project where a lot of new technologies are of interest. And there are research and development projects in progress on a lot of different subjects. There are projects related to renewable energy and

how one can use the road to produce energy. Projects including energy storage, production of renewable energy along the road and implementation of environmentally friendly energy are some of the topics[2].

Sognefjorden is considered as the most difficult fjord to cross. At today's ferry service the fjord is 3.7 kilometres wide and up to 1300 meters deep. The fjord has steep walls and a flat seabed mid-fjord[3]. Today there are no technical solutions that are capable to cross Sognefjorden, so it is necessary to develop new technological solutions. Hence, if it is possible to cross Sognefjorden, it is also possible to cross the other fjords along E39. A lot of feasibility studies are performed by several different companies for Sognefjorden and still more possibilities are considered.

2.2 ÅF Reinertsen's Concept

ÅF Reinertsen has developed a concept of a combined floating bridge and submerged floating tunnel, shown in Figure 2.1. Data from Sognefjorden are used as basis for the structural design. The bridge is anchored to two submerged steel bundles. The bundles has a parabola shape, and facing in opposite directions. This support structure is shown in Figure 2.2 and is called an artificial seabed.



Figure 2.1: The bridge crossing concept for Sognefjorden (Source: ÅF Reinertsen)

Mid-fjord is it a submerged floating bridge, in such a way that it is possible

for ships to pass through. The gap is 400 meters wide and 20 meters deep[3]. The tunnel part is approximately 1600 meters long and is anchored to the artificial seabed. The bridge part floats on concrete pontoons. These are anchored to the artificial seabed and are placed every 100th meters. The road are to be designed for an annual average daily traffic, AADT, of 4000 and a speed limit of 80 km/h. It is not allowed with an incline higher than 5 % for the road.

Documentation for feasibility of temporary phases shall also be accomplished. The transportation phase are to be evaluated with respect to material integrity and stability of the sections. The installations phase covers the time from the parts have arrived the destination to the bridge is installed and available from the abutments[3]. This thesis covers a part of the installation phase.

2.2.1 Artificial Seabed

Artificial seabed is a new kind of foundation for floating bridges and submerged floating tunnel across long distances. A bridge attached to the artificial seabed is shown in Figure 2.2. The purpose is to give lateral stiffness to the bridge, which is a very slender construction. An artificial seabed is suitable for locations where it is too deep or unsuitable for anchoring to the natural seabed.

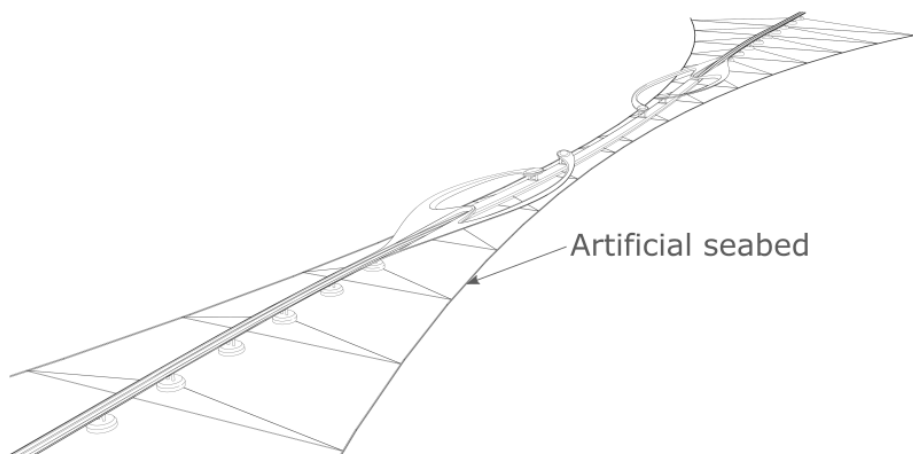


Figure 2.2: The bridge anchored to the artificial seabed (Source: ÅF Reinertsen)

The artificial seabed consists of two pretensioned steel bundles, where one bundle consists of three steel pipes attached to each other. They are submerged into the sea and are designed to have a neutral buoyancy, i.e. a D/t -ratio of 30 for steel pipes[3]. The ends of the bundles are to be anchored to the ground on either side of the fjord and the bundles keep their pretensioned shape by 13 transverse stays. The abutments are assumed to be solid bedrock. The artificial seabed are to be pre-tensioned to 40 % of yield stress, i.e. 192 MPa. The ends of the stays are attached to one bundle each.

To make it possible for vessels to pass, the artificial seabed is placed at a depth of approximately 30 meters below sea level.

The material properties for the steel used for the artificial seabed are shown in Table 2.2.

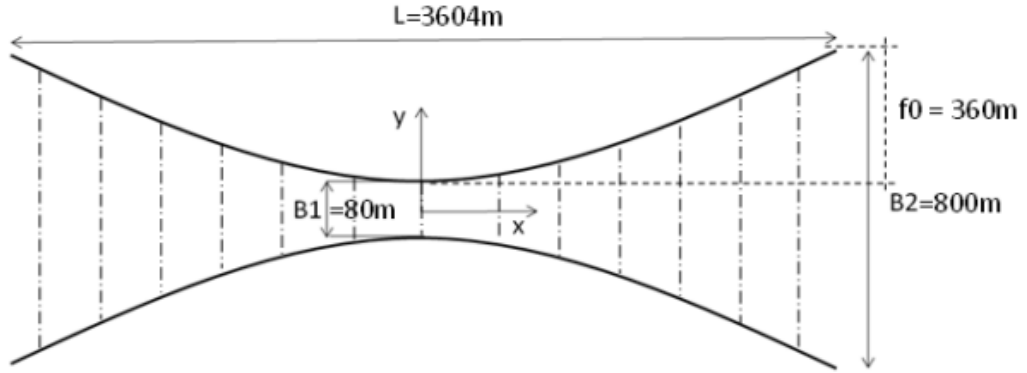


Figure 2.3: Dimensions for the artificial seabed (Source:[4])

The cross section of a bundle is shown in Figure 2.4. A pipe has the diameter D and wall thickness t , while S gives the spacing between the steel pipes. The dimensions are stated in Table 2.1. Neither the spacing between the pipes nor the orientation of the bundle is decided at present time. The overall dimensions for the artificial seabed are shown in Figure 2.3.

Table 2.1: Dimensions for the bundle[4]

Name	Value[mm]
D	914.4
t	30.5
S	Not decided yet

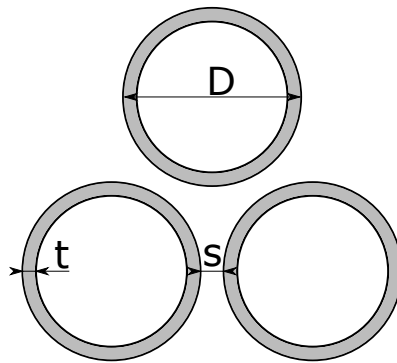


Figure 2.4: Cross section of a bundle

Table 2.2: Steel quality used for the bundles in the artificial seabed

Yield stress	Young's modulus	Poisson ratio	Density
480 MPa	207 000 MPa	0.3	7850 kg/m ³

2.2.2 Shoe-lacing Principle

To obtain the right pre-tensioned shape the shoe-lacing principle is introduced. This is a mounting procedure for the artificial seabed. The bundles are to be pulled together to the right position before the transverse stays are mounted. Several methods to mount the transverse stays are evaluated, but the shoe-lacing principle is chosen as the most appropriate solution to continue work with[5]. It's also possible to use the shoe-lacing principle for maintenance.

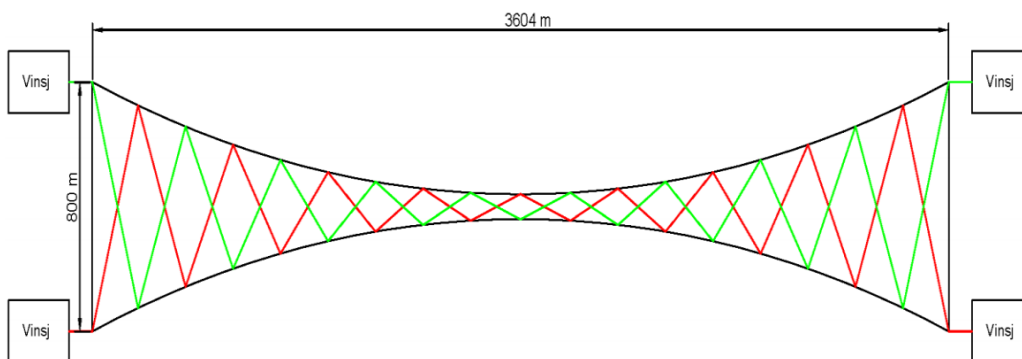


Figure 2.5: Model of the shoe-lacing principle (Source:[5])

The shoe-lacing principle is fibre ropes attached in a zigzag pattern in between the two bundles in the artificial seabed, as shown in Figure 2.5. The fibre rope is attached to the bundles through pulleys. There are two wire

spans, represented by the green and red line. At each end it is attached to a winch, to pull the wire out of the system and pre-tension the structure, shown in Figure 2.6.

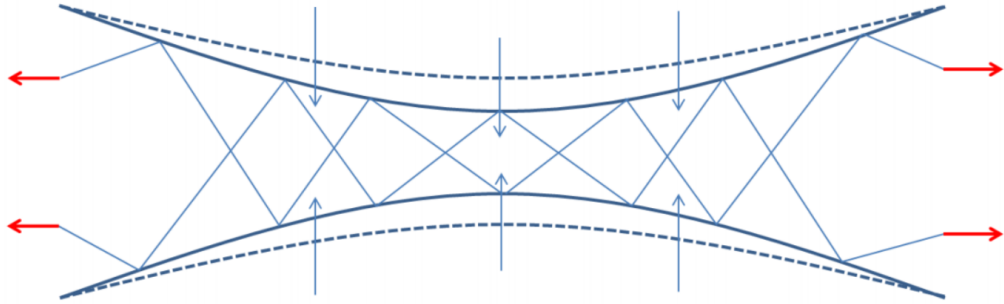


Figure 2.6: Schematic outline of the shoe-lacing principle (Source:[6])

The advantage of the shoe-lacing principle is that it's a cheaper solution, due to the land-based winches. Winches are used instead of tugboats or anchor handling tug supply vessels, AHTS.

The challenge with the shoe-lacing principle is to place the right amount of pulleys with the right spacing, to obtain the desired pre-tensioned shape[5]. This is one of the possibilities to test with ASAT.

2.3 The Artificial Seabed Analysis Tool

This section aims to give the reader a thorough introduction to the application of the Artificial Seabed Analysis Tool, ASAT. Some of the theory is described here, but for those who are interested in a deeper understanding of the theory behind ASAT is it referred to Snersrud's Master's thesis[6].

2.3.1 Why ASAT?

The major advantage of ASAT, compared to standard FEM software, is the efficiency. The whole model is built up based on predefined parameters in the script and some user defined parameters. The average analysis time for ASAT is approximately 30 seconds, which is very fast compared to conventional FEM analysis. This makes ASAT a very powerful and useful tool.

2.3.2 The Theory of ASAT

ASAT is a Python code developed by Bjørn Harald Snersrud in his Master's thesis the spring 2015. The code utilizes Abaqus to execute FEM analyses of the artificial seabed and the shoe-lacing principle. The code simulates the pre-tensioning of the artificial seabed, which is the winching process of the shoe-lacing principle. The code is developed using Abaqus 6.12 and

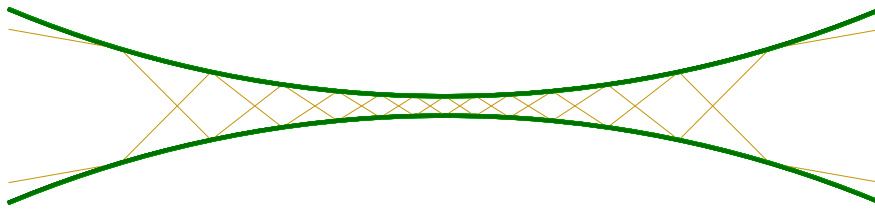


Figure 2.7: A typical model from ASAT

version 3.4 of Python. A typical model of the artificial seabed and the shoe-lacing principle is shown in Figure 2.7. The green lines represents the bundle and the orange lines are the two wire spans. The winches are placed at each end point of the wire spans. The winches are only represented by a point, so they are not visible. By default the bundles are scaled up by a factor of ten, due to visibility for the post-processing[6].

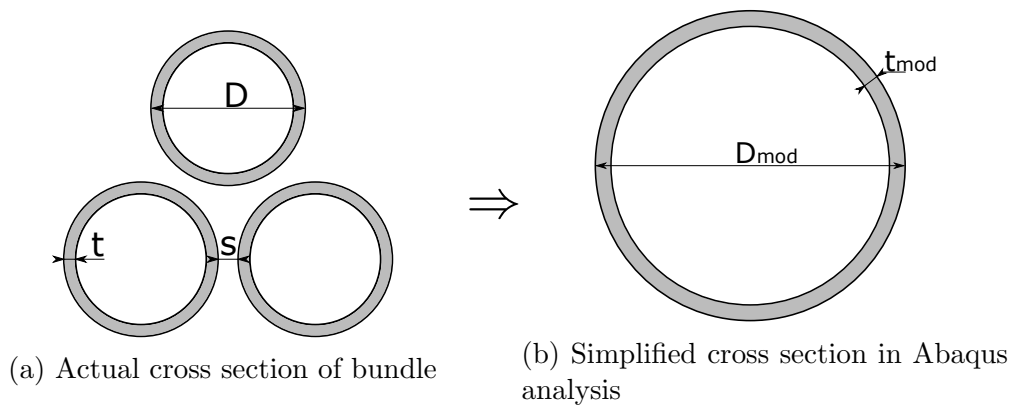
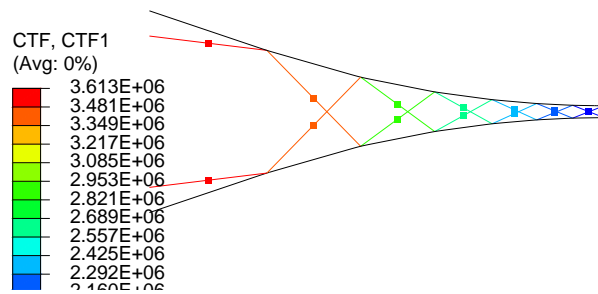


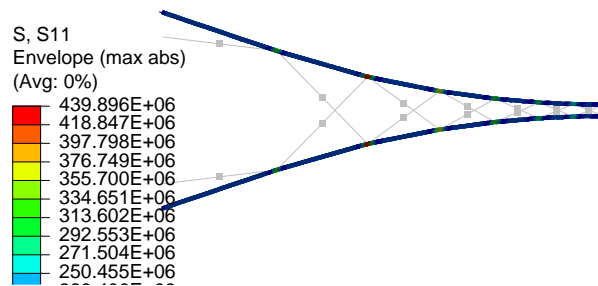
Figure 2.8: Simplifying of bundle

The code is developed to reduce the time consumed related to redefining the model. The code creates a model, executes an analysis and writing post-processing files in Abaqus, next the output files are post-processed by Python. The final result from an analysis is several graphs comparing the

results from all of the analyses performed by Abaqus and images that shows stresses and forces for each analysis, shown in Figure 2.9.



(a) Plot of wire force



(b) Stress plot

Figure 2.9: Plots generated by ASAT

The actual bundle consists of three steel pipes. In ASAT these are simplified to one single pipe, as shown in Figure 2.8. Since the orientation of the bundle isn't decided yet, Snersrud took a closer look into the bundle's stiffness based on the orientation. He found out that the bundle cross section has the same stiffness, independent of the orientation[6], and is shown in Figure 2.10. In ASAT the pipe diameter and wall thickness are calculated based on the chosen spacing between the pipes. The modified pipe has the same cross section area and second moment of area as the bundle, to take care of the bending and axial stiffness.

Another simplification made in ASAT is the shape of the bundle. The initial shape of the real bundle is straight, but in ASAT are the bundles modelled as a circular arc. I.e. the initial shape in ASAT should have some bending stresses. However, if one takes a straight stress free bundle and

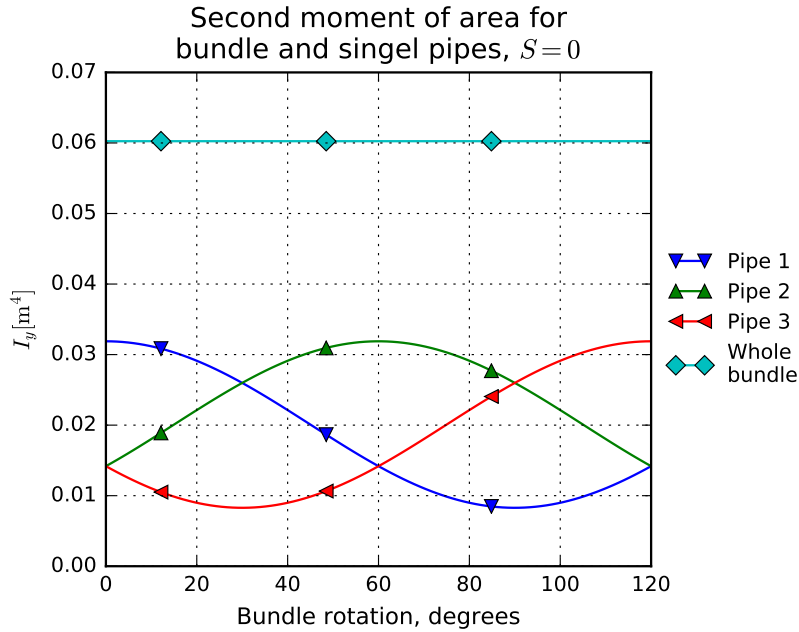


Figure 2.10: Second moment of area for each of the pipes and the whole bundle. Zero spacing between the pipes

makes an arc with the same radius as used in ASAT, the bundles gets a maximum bending stress level of 0.02 MPa, given zero spacing between the pipes ($S = 0$ m)[6]. This is considered as a neglectable difference and is not dealt with any further.

The analysis in ASAT is a dynamic explicit analysis. However, an equilibrium should occur before the analysis ends. Four of the input parameters mentioned in subsection 2.3.3 influence the numerical stability.

This is: T , t , D and Le . Chapter 4 in Snersrud's Master's thesis deals with this objective. It aims to find the optimum numerical values for ASAT, i.e. the lowest analysis time and the highest element size which still give an accurate solution. The final numerical optimum is found in Table 2.3[6].

MARK: The optimum numerical values are meant for the version of ASAT developed by Snersrud, NOT the new version developed as a part of this thesis. Optimum numerical values for the version developed in this thesis are found in Table 4.1, and are used together with the new options.

In addition to Abaqus 6.12 and Python 3.4 the original version of ASAT requires the Python module *matplotlib*, version 1.4.3, installed and is only guaranteed to work with computers with Windows 7[6]. For further and more detailed information about ASAT, please refer to Chapter 3 in Sner-

Table 2.3: Optimum numerical input parameters

Name	Value
T – Analysis time	20 sec
t – Winching time	5.95 sec
D – Mass damping coefficient	1.05
Le – Element length	10 m

srud’s Master’s thesis. The autumn 2015 Tryg-Arne Alnes Løkkeborg wrote a project thesis about the same topic. He upgraded some of the code to keep up with changes in Abaqus. This version of ASAT is compatible with Abaqus 6.14 and Windows 8.1. This version is verified to give the same results as the old version and no bugs are found yet.

2.3.3 ASAT in Use

In general is ASAT a very simple code to use, especially compared to Abaqus and other FEM programs. However, a briefly introductions to the scripts and input parameters is useful.

The Scripts

ASAT consists of four different scripts. One of them contains the user inputs, the three others isn’t it necessary to edit to run an analysis. The four scripts are:

ASAT.py is the main scripts. This is the script one have to run to run the whole ASAT code. The script also contains the post-processing of the output files from the analyses and makes plots of the results

input.py contains all of the input parameters. This is the script one has to edit to make a new analysis. The script also contains a definition of a function for placement of winches and some processing of the input values

exceptions.py is the file checking that all of the setting for the analysis are correct. If a parameter is invalid an error message is shown and ASAT is terminated

mechinery.py is the tailor-made Abaqus code. This is the script run in Abaqus by the *ASAT.py*-file

General Settings

ASAT has a lot of input arguments. Some of these doesn't affect the analysis itself, but are more like settings for the analysis. This could be the path to the saved results from the analyses or whether to run the analysis or not. All of these arguments are found in the beginning of the the *input.py*-file.

analysisType The analysis is stored in folders with a path relative to the *ASAT.py*-file's path. The path has two levels, where this is the name of the first level

analysisName The name of the analysis. This is the second level of the folder path

doAnalyse tells ASAT whether or not to run an analysis. If *doAnalyse* = 'False' one can plot a selection of the results from a previous analysis

doPlot decides whether or not to make plots of the results after the analysis has finished. The plots can be made at a later time

doDisplayPlotsWhenDone decides whether the plots should pop up at the end of the process or not.

useGUI decides if the Abaqus GUI should start. If not, the analyses are run as a background process

plotSelection is used when *doAnalyse* = 'False'. One can plot just a selection of the iterations from an already existing analysis

nIterations is the number of analyses to run

The combination of *analysisType* and *analysisName* has to be unique for every analysis. If an analysis exists in the folder already, ASAT asks whether to abort the analysis or delete the content in the folder. If one run several analysis with same purpose, it is suitable to keep *analysisType* unchanged and just change *analysisName*. The analyses are then saved in the same parent folder, but in different sub folders.

It is also possible to use ASAT as a pure plotting tool, based on already executed analyses. If you have run a lot of iterations, but only a few of these are of interest, is it possible to plot a desired selection of these iterations. One sets *doAnalyse* = 'False' and choose the desired analyses for the plot with *plotSelection*. Note, the first analysis is 0 and the last is *nIterations* - 1

If one sets *useGUI* = 'False' the Abaqus GUI doesn't start up. If the analyses are run as a background process, this is a faster alternative[6].

Input Parameters

ASAT has twelve different input parameters. Eleven of these are assigned a maximum and minimum value, the exception is *cutMethod*. All input parameters has to be SI Units to get the right units for the output data. ASAT has the following input parameters:

T is the total analysis time for the *winching* step

t is the winching time

D is the mass damping coefficient

Lw is the distance between abutment and winch. Towards center is the positive direction

cutMethod is the method for how the pulleys are placed. Valid values are: 'linear', 'quadratic' and 'quartic'

$Lmid$ is weighting of distance between two pulleys mid-fjord

$Lquart$ is weighting of distance between two pulleys at quarter points

nP is the number of pulleys along each bundle. Has to be an odd number

Mu is friction coefficients for the pulleys

dL is the amount of wire winched out of one wire-span. The amount of wire winched out at each winching point is $\frac{dL}{2}$

Le is element length

S is the spacing between the pipes in the bundle

The mass damping coefficient, D , is introduced to create numerical stability. It is not based on the real conditions for Sognefjorden, so the value should be tuned to give as short analysis time as possible. The mass damping coefficient are used to introduce an equilibrium and damp out vibrations in the system as fast as possible.

The *cutMethod*-function decides where the pulley are placed. The three different options are based on three different functions, which tells ASAT where to put the pulleys along the bundle. The 'quartic' choice gives the highest pulleys density at mid-fjord, while 'linear' gives the highest pulley density close to the shore.

One should note that it is only allowed to vary one parameter for each analysis. The user decides a minimum and a maximum value for the varied parameter, the remaining parameters have to have the same maximum and minimum value, and ASAT executes the desired number of analyses with a constant step from the starting value to the end value. For example by using $nIterations = 5$, $nP_min = 9$ and $nP_max = 17$ produces results for $nP = \{9, 11, 13, 15, 17\}$.

Optional Setting

There are some optional input arguments too. These are generally not varied for different analyses, but one has the option.

doLockAll can change the boundary conditions for the bundles to fixed instead of pinned

requestedFrames is the number of frames produced for each step in Abaqus. The default in Abaqus/ASAT is 20 frames

nHistoryOutputPoints gives the number of saved data points for each step in the analysis

nMarkersMax sets the highest numbers of markers in the plots

doRaiseErrors is possible to set to 'False', if one want to skip the *exceptions.py*-script. This argument is found at the bottom of the *input.py*-file. If 'False' is chosen, ASAT doesn't checks for invalid input parameters

2.4 Loads on the Artificial Seabed

In the original version of ASAT there are no external forces included. Some of the objectives for this thesis is to include external forces in ASAT and run parameter studies. The loads aren't calculated yet, but there exists enough data to calculate them. This section contains necessary formulas and data to make calculations of the water current and buoyancy.

2.4.1 Water current

A report from ÅF Reinertsen[3] says that the current load for a submerged cross section are to be calculated from the following equation.

$$F_{current} = \frac{1}{2}\rho_w C_D A v_{current}^2 \quad (2.1)$$

where

$F_{current}$ is total force

ρ_w is density of sea water

C_D is drag coefficient for the geometry

A is the area of the cross section projected toward the current

$v_{current}$ is flow velocity of the sea water, relative to the geometry

Equation 2.1 gives the total force for the body. If one divide by the length on each side, one gets a line load instead of the total force. One has to use the height, h , instead of the area, A . The formula then reads

$$F_{current} = \frac{1}{2}\rho_w C_D h v_{current}^2 \quad (2.2)$$

where

$F_{current}$ is the force as a line load along the object

h is the height of the area projected towards the current direction

In a report by SINTEF there are calculated flow velocities for the sea water by numerical simulations[7, 3]. The data are presented in Table 2.4.

Table 2.4: Flow velocities for Sognefjorden, extremal and average values

Depth[m]	U_{out} [m/s]	U_{mean} [m/s]	U_{in} [m/s]
0 - 10	-1.06	-0.533	1.27
30	-0.55	0.258	0.48
75	-0.44	0.257	0.39

The density of the water is shown in Table 2.5. It is based on an average of 1015 kg/m³, with a deviation of 1 % to allow for variations of salt content in the sea water. The most unfavourable value are to be used for each calculation[3, 8].

Table 2.5: Density of sea water

	Density [kg/m ³]
Minimum	1005
Average	1015
Maximum	1025

Drag Coefficient

Simen Grevstad wrote about vortex induces vibrations on the artificial seabed in his Master's thesis. As a part of this work he performed some tests. Based on these tests did he calculate the drag coefficients for the pipe bundle[9]. He tested the drag coefficient for three different orientations of the bundle, as shown in Figure 2.11. The spacing between the pipes in the bundle is equal zero, $S = 0$, for all of the configurations. The resulting drag coefficients are listed in Table 2.6.

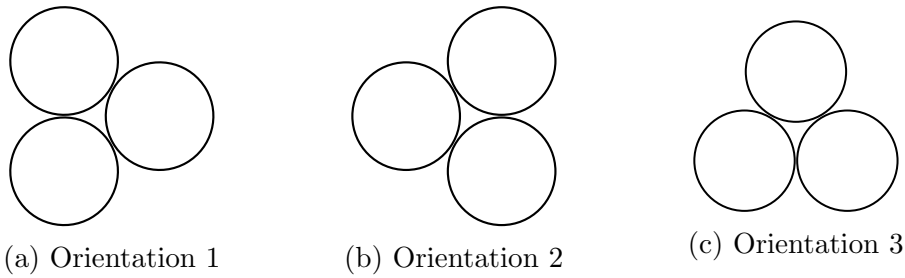


Figure 2.11: Orientations for testing of drag coefficient, current from right to left

Table 2.6: Drag coefficient for different orientation of the artificial seabed

	C_D
Orientation 1	1.1
Orientation 2	1.5
Orientation 3	0.5

From Table 2.6 one can see that orientation 2 gives the highest drag coefficient. In this orientation the height is equal twice the diameter plus the spacing. The height, h , in Equation 2.1 and 2.2 then reads:

$$h = 2D + S \quad (2.3)$$

2.4.2 Buoyancy

From Archimedes' law we have that the buoyancy is equal to the weight of the displaced water.

$$F = \rho V g \quad (2.4)$$

where

F is total buoyancy force

ρ is mass density of sea water

V is the volume of the immersed body/displaced water

g is the gravitational acceleration

If one divide by the length, L , on each side in Equation 2.4 one gets a line load along the body

$$F = \rho A g \quad (2.5)$$

where

F is buoyancy force per length of the body

A is the cross section area of the body

By combining the equation for buoyancy and an equation for the weight of the body one can calculate the immersed weight for the body.

2.5 Abaqus

Abaqus is a program developed by Simulia Corporation and is the program utilized by ASAT to execute FEM-analyses. Abaqus is very close related to Python, which is built-in in Abaqus. For Abaqus there is made an application programming interface, API, called the Abaqus Scripting Interface, ASI. ASI is an extension of Python and it is possible to run Python scripts with ASI commands with Abaqus. With ASI commands one can modify and create Abaqus models and analyses and handle the output database from an analysis[10]. Most of the functions in the Abaqus GUI have its own commands in ASI.

During every session in Abaqus a replay(.rpy) file is recorded. This file contains information about everything performed in Abaqus as Python commands. There are created a new file for every time Abaqus is opened. By running this file is it possible to recreate everything one did in this session. Abaqus also creates a recovery(.rec) file during the work in Abaqus. This file contains everything performed since last time the model was saved. The recovery file is deleted when one saves the model. This file can rebuild the model if Abaqus shuts down unexpected without saving the model[11].

2.5.1 Macro Manager

In addition to the .rpy-files is it possible to use the *Macro Manager*. The *Macro Manager*-function in Abaqus is a very useful tool for Python scripting. With this function is it possible to record a chosen part of the work[11]. Everything one does are recorded and saved as Python commands in the same row as they appear. The file is a Python(.py)-file and is executable in Abaqus. If one is uncertain about a command, this function becomes very helpful.

Some functions change between different versions of Abaqus, and so does the commands. If one has a script which is out of date, is it possible to use the *Upgrade Scripts*-function. This function detects outdated commands and updates them[11]. One choose the old and new version and Abaqus scans through the document and makes the necessary changes.

2.5.2 The Slipping Connector Element

The slipping connector element is used to represent the fibre ropes and the pulleys in the shoe-lacing principle. A slipping connector models material flow and stretching between two node point and is suitable to model a pulley system[12]. Maximum two slipping connector can be attached to a node. If two connectors are connected to one node, the node has to be the end point for one element and the starting point for the other point. I.e. one slipping connector has to go from node a to node b and the next from node b to node c, so the line a-b-c is created, as shown in Figure 2.12. To calculate the friction in a pulley the angle between two slipping connectors is used. This is a Coulomb-like friction and calculated from the following formula:

$$f_{ab} = f_{bc}e^{-\mu\alpha} \quad (2.6)$$

where

f_{ab} is the tension in element ab

f_{bc} is the tension in element bc

μ is the friction coefficient

α is the angle between element ab and bc

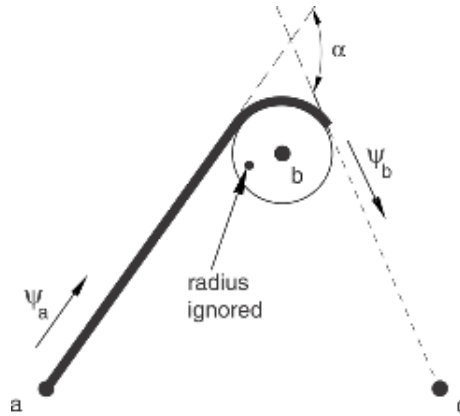


Figure 2.12: Two slipping connector element (Source:[12])

For analyses one should note some output variables with a different meaning than usual:

CP1 – distance between the nodes, i.e. the length of the connector/wire

CP2 – material flow at node b

CP3 – material flow at node a

CU1 – strain in the connector

For a slipping connector a flow from node a to node b is the positive direction. Hence, a material flow out of the element at node a, *CP3*, is negative, while it is positive at node b, *CP2*. Material flow in ASAT is equal to the magnitude of wire passing through a node. At the winching points the material flow is equal $\frac{dL}{2}$, where dL is set as a boundary condition.

One can state the axial stiffness for a slipping connector, where it is possible to choose between rigid, linear and non-linear behaviour. If one choose linear elastic behaviour, one has to state the constant D_{11} . For a slipping connector the unit of the constant is a force[13].

Chapter 3

Method

This chapter contains a description of the performed work during this project. The chapter is divided into two part, where the first part is about ASAT and the latter is about analyses. The part about ASAT contains a description of the upgrading with water current and an elastic wire. In addition is the testing of the elasticity for the wire described. The analysis part takes care of analyses with water current and buoyancy and calculation of these loads.

3.1 Upgrading of ASAT

The original version of ASAT doesn't include any external forces. It is only an analysis of a pure winching procedure. Earlier some analyses with external forces, water current, are performed, but they wasn't included in the ASAT-code. These analyses were performed manually. The analyses were executed with a line load, representing the water current. The load was applied both before and after the winching procedure.

3.1.1 Water Currents in ASAT

One of the objectives for this Master's thesis was to include water current in the ASAT code. In this way is it possible to perform parameter studies of the influence of the water current with respect to the other parameters. This makes it for instance possible to find out whether a parameter has the same influence to the artificial seabed with or without water currents. The rest of this subsection contains a description of how the ASAT code were updated to include water current.

New Input Parameters

In the new version of ASAT there are several new input parameters, four of these are directly associated to the implementation of a water current. This is Tb , Ta , Fb and Fa . It is possible to assign a maximum and a minimum value to all of these, so one can run through several iterations for one parameter. Below follows a description of the new parameters related to the water currents.

Tb sets the analysis time for the step before the winching procedure

Ta is used to decide the analysis time for the step after the winching procedure

Fb decides whether or not to apply a load in the step before winching. This is a True/False statement, so other input values aren't allowed

Fa is also a True/False statement. With this parameter one can apply a load after the winching step. It is ignored if $Fb = 'True'$, because a load is already applied

Since Fb and Fa are True/False statements, they only have two valid input values. So if one of these parameters is the varied parameter, *parameterName*, this analysis is limited to two iterations, i.e. $nIterations = 2$.

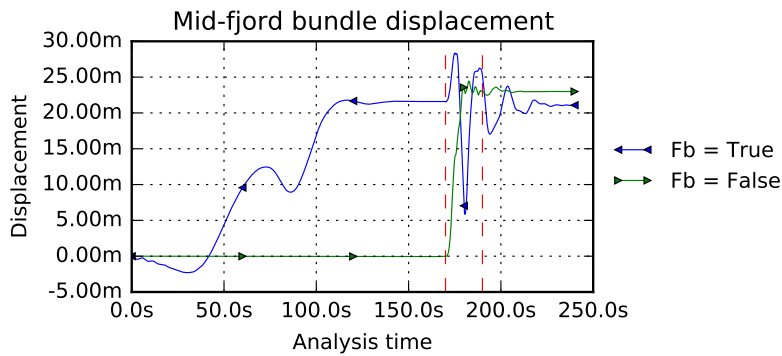
New Steps

The original version of ASAT has one step, the *winching* step. To include the water current it was appropriate to augment the number of steps. If a load is applied to the structure before the winching, an equilibrium should be reached before the winching starts. Equally an equilibrium after the winching should take place before a force is applied, if the load is applied after the winching. Based on this there are three distinct phases in the analyses, hence two more steps were added to the analysis. There are added one step before and one after the winching step, named *before* and *after* respectively.

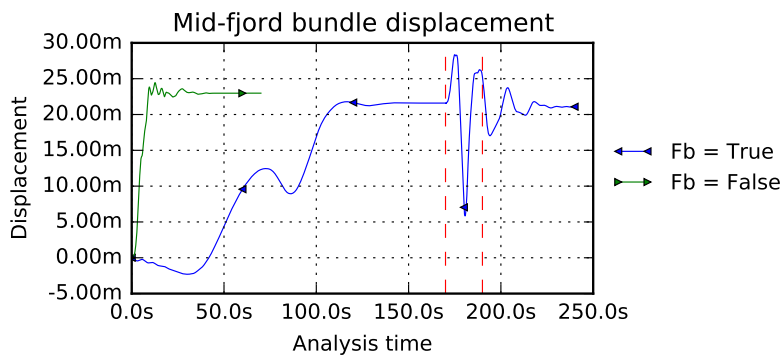
It is possible to include the whole analysis in one step, which is a faster alternative than with three steps. This alternative was rejected due to the readability of the code. It is assumed that it is easier to understand the code for a new reader if there are three steps instead of one.

To decide whether or not to create the steps before and after the winching step, two new variables are introduced: *makeBefore* and *makeAfter*. They are found in the *input.py*-script. They are True/False statements and are

used to create the steps *before* and *after* and features related to these steps. *makeBefore* is set to True if *Fb* is True for one or more of the iterations, i.e. *parameterName* = 'Fb' or *Fb* is True for all of the iterations. *makeBefore* is set to True even if *Fb* = False for some of the iterations, due to the readability of the plots. If you have the same steps for all of the iterations, it is much easier to compare the plots in the diagram. The steps then starts at the same places in the diagram. For instance the winching starts at the same time, instead of at the start and in the end of the plots, as shown in Figure 3.1a and 3.1b.



(a) Both analyses have a step before winching



(b) Only the analysis with a load before has a step before winching

Figure 3.1: Comparison of plots with and without steps before winching

Exceptions

The *exceptions.py*-script is updated to include the changes and new functions. The new parameters are added to the old expressions, where this is necessary. There are also two new exceptions. The first one checks that $nIterations = 2$ if *Fb* or *Fa* are the varied parameter, as explained in an earlier paragraph. The latter one verifies that input values for *Fb* and *Fa* only is True or False, everything else is rejected.

It is not allowed to choose *Fa* as varied parameter for $Fb = \text{True}$. A load is applied in this step regardless of the value of the parameter. *Fa* is ignored when $Fb = \text{True}$.

ASAT script

In the ASAT script there are only made a few minor changes. If the varied parameter, *parameterName*, is *Fb* or *Fa*, the variable *parameterValues* are modified. When True and False are put into a NumPy array, they are replaced with 1.0 and 0.0 respectively. Zero and one are then replace with 'True' and 'False' again, as shown in Listing 3.1. This is done to increase the readability of the plots, so the legends shows True/False instead of 1.0/0.0.

Listing 3.1: From the *ASAT.py*-file

```
#If Fb or Fa is the varied parameter, 1 and 0 are
    replaced with True and False. Used for the legend in
    the plots
parameterValues = vars.parameterValues
if vars.parameterName == 'Fb' or vars.parameterName ==
    'Fa':
    tempParameterValues = list()
    for i in range(len(parameterValues)):
        if parameterValues[i] == 1:
            tempParameterValues.append('True')
        elif parameterValues[i] == 0:
            tempParameterValues.append('False')
        else:
            tempParameterValues.append(parameterValues[
                i])
    parameterValues = tempParameterValues
```

Another modification to increase the readability of the plots are the vertical separation lines. If the steps *before* and/or *after* are created and the analysis time is constant for all iterations, some vertical lines are plotted in

the plots. The vertical lines shows where a step ends and a new step starts. One can see these lines as red dashed lines in Figure 3.1a.

Abaqus codes

To include all of the necessary changes related to the water currents, is it required with some changes in the *machinery.py*-script. It is in this script most of the changes take place. This sections contains a description of these changes. In the new code there are three in stead of one step, and a lot of the changes were necessary due to the creation of the new steps.

When one creates the first step in Abaqus, there are some default Field- and History-outputs that are created automatically. If one creates a new step that takes place after the first step, the default F- and H-outputs are propagated to the new step. But if one creates a new step before the first one, the default F- and H-outputs aren't transferred. This is something one should pay attention to for further changes. To solve this is the code built up so the first step is always the first created step, independent of it is the step *before* or *winching*.

Some functions are dependent of the first or last step. Due to this two new variables are introduced, *firstStep* and *lastStep*. These variables are strings, and the assigned value is the name of the first and last step step. *firstStep* is for instance useful for the making of new History-outputs, which should be created from the first step. There are a lot of manually created Field- and History-outputs in the *machinery.py*-script, so this variable was very useful for this purpose. If this variable wasn't introduced, the plots would only shown the results from the *winching* step, regardless of the number of created steps. *lastStep* is useful for the images, which should show the state at the end of the last step. In Figure 3.2 one can see a comparison for a analysis with a load applied after the winching procedure. Note the asymmetric wire forces in Figure 3.2b, which doesn't occur in Figure 3.2a. This is because of the load. In Figure 3.2b is the variable *lastStep* use, while it isn't in Figure 3.2a.

One of the major changes in the code is the implementing of the water current. The load is introduced as a constant line load along each bundle. In the command a variable called *loadStep* is used. This variable contains the name of the step the load should be applied to. *loadStep* has either the value *before* or *after*. If $Fb = 'True'$ for the present iteration $loadStep = 'before'$, no matter the value of Fa . If $Fb = 'False'$ and $Fa = 'True'$ is $loadStep = 'after'$. If both of the statements are False, the whole block is skipped and ASAT only analyses the winching procedure, hence ASAT runs with one step and equally to the original version of ASAT.

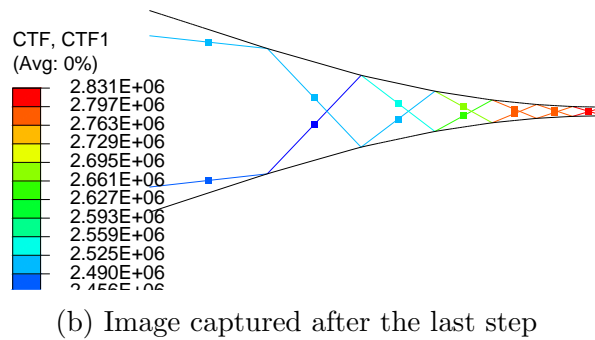
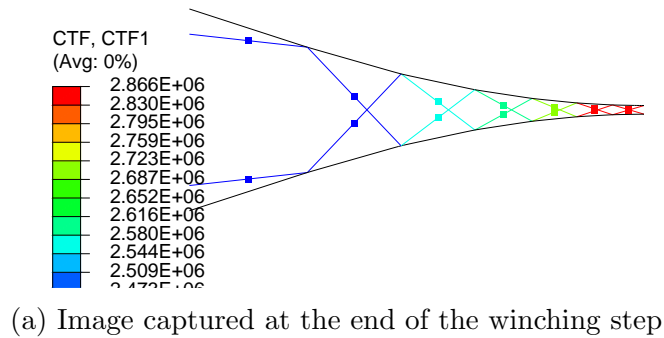


Figure 3.2: Images for an analysis with a load applied after the winching procedure

When several steps are created, is it also necessary to modify the material flow through the points simulating the winches. If the material flow boundary conditions are unchanged, you have no boundary condition for the step *before* and it's propagated to the step after winching. Both of these steps have no boundary condition that lock the winches, hence one has free material flow. The material flow should be zero through the winches in step *before* and *after*.

To solve this as simply as possible, a boundary condition with zero material flow is assigned in the initial step. It is then propagated to the step *before*, if it is created, so no additional modifications are necessary. So if the step *before* is created the material flow is set to zero. Further the right winching magnitude is assigned for the winching step. Finally the material flow is set to zero again for the last step, if this step is created. Now, the only material flow through the winching points are the winching magnitude

set in the *input.py*-file, and for the rest of the steps it is zero.

The last challenge was the XY data reports. When one is saving data from the H-output, one has to choose the steps to include. In ASAT one wish to choose all of the steps in the analysis. When the GUI is used manually, all of the steps are chosen by default. When ASI is used, one has to state the name of the steps. There is not found a command to choose all of the steps. After some trial and error one found out that it is possible to use a list as input parameter for the command. A variable called *activeSteps* is introduced to solve this. This is a list and contains the name of the steps in this particular analysis. *winching* is always added, but *before* and *after* are only added to the list if the steps are created in this analysis. The code block is shown in Listing 3.2.

Listing 3.2: Finding created step(s) for the current analysis

```

activeSteps=list ()
if vars.makeBefore == True:
    activeSteps.append('before')
activeSteps.append('winching')
if vars.makeAfter == True:
    activeSteps.append('after')

```

The plots in the figures have some markers. These are either a diamond or a triangle. The number of markers for each plot are decided from the variable *nMarkersMax*. Based on *nMarkersMax*, *nHistoryOutputPoints* and *T*, which is the winching time, a marker frequency, *markEvery*, is determined. When one include a step before and/or after *winching* the total analysis time increases a lot, hence the markers are very tight placed in the plot. The time *T* is now replaced with a variable called *Ttot*, which is the total analysis time. In addition is a variable called *nSteps* introduced, which contains the number of steps, to find the right marker frequency.

MARK: The part regarding the data sampling frequency is moved. Snerud's Master's thesis says that it is found around line 106 to 112 in *input.py*. It is now found between line 258 and line 273 in the same script.

3.1.2 Elastic Wire

In the earlier versions of ASAT the wire is modelled as infinite rigid, i.e. the wire has no elongation, no matter of the axial force. The influence of an elastic wire is unknown, so this was a part to study. In the *input.py*-file the are two new variables for this part:

wire Decides whether the wire is elastic or infinite rigid. Takes values ‘rigid’ and ‘elastic’

EA Sets the values for the elongation of the wire. The value is Young’s modulus (E) [Pa] multiplied by cross section area (A) [m²] and has the unit Newton[N]

The cross section area and the Young’s modulus are not decided yet. Therefore is the input parameter *EA* introduced, so one can investigate the effect of an elastic wire. The results from these analyses may influence the selection of the wire. By finding a required axial stiffness one can find the required combination of Young’s modulus and wire diameter.

In the *exceptions.py*-file there is added an argument that checks that the value of *wire* always is ‘rigid’ or ‘elastic’. The establishing of the wire properties for the model is found in the *machinery.py*-file.

3.2 Testing of Wire Elasticity

One of the objects for this thesis is to include an elastic wire for the shoe-lacing principle. To do this one needs to state a constant called D_{11} as a part of the definition of the slipping element. This is the property of the axial stiffness. In the Abaqus CAE GUI there is no information about this constant, so some further work was required to find out more about it.

Based on earlier experiences and discussions, it was assumed that the wire stiffness is either EA or EA/L . Therefore the analysis set-up aims to be as suitable for this purpose as possible.

One decided to build up a model in Abaqus and run some analyses with varying parameters for the wire/slipping element and find out how the model behaves with varying input parameters. Three different configurations were tested, they are shown in Figure 3.3, 3.4 and 3.5. Below follows an explanation of each of them:

Configuration 1 This model has only a wire in its analysis. An analysis requires at least one element, so a beam is introduced. This beam is separate from the wire and doesn’t influence the result. The wire is attached to freely supported points at its ends. Wire is pulled out of the system at the left end.

Configuration 2 This model has a beam, which is fixed at its lower end. A wire is attached to the upper end. The wire goes through a fixed pulley with no friction and is attached to a fixed end point. The wire is pulled out through this point.

Configuration 3 The beam is fixed at its left end. A wire is attached to the right end of the beam. At the wire's right end point wire are pulled out of the system.



Figure 3.3: Configuration 1: Only a wire. Freely supported at its ends

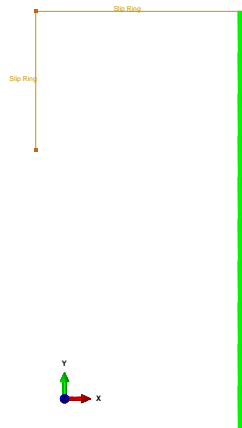


Figure 3.4: Configuration 2: A cantilever beam where the wire introduces a bending force

It was hard to find analyses with good input parameters. For some reason a lot of the analyses ended up with zero force in the wire. Configuration 2 worked very well for the analysis. The winching of the wire introduces a bending stress and a small axial force in the beam. The combination of these two makes the reading of the result difficult. Configuration 1 did also



Figure 3.5: Configuration 3: The final model, used for the testing of D_{11} . Pure axial loading

arise some errors, especially related to the lack of wire force. Configuration 3 didn't work well in the beginning either. But since this one was considered as the best alternative, some extra effort was put into to get this work. After a lot of trial and error and tuning of parameters, one got a model that worked as wanted.

Configuration 3 is simple modelled. One get pure axial stress in the beam, so the results are easy to read off. For all of the configurations the beams were modelled as circular rods, but the diameter and length varied, based on a proper stiffness. Results from the analyses with configuration 3 are found in section 4.3 on page 46. The physical measurements for the beam and the wire are found in Table 3.1 and material data in Table 3.2.

Table 3.1: Properties for the rod and wire used in configuration 3

Rod		Wire		
Length	Diameter	Length	D_{11}	Material flow
1000 mm	10 mm	500-4000 mm	1 000 000[?]	0.020 m

Table 3.2: Material properties for the rod in Table 3.1

Density	Young's modulus	Poisson's ratio	Mass damping coefficient
7800 kg/m ³	210 000 MPa	0.3	1.0

To calculate the wire stiffness, a lot of data from the analyses were used. The calculated stiffness were compared with the stiffness set as a property in the model. The following results from an analysis were used:

CTF The tension force in the wire

U1 Displacement of the common node between the wire and the pole

S-Mises von Mises stress in the pole

Based on the information in this section and the results shown in Appendix D the calculations of the wire stiffness were executed. The results are shown in section 4.3.

First one has to calculate the undeformed length after the material flow. The material flow is the same boundary condition as used for the winching magnitude in ASAT.

$$l_0 = l - \Delta l \quad (3.1)$$

where

l_0 is the undeformed wire length after the material flow

l is the start length of the wire, i.e. before material flow

Δl is the material flow

Further the deformed length of the wire is calculated

$$l_1 = l - U1 \quad (3.2)$$

where

l_1 is the deformed length of the wire

$U1$ is the elongation of the pole

This gives the elongation of the wire as

$$\delta l = l_1 - l_0 \quad (3.3)$$

where δl is the elongation of the wire

From the elongation one can calculate the strain of the wire

$$\epsilon = \frac{\delta l}{l_0} \quad (3.4)$$

where ϵ is the strain of the wire

From the finite element method one has that[14]

$$\mathbf{S} = \mathbf{k}\mathbf{v} \quad (3.5)$$

where

\mathbf{S} is the force at a node

\mathbf{k} is the elements stiffness matrix

\mathbf{v} is the displacement at a node

For a pole with pure axial loading the equation reads

$$F = \frac{EA}{l_0} \delta l \quad (3.6)$$

where

F is axial force

E is Young's modulus

A is cross section area

By using this equation one can get two different expressions for the stiffness

$$\frac{EA}{l_0} = \frac{F}{\delta l} \quad (3.7)$$

$$\begin{aligned} EA &= \frac{F}{\delta l} l_0 \\ &= \frac{F}{\frac{\delta l}{l_0}} \\ &= \frac{F}{\epsilon} \end{aligned} \quad (3.8)$$

For the beam the strain is calculated as

$$\epsilon = \frac{U1}{l} \quad (3.9)$$

where l is the length of the rod

The stress is then calculated from

$$\sigma = E\epsilon \quad (3.10)$$

The equations above are used to calculate the results shown in section 4.3 and Appendix D.

3.3 Calculation of Loads

In this section all of the calculations for the loads are gathered, i.e. drag force due to water current and buoyancy. Theory about the equations and the equations itself are found in section 2.4.

3.3.1 Water Current

There aren't found any reports where the drag force due to the water current is calculated. By combining data from several different reports regarding the artificial seabed project is it possible to calculate the drag force. A report by ÅF Reinertsen[3] says that Equation 2.2 are to be used. The sea water density is stated in Table 2.5, drag coefficient in Table 2.6 and water current velocity in Table 2.4. As provided by the Norwegian Public Roads Administration's Handbook 185[8] the most unfavourable values are used. I.e. the highest values in Table 2.5, 2.4 and 2.6, which gives the highest drag force. The height, h , is calculated from Equation 2.3. Most of the analyses, both in this thesis and in Snersrud's and Grevstad's Master's theses, are run with a spacing between the pipes of 0 m. Hence, $S = 0$ m are used for calculation of the cross section height too.

$$\begin{aligned} h &= 2D + S \\ &= 2 \times 0.9144 + 0 \\ &= 1.8288 \end{aligned} \tag{3.11}$$

All together one can calculate the drag force due to the water currents.

$$\begin{aligned} F_{current} &= \frac{1}{2} \rho_w C_D h v_{current}^2 \\ &= \frac{1}{2} \times 1025 \times 1.5 \times 1.8288 \times 0.55^2 \\ &= 425 \text{ N/m} \end{aligned} \tag{3.12}$$

A value of 425 N/m are used both in ASAT and other analyses with water current.

3.3.2 Buoyancy

The buoyancy on the bundle is equal the difference between the mass of the immersed water and the gravitational force on the bundle. The dimensions for the bundle are found in Table 2.1, material properties in Table 2.2 and density of seawater in Table 2.5. As provided by the Norwegian Public Roads Administration's Handbook 185[8] the most unfavourable value are used. I.e. the lowest value in Table 2.5, which gives the lowest buoyancy force. The weight of the bundle are.

$$\begin{aligned}
G &= \rho Ag \\
&= 7850 \times 3 \times \pi \times \frac{0.9144^2 - (0.9144 - 2 \times 0.0305)^2}{4} \times 9.81 \quad (3.13) \\
&= 19566 \text{ N/m}
\end{aligned}$$

By using Equation 2.4 one finds the buoyancy, which is the mass of the immersed water. The bundles are watertight, therefore the cross section is assumed as a closed cross section.

$$\begin{aligned}
F_B &= \rho Ag \\
&= 3 \times \pi \times \frac{0.9144^2}{4} \times 1005 \times 9.81 \quad (3.14) \\
&= 19423 \text{ N/m}
\end{aligned}$$

The difference between Equation 3.13 and 3.14 gives the weight of the bundle in sea water.

$$\begin{aligned}
\Delta F &= G - F_B \\
&= 19423 - 19566 \quad (3.15) \\
&= -143 \text{ N/m}
\end{aligned}$$

From Equation 3.15 one gets that one bundle totally has a negative buoyancy of 143 N/m in sea water.

3.4 Simulations

Before the wire and the pulleys for the shoe-lacing principle are mounted between the two pipe bundles, they have no support, except of the ends. In the period before the shoe-lacing principle is mounted, the bundles need extra support to maintain the material integrity. Tugboats and barges are meant for this operation. One or more tugboats or barges are placed along the bundle to keep the initial shape, and withstand external forces as water current and buoyancy. To keep the costs as low as possible one wants to hire as few as possible vessels, but still one has to take material integrity into account.

3.4.1 Water Current

The two bundles have a curvature facing towards each other, i.e. water current have opposite influence on the bundles, shown in Figure 3.6. It is desirable to keep the shape as close up to the initial shape as possible, both with respect to material stresses and mounting of the shoe-lacing principle. The water currents are introduced as a line load along the bundles, where

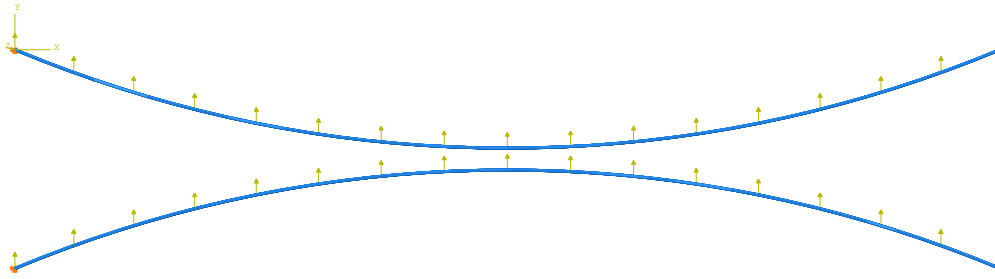


Figure 3.6: Water current load on the bundles

the value is calculated in section 3.3. The boundary conditions at the ends are freely supported, i.e. zero displacement and free rotation. The spacing between the pipes in the bundles, S , is set to zero, when the simplified singular pipe is calculated. The forces from the tugboats are placed as point loads on the bundle.

In the beginning one tried to vary the position of the tugboats to find a optimum placement, but after awhile one ended this work. This work gave too many possible solutions and analyses, and became too time-consuming. Therefore the tugboats are evenly distributed along the bundle, hence when one tugboat is used it's placed at the mid-point, two tugboats at the third point and so forth.

It is not yet decided what kind of tugboats that are going to be used, so one doesn't know the bollard pull for the tugboats. Therefore are the analyses run for a wide span of forces, to figure out whether there is a optimum force or not and to cover a wide span of tugboats.

For small forces Abaqus doesn't find an equilibrium for the analyses, so they are aborted before they are finished. For each configuration the lowest possible force is found. Each configuration is based on this force and do analyses for values equal and higher than this force. The lowest force varies for each configuration, but decreases for an increasing number of tugboats. The lowest possible force represent when one will get a snap through of the bundle.

To run the analyses as efficient as possible several Python script were used. Earlier a script, which builds up a model, was made. This script was used again, but with adjusted input parameters. Further were boundary conditions, loads and the first analysis for each analysis made manually. Finally a new script was run. This script contains all of the loads. The scripts goes through a for loop for each load. Briefly one loop sets the value of the load, runs the analysis and saves images of deformation and von Mises stress. This script is found in Appendix A, as an example of how a Python script for Abaqus can look.

3.4.2 Buoyancy

The model from the analyses with water currents were reused. The buoyancy force calculated in section 3.3 were used. In these analyses barges instead of tugboats were used. The barges were evenly distributed along the bundle. A barge holds the bundle in the vertical position. The boundary condition isn't a force, but the displacement is set to zero in the vertical direction.



Figure 3.7: 2 barges, deformation in the horizontal plane. Deformed and undeformed shape



Figure 3.8: 3 barges, deformation in the horizontal plane. Deformed and undeformed shape

In Figure 3.7 one can see the deformation with 2 barges. The bundle was deformed to a straight line across the fjord, but, as seen in Figure 3.8, with 3 barges the shape was kept much better. To keep the shape of the bundle

with 2 barges an extra force was introduced. The force represents a tugboat and is placed in the same points as the barges but acting in the Y-direction. The maximum force is equal to zero deformation in the Y-direction in this point, and is stepwise reduced to zero for the analyses.

3.4.3 Water Current and Buoyancy

A series of analyses with a combination of water current and buoyancy were run, to find out how these are acting together.

The same boundary conditions and loads as previously used in this section were still used, but now all together. An equal number of barges and tugboats were used. A tugboat were represented with a horizontal force in Y-direction, while a barge were simulated with zero displacement in Z-direction.

To run the analyses as effectively as possible, the same script as used for the water current were used, but now with some modifications and extensions. Due to the results from the previous analyses, these analyses were only run with three and four tugboats and barges.

3.4.4 Tugboat with Vertical Force Component

So far the force from the tugboat is used as a horizontal force in Y-direction. However, this is not a realistic case, because the force needs a vertical component too. One want to find a vertical component, so one can calculate the total force. In addition is it of interest to find a required length of the stay between the bundle and the tugboat.

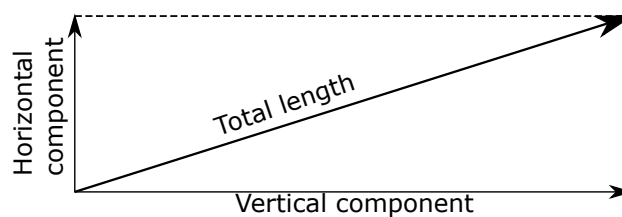


Figure 3.9

The stay is probably a wire, or something similar. A wire is long and slender, therefore it only transfer tension forces and no moments. Hence, the stay and the force are parallel, which means that they creates two similar and perpendicular triangles. The Y- and Z-components are the catheti and the total length/force is the hypotenuse, as shown in Figure 3.9. The following equation gives the relation between the components:

$$\frac{l_Y}{l_Z} = \frac{F_Y}{F_Z} \quad \Rightarrow \quad l_Y = \frac{F_Y}{F_Z} \times l_Z \quad (3.16)$$

where

l_Y is the horizontal component of the length

l_Z is the vertical component of the length

F_Y is the horizontal component of the force

F_Z is the vertical component of the force

l_Z is equal the submerged depth of the artificial seabed, F_Z is found from the analyses and F_Y is an input force to the analyses. By using the Pythagorean theorem one finds the total length of the stay.

$$\begin{aligned} l_0 &= \sqrt{l_Z^2 + l_Y^2} \\ &= \sqrt{l_Z^2 + \left(\frac{F_Y}{F_Z} l_Z\right)^2} \\ &= \sqrt{l_Z^2 \left(1 + \left(\frac{F_Y}{F_Z}\right)^2\right)} \\ l_0 &= l_Z \sqrt{1 + \left(\frac{F_Y}{F_Z}\right)^2} \end{aligned} \quad (3.17)$$

l_Z is decided and is 30 meters, which is the distance from the artificial seabed to the sea level. Hence, it is the F_Y/F_Z -ratio that decides the length of the stay. When the F_Y/F_Z -ratio increase the expression in the square root is approximately equal $(F_Y/F_Z)^2$. Therefore, Equation 3.17 has an approximately linear behaviour for high values. The equations is plotted in Figure 3.10.

One wants to avoid that the bundle is pulled upwards due to the vertical component of the tugboat force. Since a tugboat and a barge are attached to the same points, the vertical component from the tugboat is directly affecting the force from the barge. When one runs the analyses with only a horizontal component for the tugboat, the barge takes all of the vertical forces. When the vertical tugboat force component is introduced, this force is a direct reduction of the force from the barge.

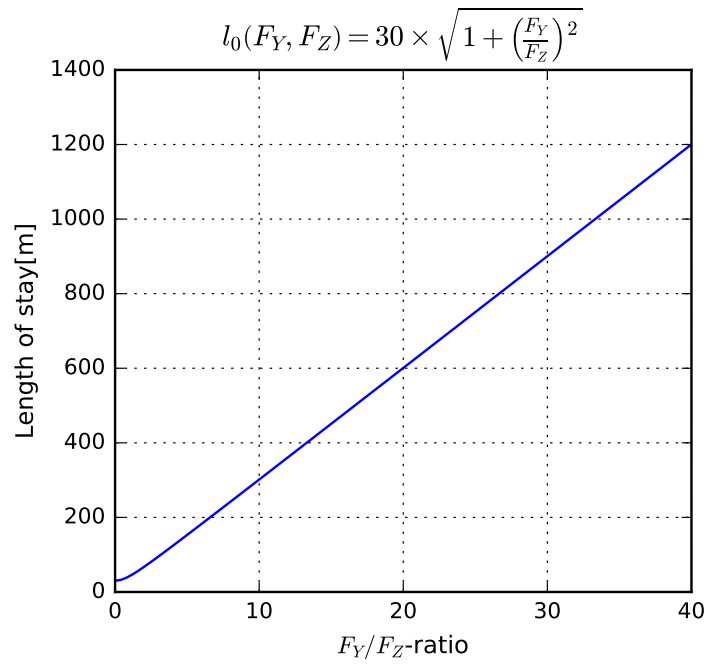


Figure 3.10

To avoid that the bundle is pulled upwards, the vertical force from the tugboat can't exceed the magnitude of the barge force, when the vertical force from the tugboat is zero. This makes a limit for F_Z . Therefore one needs a longer stay, if one needs to increase the horizontal force without influencing the vertical force.

Chapter 4

Results

In this chapter the most interesting results from the analyses are collected and presented. The new version of ASAT isn't attached to this chapter, but handed in a separate own attachment. All of the results are further discussed in chapter 5 Discussion. For more results, please go to the appendices to this report.

4.1 New Version of ASAT

The verification and a test run of the new version of ASAT are shown in this section. The first part shows that it is still possible to run ASAT similar as the old version, while the latter part shows how an analysis with the new options can look.

4.1.1 Comparison of New and Old Version

It is still possible to run ASAT similar to the old version of ASAT. To show this and verify the changes, a analysis with the same input parameters is run with both of the versions of ASAT. In Figure 4.1, 4.2, 4.3 and 4.4 some of the results from both of the analyses are shown. The remaining plots are found in Appendix C. The input parameters for both of the analyses are shown in Table E.2 in Appendix E.

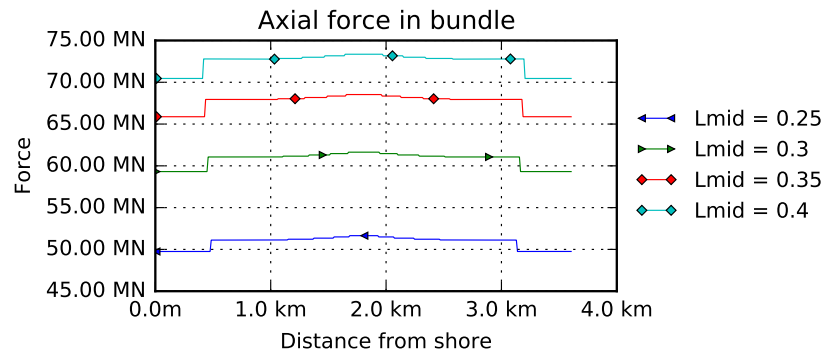


Figure 4.1: From old ASAT version

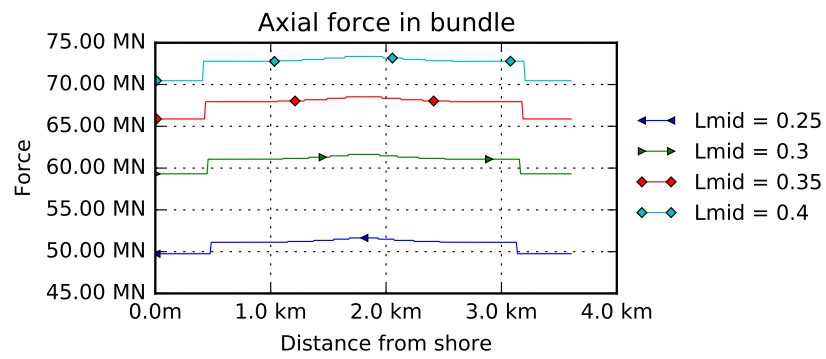


Figure 4.2: From new ASAT version

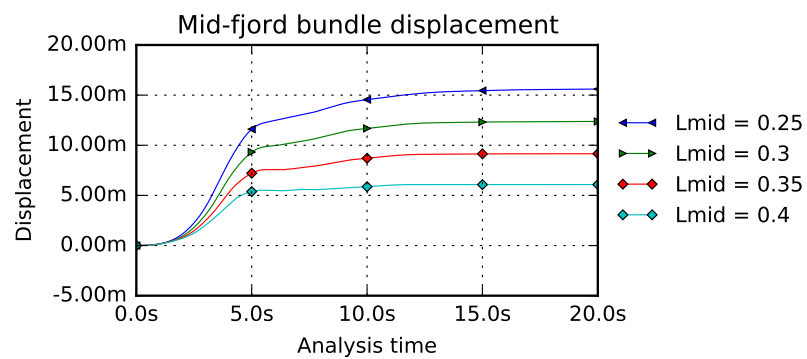


Figure 4.3: From old ASAT version

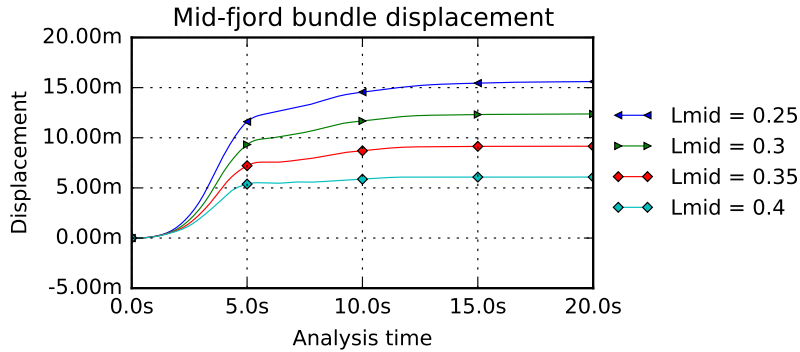


Figure 4.4: From new ASAT version

4.1.2 Example of Analysis in New Version of ASAT

This part is mainly included to show that the functionality of the new version of ASAT works well. At the same time one have some phenomenons that are worth to mention. The input parameters for this analysis is found in Table E.3.

As seen in Figure 4.5 the behaviour of the bundle when applied to water current depends on the pulley configuration. For a low mid-span weighting, L_{mid} , the center point of the upper bundle drift away from the center of the construction, while it drifts towards the centre for a higher L_{mid} .

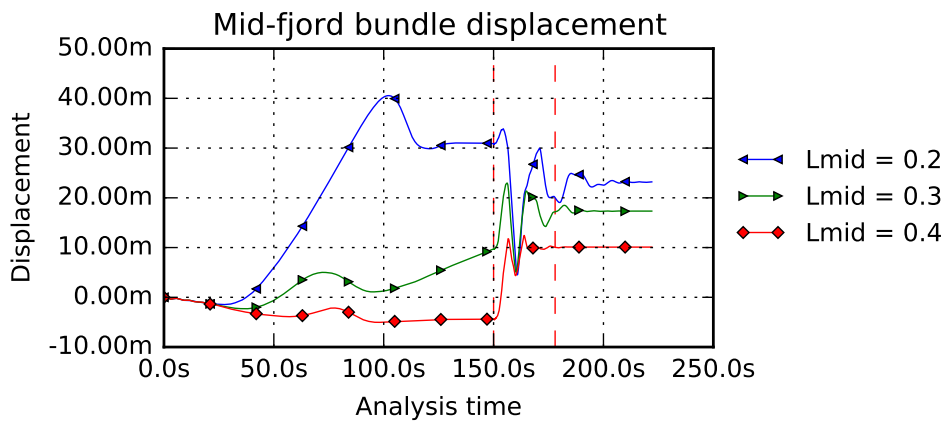


Figure 4.5

As seen in Figure C.16 the relative deviation of axial force in the bundle

is low. For $L_{mid} = 0.2$ one gets a relative high drop of axial force mid-fjord. For some configurations one gets a drop of axial force mid-fjord, but not as high as in this case.

4.2 New Numerical Optimum

After the changes of ASAT made in this thesis, the optimum numerical values has changed. In addition are two new numerical input parameters added, T_b and T_a . The winching time, t , and element length, L_e , are assumed as unchanged. The input parameters used for these analyses are shown in Table E.1.

The water current introduces displacements of the bundles before the winching starts. A higher mass damping coefficient gives a higher resistance to displacements, i.e. the bundle moves slower but vibrations are damped more efficient for a higher mass damping coefficient.

The displacements of the mid-point of the bundle for different mass damping coefficients are shown in Figure 4.6. A plot of analyses with a wider span of D , is shown in Figure C.17. As seen, the optimum numerical value, are much lower than the old values in Table 2.3. It looks like the numerical optimum is $D = 0.10$

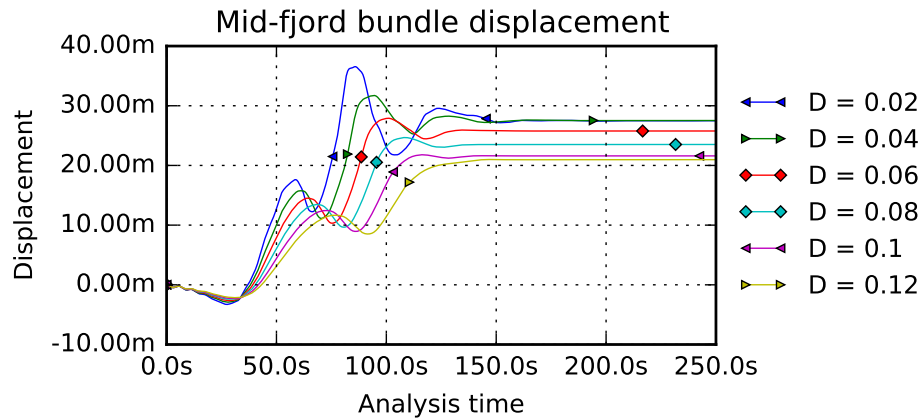


Figure 4.6: Equilibrium for different mass damping coefficients

The equilibrium for $D = 0.10$ in Figure 4.6 occurs after approximately 150 seconds. Hence, this is the optimum numerical value for T_b .

Since the mass damping coefficient is much lower than in Table 2.3, the bundles need more time to find an equilibrium. Figure 4.7 shows the dis-

placement when the water current are applied before the winching step, $Fb = 'True'$. One can see that an equilibrium are reached after 72 seconds. Since nothing are changed from the step *winching* to *after*, the total length of these steps must exceed 72 seconds. The length of the single steps doesn't matter, except $T \geq t$.

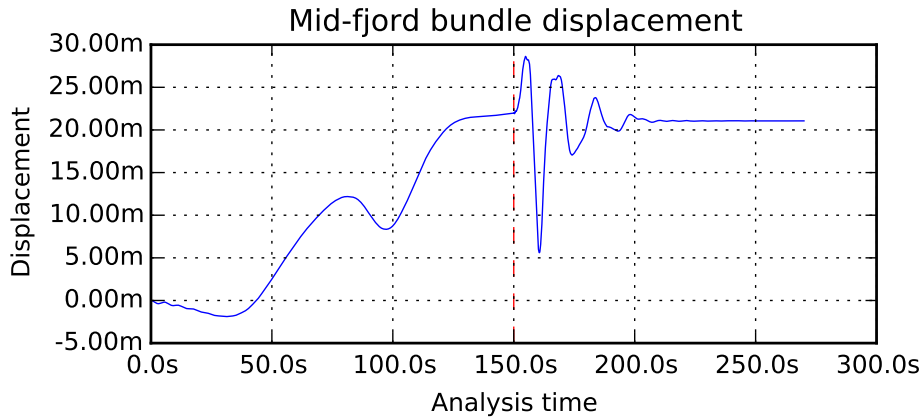


Figure 4.7: Equilibrium for winching procedure

Figure 4.8 shows the equilibrium for the shoe-lacing principle when the water current is applied after the *winching* step. An equilibrium occurs after 28 seconds in step *winching* and 22 seconds in step *after*.

The new optimum numerical values are summed up in Table 4.1.

Table 4.1: New numerical optimum

Parameter	Value
Tb – Time step <i>before</i>	150 s
T – Time step <i>winching</i>	28 s*
Ta – Time step <i>after</i>	22 s*
t – Winching time	5.95 s
D – Mass damping coefficient	0.10
Le – Element length	10 m

*When $Fb = 'True'$ the sum of T and Ta has to be 72 s and $T \geq t$

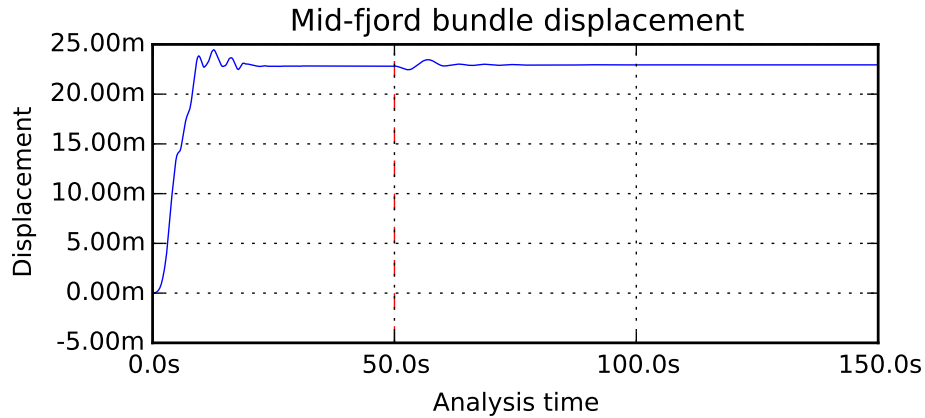


Figure 4.8: Equilibrium when force is applied after *winching*-step

4.3 Wire Elasticity

Based on the results from the analyses, the stiffness for the wire is calculated. All of the analyses are run with the same wire stiffness, but with a varying wire length. The results from the analyses are used to go backwards from the results to the wire stiffness and compare the answer with the input stiffness. As described in section 3.2 two different approaches for the stiffness are evaluated.

The calculations are compared with the true stiffness in Figure 4.9. The results from the EA and $\frac{EA}{L}$ calculations are also shown in Table D.2. Complete tables with all of the calculations are found in Appendix D.

As one can see from Figure 4.9 the calculations for EA always are close to the true value, while the EA/L -calculations are decreasing with an increasing length of the wire.

4.4 Water Currents

The results from the analyses of the tugboat capacity are summed up in Figure 4.10. The start point of the curves represents the lowest possible force without a snap-through. The stress is the maximum von Mises stress in the bundle. Note, the tugboat force at the X-axis is per boat. A scaled up version of the most interesting part is shown in Figure C.18. From the curve in Figure 4.10 one can see that for an increasing number of tugboats the minimum required force per tugboat and the stresses are decreasing, while

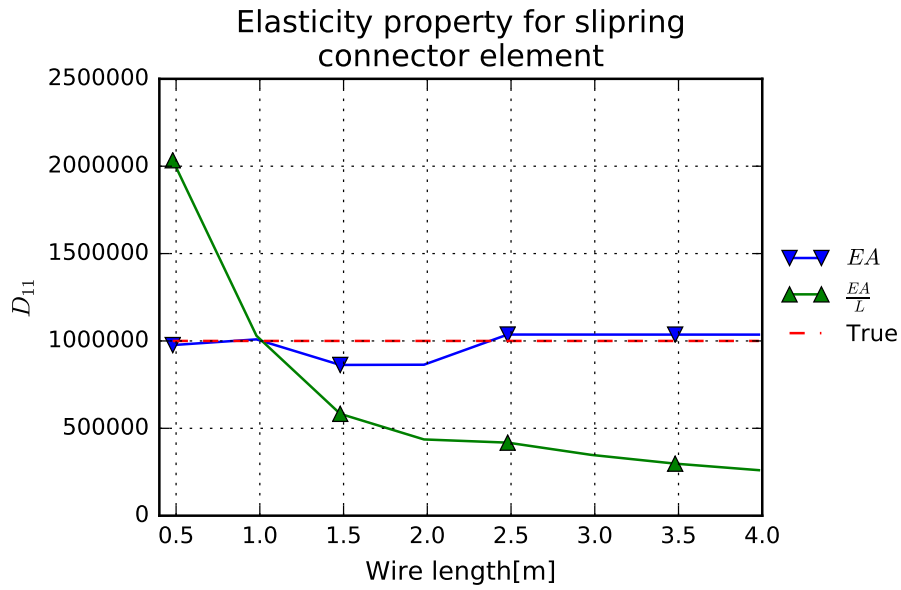


Figure 4.9: Calculated wire elasticities compared to true elasticity

the total tugboat force requirement is increasing. If minimum two tugboats are used, these is also a low point for the curves.

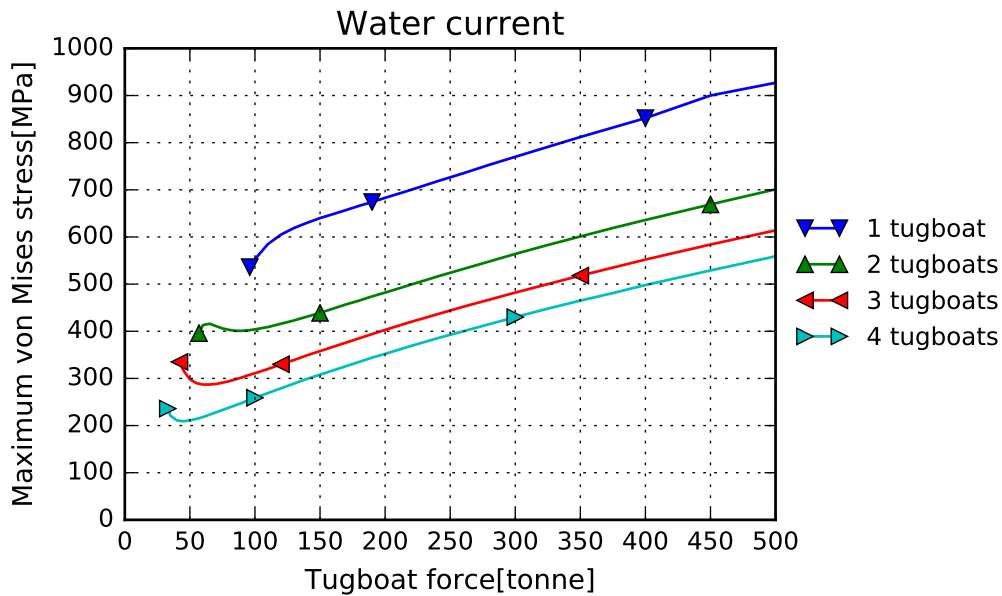


Figure 4.10: Maximum von Mises stress in the bundle

In Table 4.2 the lowest possible force for each of the configurations are shown. This is the start point of each curve in Figure 4.10.

Images of stress and deformation of the bundle are shown in subsection C.7.1.

Table 4.2: Lowest possible force with water current

	1 tugboat	2 tugboats	3 tugboats	4 tugboats
Force[tonne]	96	57	42	33

4.5 Buoyancy

As seen in Figure 4.11 there are huge differences in the deformation for the bundles, dependent on the number of barges. The analysis with two barges clearly stand out from the other. The analysis with one barges didn't find any equilibrium and is excluded from this plot, but has probably equal deformation in Y-direction as for two barges.

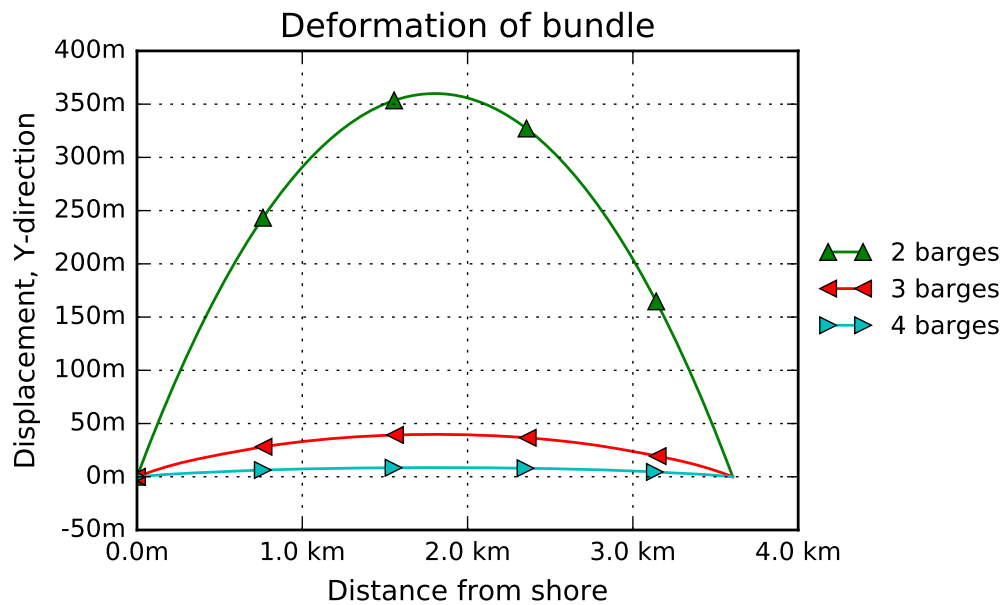


Figure 4.11: Deformation in Y-direction

Figure 4.12 shows the deformation for the bundle with two barges and an additional force from tugboats. The force that gives zero displacement is 134 kN and is denoted as 1.0F. Other forces are stated relative to this force.

As one see from Figure 4.12 a relative small force gives a huge effect on the deformation. With a force at only $0.4F = 53 \text{ kN}$ (5.3 t) the deformation is equivalent with the deformation for three barges.

A similar plot is made for one barge, and is found as an appendix in Figure C.20. For this plot the deformation is more spread. Plots showing the vertical deformation and the von Mises stress in the bundles are also found in section C.4.

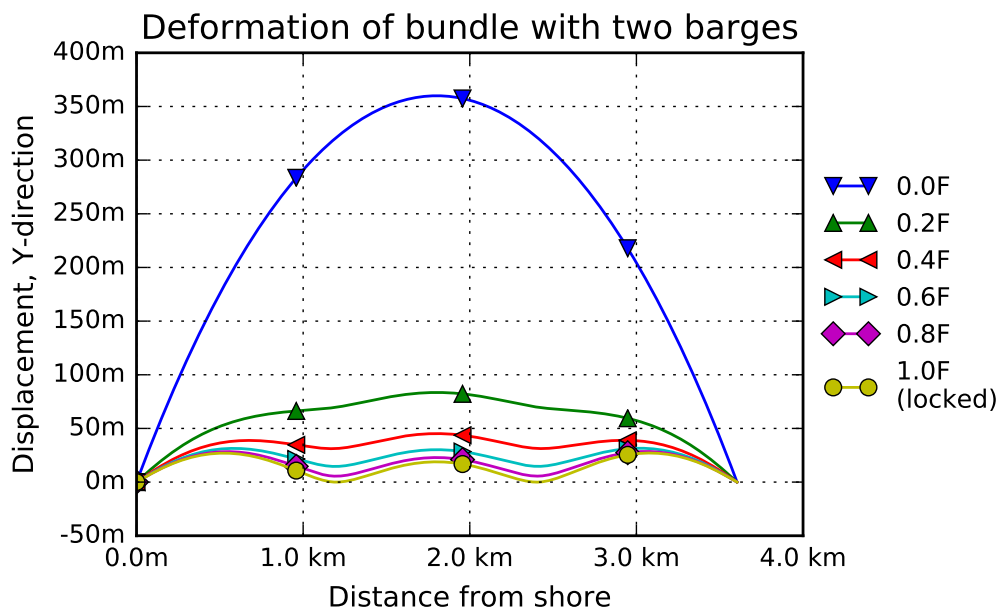


Figure 4.12: 2 barges, varying tugboat force

4.6 Water Current and Buoyancy

In Figure 4.13 the maximum von Mises stress for each tugboat force is plotted. The lowest possible force are equal with the forces stated in Table 4.2. The curves have also a low point in this plot, but is not similar to the low point found with only water current. A scaled up version of this part is found in Figure C.25 on page 90.

Images of stress and deformation of the bundle are shown in subsection C.7.2.

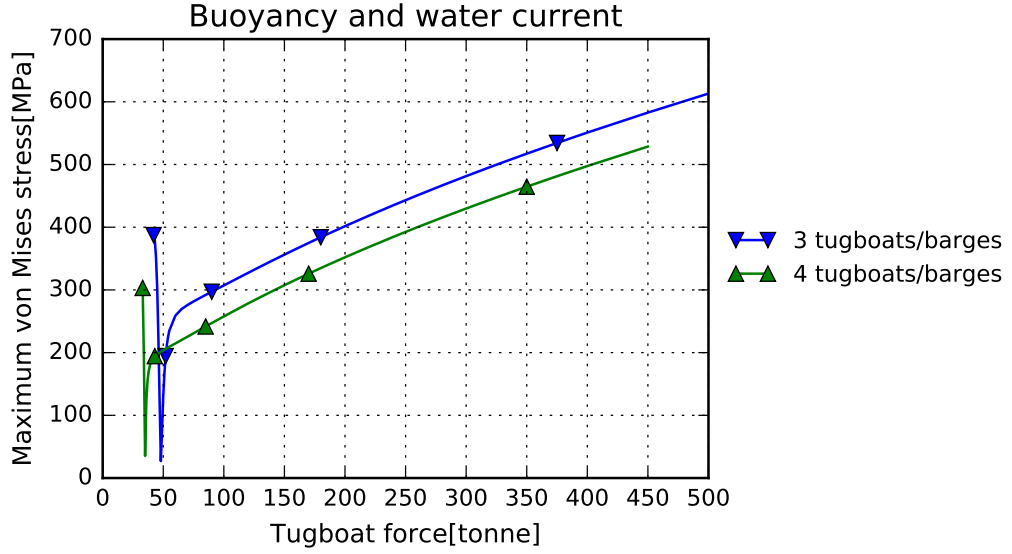


Figure 4.13: Simulations with both water current and buoyancy

4.7 Tugboat with Vertical Force Component

Based on the already executed analyses, the best alternative is to use three tugboats. The ideal towing force is probably somewhere between 50 and 55 tonnes. From the analysis with 50 tonnes in section 4.6 the force for the middle barge is 130 kN. If one assumes that the tugboat should take the whole force, the total force is then 51.7 tonnes. From Equation 3.17 one can find a minimum stay length:

$$l_0 = 30 \times \sqrt{1 + \left(\frac{50 \times 10^4}{130217}\right)^2} = 119 \text{ m} \quad (4.1)$$

From Equation 3.16 one can find the horizontal distance between the tugboat and the bundle

$$l_Y = \frac{50 \times 10^4}{130217} \times 30 = 115 \text{ m} \quad (4.2)$$

In Figure 4.14 one can see how the length of the stay changes with respect to the vertical component. The X-axis is normalized with respect to the maximum possible force, 130 kN.

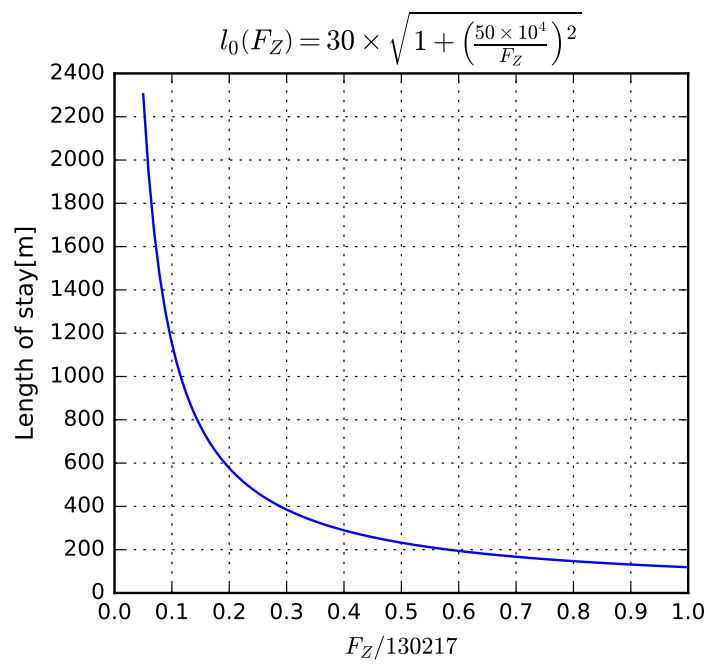


Figure 4.14: Length of stay, with a normalized X-axis

Chapter 5

Discussion

In this chapter are the findings from chapter 4 Results discussed. This chapter has the same structure as the Results chapter.

5.1 New Version of ASAT

As seen from the plots in section 4.1 and Appendix C the results from the two different versions of ASAT are equal. Hence, one can say that the upgrading is executed without influencing the original functionality of ASAT. Therefore, by using $Fb = 'False'$, $Fa = 'False'$ and $wire = 'rigid'$ ASAT produces results equal to the original version of ASAT.

The new version also work well. During the work with the upgrading of ASAT test runs were executed regularly. After every major change a test were run, to verify that ASAT runs as planed and gives expected results. If there were found any deviations, one took a closer look into the code to find out what caused the error. Any error were debugged before new changes were made. At present time there are no known errors in the code.

As seen in Figure 4.5 and Appendix C the plots look reasonable. The deformation and stress looks similar to earlier analyses. Except of the small vibrations that causes the peaks in the plots of wire force, which is dealt with later in this chapter, the wire force looks sensible.

For the lowest $Lmid$ the axial force has a relative high drop mid-fjord. Due to the water current the bundles are deformed before the winching. The wire in the shoe-lacing principle is redistributed in the system and therefore the bundle doesn't behave similar to a bundle not subjected to water current. In addition is it tighter spacing between the pulleys, which gives a lower angle for the wire through the pulley. Therefore are the shear forces higher and the axial forces lower, compared to the analyses with higher $Lmid$. The result

of a higher shear force can be seen in Figure C.12, which gives the highest deformations mid-fjord, even though the bundle has the lowest stress level.

The wire-pulley configuration does also give quite different equilibrium points for the deformation before the winching. For a high L_{mid} the bundle drifts towards the center of the construction, while it drifts away for a low L_{mid} .

In the earlier versions of ASAT are the deformations and stresses equal for both of the bundles, the model is symmetric about both the X- and Y-axis. Hence, it is indifferent whether one picks data from the upper or lower bundle. When the water current is introduced, the symmetry about the X-axis ceases. In ASAT are all of the data captured from the upper bundle. The water current's direction is set to positive Y-direction, so the biggest influences are on the upper bundle. With this direction is it possible that the upper bundle can snap through and the bending stresses are higher.

ASAT is also run with the elastic wire selection. Analyses with the new version of ASAT with an elastic wire is found in Appendix B.

5.2 New Numerical Optimum

The new numerical optimum is shown in Table 4.1. However, this only applies to analyses where either Fb or Fa or both are 'True'. If both Fb and Fa are set equal 'False', ASAT runs with only the *winching* step, as in the old version. I.e. the numerical optimum are unchanged, and equal the optimum stated in Table 2.3.

As one can see from Figure 4.6 the equilibrium point is dependent on the mass damping coefficient. Different values for D gives different displacements at equilibrium. To avoid getting different solutions, one has two possible actions: One can either use the numerical optimum mass damping coefficient or find a mass damping coefficient which is representative for the conditions in Sognefjorden. Since the mass damping coefficient was introduced to create numerical stability, the most appropriate solution is to use the numerical optimum mass damping coefficient. At a later point, when one knows more about the behaviour of the shoe-lacing principle, one should consider to use a more realistic mass damping coefficient.

Due to the varying mass damping coefficient, one gets different displacements of the bundle during the analyses. Since the mass damping resists the displacement, the iterations ends up with different equilibrium points, even though the final state is a static solution. However, the equilibrium is influence by more than the mass damping coefficient. During the deformation the bundle has both speed and acceleration, and due to the damping this do also

affect the equilibrium. For instance, the speed is influenced by the winching time, t . A lower winching time gives the bundle a higher speed. Due to the pulley friction is the force reduced through the system and different forces gives different equilibriums.

Another parameter that influences the numerical stability is the winching magnitude, dL . A higher dL means more wire winched out of the system and, for the same number of pulleys, higher stresses and strains. If one increase the winching magnitude one gets a stiffer construction, which causes a quicker equilibrium, as seen in Figure 5.1 where the water current is applied after the *winching* step. Therefore one should consider to change the analysis times for step *winching* and *after*, T and T_a , if number of pulleys, pulley distribution or winching magnitude are changed. There aren't made up any recommended analysis times for other input values than given in Table E.1.

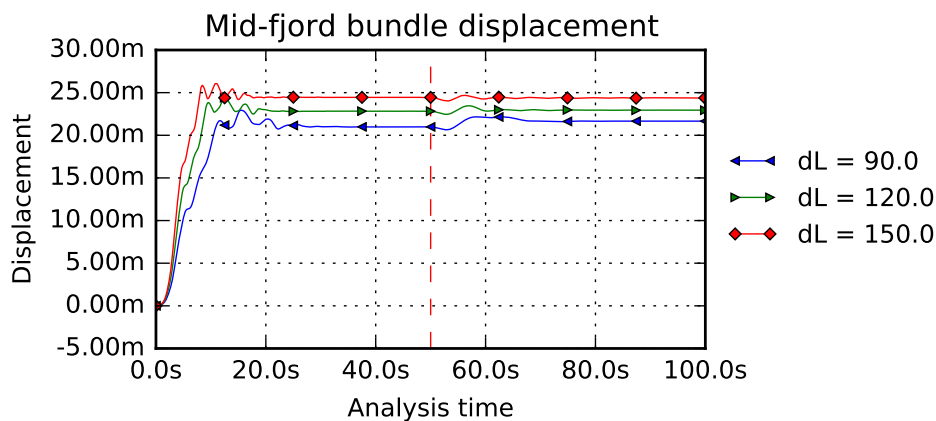


Figure 5.1: Water current applied after winching

A disadvantage with the low mass damping factor is that small vibrations take very long time to damp out. As seen in Figure 5.2 it takes a very long time to find an equilibrium for the wire forces. There are still some small vibrations in the bundles that raises a varying force in the wire. The vibrations are very small, a magnitude of ± 20 mm. This is neglectable for the equilibrium of the displacement, because it is much smaller than the total displacement. But it causes some problems for the wire force. However, in most cases one clearly sees approximately where the equilibrium for the force are going to end up. Since this task mainly take global effects into account, it is not dealt with further. To avoid this problem is it possible to increase the mass damping factor, but this increases the analysis time as well, or use a higher analysis time for the steps.

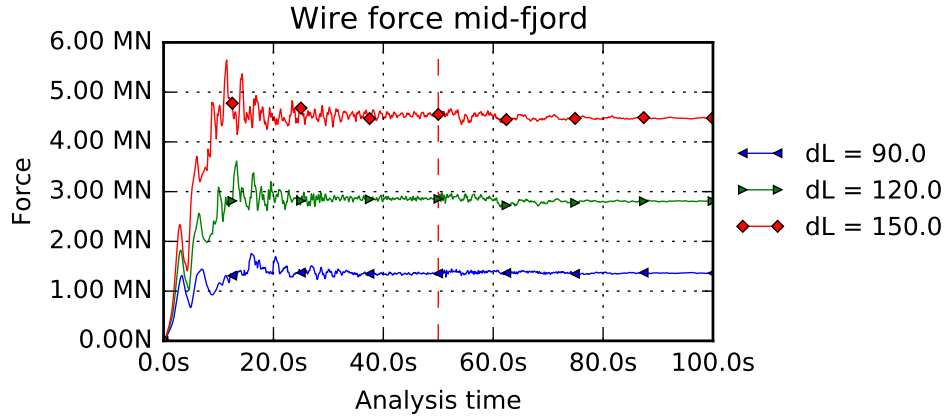


Figure 5.2: Small vibration in bundle causes a non-existing equilibrium for the wire force

5.3 Wire Elasticity

As one sees from Figure 4.9, the calculations for EA always are close to the true value of the stiffness, while EA/L decreasing with an increasing length of the wire. The Abaqus documentation also says that the unit for D_{11} is a force[13] for the slipping connector element. EA/L has the unit force per length, while EA's unit is a force. Hence, all together it is very likely that D_{11} is equal EA.

The possibility for other values for the stiffness isn't considered. Since EA and EA/L by far is the most common values, other approximations are considered as very unlikely and therefore not evaluated. EA is so close to the true value that it is not necessary to look into other possibilities.

5.4 Water Currents

To find the recommended number of tugboats, one has to take deformation, logistics, cost, stresses and the tugboats bollard pull into account.

An increasing number of tugboats on the fjord makes the logistic much harder. More tugboats on the fjord means less space for each vessel and less margins. The cost does also increase by the number of tugboats. Therefore is it favourable with as few as possible tugboats with respect to cost and logistics.

The yield stress for the steel used for the bundles is 480 MPa. From

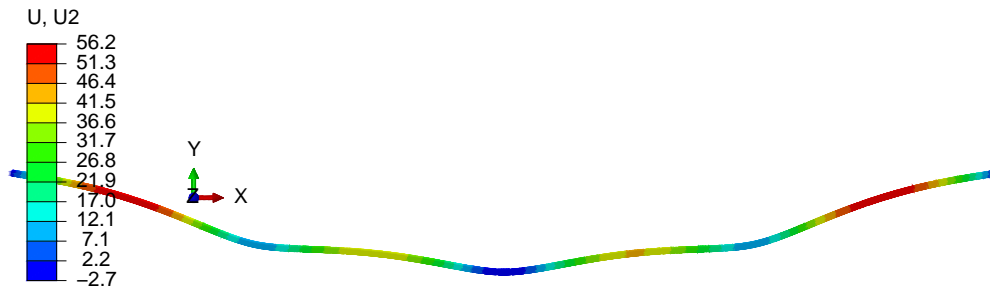


Figure 5.3: Deformation for the bundle with 3 tugboats with 55 t force

Figure 4.10 one can see that with one tugboat the stresses is higher than this. With two tugboats are the stresses below the yield stress, but still too high. The stresses in Figure 4.10 represents maximum values. As one can see from Figure 5.4 the stresses are much lower between the tugboats. In addition the tugboat forces are applied as point loads. If one use a clamp one spreads them out and the stresses will decrease.

Several tugboats gives shorter spans between the tugboats. In addition to the reduced stresses, the deformations also do decrease. A shape close to the initial shape is an advantage with respect to the amount of wire used in the shoe-lacing principle.



Figure 5.4: Von Mises stress for bundle with 3 tugboats with 55 t force

Taking these aspects into account three tugboats with a towing force of 55 tonnes each is a good choice. The deformation for this choice is shown in Figure 5.3 and stresses in Figure 5.4.

5.5 Buoyancy

The bundles are heavier than the mass of the immersed water, therefore they sink in sea water. As seen in Figure 5.5 and Figure 5.7 the stresses are far

from a critical level. The deformation in Z-direction for the bundle with three barges is shown in Figure 5.6.



Figure 5.5: 3 barges, von Mises stress in bundle

As expected the deformation and the stress decreases for an increasing number of tugboats and barges. The von Mises stress for the bundles are shown in Figure 5.7. If it is possible to reduce the peak stress for two barges, the stress level is sufficient for all of the analyses. The boundary conditions are set to a single point, so if one introduces several attachment points the stress should be on a sufficient level. It is favourable to have a so small deformation as possible, due to the mounting, both in vertical and horizontal direction. In these analyses no tugboats are used, and they will better the situation.

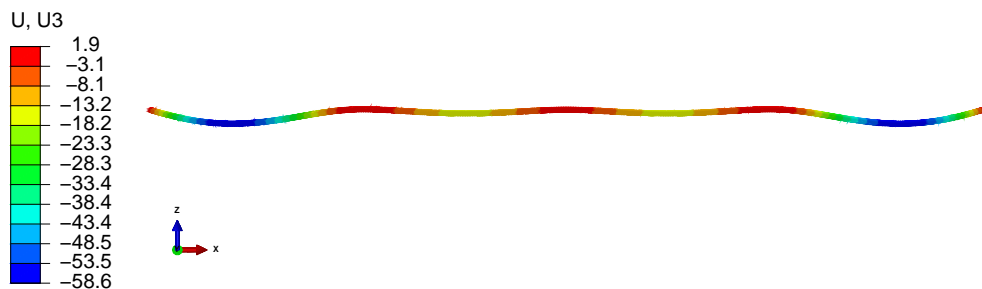


Figure 5.6: 3 barges, deformation in Z-direction

If one uses two barges, the bundle is deformed so it is a straight line in the XY-plane. This causes very large deformation in the vertical direction. Because of this the analyses with an extra external force were introduced. As one can see from Figure C.23 the vertical deformation is reduced. At the mid-span the deformation without any tugboat force is among the lowest, but much higher elsewhere.

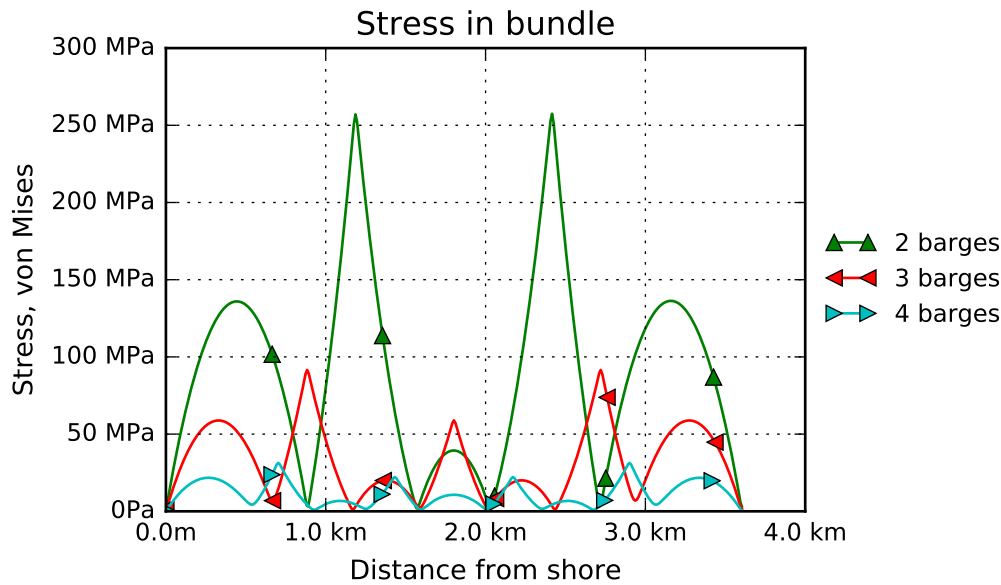


Figure 5.7

With only one barge and a tugboats, the configuration with the lowest tugboat force has the most unfavourable case for all criteria. It is little likely that only one barge will be considered as an option, and is not dealt with further.

For the calculation of the buoyancy the lowest force from Table 2.5 is used. If one calculates the buoyancy with the highest values from Table 2.5, 1025 kg/m^3 , the bundle floats up. Further up in the sea are the water current stronger and wave forces higher. To avoid this, one should attach some ballast to the bundle. It is also attached ballast on the bundles during the towing operation to the mounting site[5]. This also shows that the bundle is very close to a neutral buoyancy.

5.6 Water Current and Buoyancy

As one can see from Figure 4.13 and Figure 4.10, they have several similarities. But when one introduces the buoyancy, the ideal area spans over a much smaller span of forces. In addition is it a much bigger difference between the highest and lowest stress.

The very steep and deep area of the curve looks a little strange, therefore one took a close look into this. An analysis from the linear area (60 t) was compared to an analysis from around the lowest point (49 t). The

moment and force distribution along the bundle were compared with each other. The maximum and minimum levels are stated in Table 5.1. The table shows that the analysis with 49 tonnes has the highest M_Y , M_Z and F_Z . The analysis with 60 tonnes gives a more tensioned bundle, therefore is the bundle less exposed for the external forces. A stiffer bundle gives a better distribution of the forces too. Hence, the higher forces and moments has a sensible explanation.

Table 5.1: Maximum and minimum values for bundle

	49 tonnes		60 tonnes	
	Maximum	Minimum	Maximum	Minimum
F_X [N]	5.0×10^5	3.8×10^5	1.0×10^6	9.0×10^5
F_Y [N]	7.1×10^4	-7.1×10^4	2.6×10^5	-2.6×10^5
F_Z [N]	2.4×10^5	-2.4×10^5	1.4×10^5	-1.4×10^5
M_X [Nm]	3.9×10^6	-6.6×10^6	6.6×10^6	-2.2×10^7
M_Y [Nm]	2.8×10^7	-9.5×10^6	1.3×10^7	-3.0×10^6
M_Z [Nm]	1.0×10^6	-1.0×10^6	3.5×10^5	-3.5×10^5

The lowest possible tugboat force for these analyses are equal to the analyses without buoyancy, shown in Table 4.2. As already seen, the buoyancy doesn't represent a critical factor itself. If one uses three or four tugboats, the stresses are far from a critical level and the deformations are sufficient. Hence, for the bundle is it the water current that represents the most critical factor.

When it comes to the deformation in Z-direction, these are considerable less than with only buoyancy and barges. The tugboats make the bundle more tensioned, so the buoyancy has less influence. For a sufficient tugboat force the deformation is about 20 meters at its maximum.

The analyses are very idealized and are more like a pointer than the fact of the behaviour. It is probably little likely to have a situation likely to the analysis. However, based on these analyses would a tugboat force of 50-55 tonnes be sufficient.

5.7 Tugboat with Vertical Force Component

For the case used in section 4.7, is the minimum length of the stay 119 meters. If one exceeds the calculated towing force at 50 tonnes at this length, the bundle will rise. The water current and wave forces are stronger closer to

the sea level, therefore it is disadvantageous that the bundle rise. To avoid this one should choose a longer stay, which makes it possible to increase the towing force without raising the bundle. The barge will then take care of the varying vertical force. If one sets the vertical component equal half of the vertical force from the barge, the needed stay is 232 meters and the total towing force from a tugboat is 50.4 tonnes.

5.8 A few final remarks

To reduce the number of possible solutions, it was decided to place the tugboats and barges evenly distributed along the bundle. However, this is not the ideal configuration. Since the boundary conditions for the bundles at the abutments are free to rotate, they wouldn't take up any moments. The other support points has a moment, which decreases the deformation. Therefore, a shorter span between the abutments and the first tugboat/barge and longer spans elsewhere is a better configuration. From the analyses one also found that the barges in the middle took a lower force than the barges at the outer side, which is related to the freely supported ends.

Through most of the thesis a pipe spacing where $S = 0$ is used. This is equal to the configuration Grevstad used in his Master's thesis, when he calculated the drag coefficients for the bundle. For the final bundle zero pipe spacing is not realistic. The pipes are attached to clamps, so it is necessary with some spacing between the pipes. The spacing is not decided yet, therefore the spacing consistent is set to zero, so one always uses the same parameters for the analyses.

To reduce the stresses and deformations for the bundle, the analyses shows that it is better to increase the number of tugboats and barges, instead of changing the towing force from the tugboats. If one uses several bearing points, the span between each vessel is reduced.

The problem text says that the analyses are to be run as quasi-static analyses. The first analyses were set up as quasi-static analyses. These analyses needed very long time to find an equilibrium. If one should use these analyses to run parameter studies, this would take a very long time. Hence, the analyses are run as static and not quasi-static analyses.

Figure 5.8 shows a comparison of the stress with only water current and with water current and buoyancy. For the latter case is there also used barges. The tugboat force is set to 55 tonnes and no vertical component. As one can see from Figure 4.13 the tugboat force isn't selected from the area with very low stresses. This is done on purpose, because it is probably hard to hit this area in the real life. In Figure 5.8 on can see that the stresses are lower

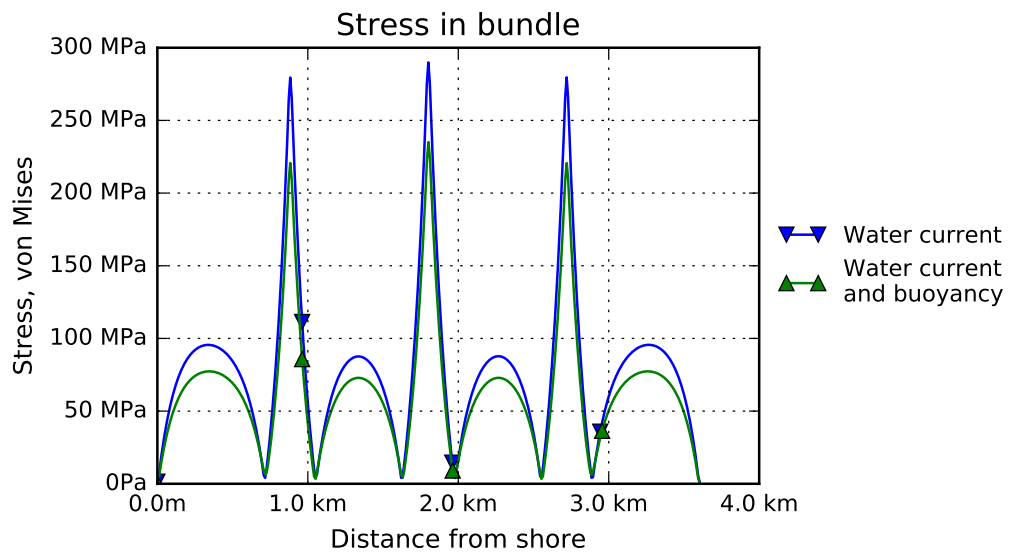


Figure 5.8: Tugboat with 55 tonnes towing force. With and without buoyancy and barges

when the buoyancy is introduced. Figure C.26 shows the deformation in the Y-direction. The deformation is larger when the buoyancy is introduced, but the differences are small. Both the stress and the deformation have equal shapes in both cases.

Chapter 6

Conclusion

Based on the analyses by ASAT, which doesn't give any deviation between the new and old version, one can say that the changes are performed without affecting the original functionality. One can still run ASAT equal to the old version. In addition are the opportunity to include water current and/or an elastic wire included. Both of these possibilities are tested and gives reasonable results.

Due to the changes of the ASAT code, was it necessary to find new numerical optimum values for ASAT. This optimum are to be used when there are applied external forces to the artificial seabed. The new numerical optimum is found in Table 4.1.

It was some uncertainties regarding the stiffness expression for the wire. Separate analyses are performed to find an expression for the stiffness. Based on the results and consultancy with the Abaqus documentation, one found out that the stiffness property is EA (Young's modulus and cross section area).

Parameter study of the bundle with water current and/or buoyancy shows that the water current represents the critical factor. These analyses were run as static and not quasi static analyses, as stated in the problem text, due to the time consumption. Based on deformations and stresses in the bundle, three barges and three tugboats with a bollard pull of 50-55 tonnes would give a sufficient situation. With this configuration one avoids too large deviation from the initial shape, both in the horizontal and vertical direction, in addition is the stresses kept low.

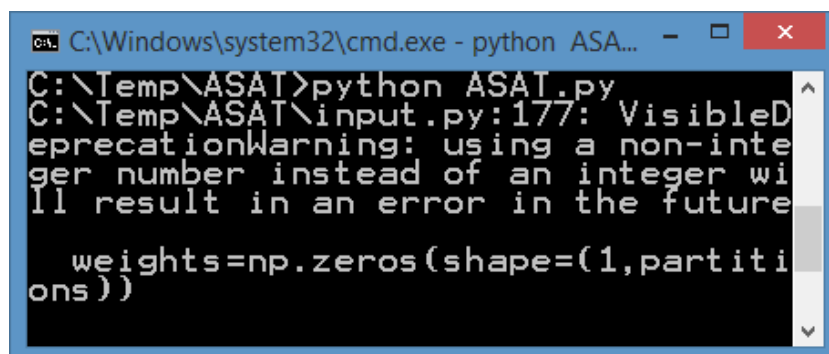
The tugboats also introduces a vertical force component. To avoid lifting the bundle, this force should be kept lower than the bearing force for the barge. For the analysis with both buoyancy and water current and a towing force of 50 tonnes, one needs a stay at minimum 119 meters to avoid lifting the bundle.

If one wants to reduce the stresses and the deformation, the best decision is to increase the number of tugboats and barges. The best alternative to this configuration presented in the previous paragraph is to use four barges and four tugboats with a towing force of 40 tonnes. This gives lower stresses and deformations, but the cost increases.

6.1 Recommended further work

There are still a lot of interesting aspects of the artificial seabed and the shoelacing principle to examine. There are both new topics and continuation of the work performed in this thesis. Below follows some suggestions to further objectives for these regarding similar topics:

- Analysis with forces from the bridge acting on the artificial seabed
- If necessary, update ASAT to keep up with changes in Abaqus and Python
- Include buoyancy in ASAT
- Find the required wire stiffness
- Ideal distributions of barges/tugboats along the bundles
- Water current both in and out of the fjord at the same time
- Use ASAT to find a procedure to mount the transverse stays

A screenshot of a Windows command prompt window. The title bar reads "C:\Windows\system32\cmd.exe - python ASA...". The command prompt shows the execution of "python ASAT.py" in the directory "C:\Temp\ASAT". A warning message is displayed: "C:\Temp\ASAT\input.py:177: VisibleDeprecationWarning: using a non-integer number instead of an integer will result in an error in the future". Below the warning, a line of Python code is visible: "weights=np.zeros(shape=(1, partitions))".

```
C:\Temp\ASAT>python ASAT.py
C:\Temp\ASAT\input.py:177: VisibleDeprecationWarning: using a non-integer
number instead of an integer will result in an error in the future

    weights=np.zeros(shape=(1, partitions))
```

Figure 6.1: Future error in ASAT

When one runs ASAT today with version 1.11.0 of NumPy, one gets a warning about a future error. The error message is shown in Figure 6.1. The

NumPy function `zeros(shape = (a, b))`, which is found several places in the file `input.py` requires integers in the future. The variable used today is also an integer, but Python doesn't understand this when importing this file. So debug the code and get rid of this warning message could be a good exercise to start with. If Abaqus are updated, a check of outdated Abaqus commands in the file `machinery.py` could be useful as well.

References

- [1] Statens vegvesen. *Ferjefri E39* [Internet], [cited 5th Apr. 2016]. Available from: <http://www.vegvesen.no/vegprosjekter/ferjefriE39>.
- [2] Statens vegvesen. *Statusrapport Ferjefri E39*. Technical report, Vegdirektoratet, May 2015.
- [3] Reinertsen. *Kunstig Sjøbunn - Kvalifiseringsstudie for nytt forankringskonsept. Laster og lastbeskrivelse*. Technical Report 2401051-02-RE-020202, rev. 02, 2014.
- [4] Reinertsen. *Kunstig Sjøbunn - Kvalifiseringsstudie for nytt forankringskonsept. Dimensjonering og materialbruk*. Technical Report 2401051-02-RE-020203, rev. 01, 2014.
- [5] DeepOcean. *Installasjon av flytebro, Kunstig Sjøbunn*. Technical Report NO.E10701, rev. 0, 2014.
- [6] Bjørn Harald Snersrud. *Analysis of a Pre-Tensioning Concept for a Floating Bridge Support Structure*. Master's thesis, Norwegian University of Science and Technology, Department of Engineering Design and Materials, Trondheim, spring 2015.
- [7] SINTEF. *Mulighetsstudie for kryssing av Sognefjorden Oppedal-Lavik. Estimert på bølger og strøm*. Technical report, SINTEF, 2011.
- [8] Statens vegvesen and Vegdirektoratet. *Håndbok 185 Bruprosjektering Eurokodeutgave*. Håndbok, Vegdirektoratet, Oslo, 2011.
- [9] Simon Grevstad. *Vortex Induced Vibrations on an "Artificial Seabed" for Support of a Floating Bridge*. Master's thesis, Norwegian University of Science and Technology, Department of Marine Technology, Trondheim, spring 2015.
- [10] Simulia. *Abaqus 6.14 Scripting User's Guide*. Dassault Systems, Providence, 2014.

- [11] Simulia. *Abaqus 6.14 Abaqus/CAE User's Guide*. Dassault Systems, Providence, 2014.
- [12] Simulia. *Abaqus 6.14 Analysis User's Guide*. Dassault Systems, Providence, 2014.
- [13] Simulia. *Abaqus 6.14 Keywords Reference Guide*. Dassault Systems, Providence, 2014.
- [14] Åge Ø. Waløen. *Dimensjonering med elementmetoden*. Kompendie. NTH, 1995.

Appendix A

Python Script for Tugboats

In this chapter you will find the Python code use for the analyses for the tugboat forces. A model of one of the bundles for the artificial seabed was already made. Briefly this code changes the value of the tugboat force, runs the analysis and captures images of the von Mises stress and the deformation.

The script is built up mainly by using the Macro Manager in Abaqus, as described in subsection 2.5.1. With this script 36 analyses were run in less than 15 minutes. The script was used several times, with only small modifications. Taking the time savings into account the time spent on making it were well used.

Listing A.1: Script used for analysis of tugboat forces

```
1 from abaqus import *
2 from abaqusConstants import *
3 import __main__
4
5 import material
6 import assembly
7 import load
8 import mesh
9 import job
10 import visualization
11
12 import time
13
14 loads = [42, 45, 50, 55, 60, 65, 70, 75, 80, 85, 90,
          95, 100, 110, 120, 130, 140, 150, 160, 170, 180,
          190, 200, 220, 240, 260, 280, 300, 325, 350, 375,
          400, 450, 500]
```

```

15
16 #Creates a file to log the time spent on the analyses
17 file=open('timeData.txt','w')
18 start=time.time()
19
20 #For loop for the decired loads
21 for load in loads:
22     #Starting the time for this particular analysis
23     startAnalysis=time.time()
24     #
25     a = mdb.models['Model-1'].rootAssembly
26     session.viewports['Viewport: 1'].setValues(
27         displayedObject=a)
28     session.viewports['Viewport: 1'].assemblyDisplay.
29         setValues(loads=ON, bcs=ON, predefinedFields=ON,
30         connectors=ON, optimizationTasks=OFF,
31         geometricRestrictions=OFF, stopConditions=OFF)
32     session.viewports['Viewport: 1'].assemblyDisplay.
33         setValues(step='Step-1')
34     #Sets the load for the analysis
35     mdb.models['Model-1'].loads['Load-3'].setValues(cf2
36         =load*10**4, distributionType=UNIFORM, field='
37         ')
38     #
39     session.viewports['Viewport: 1'].assemblyDisplay.
40         setValues(mesh=ON, loads=OFF, bcs=OFF,
41         predefinedFields=OFF, connectors=OFF)
42     session.viewports['Viewport: 1'].assemblyDisplay.
43         meshOptions.setValues(meshTechnique=ON)
44     session.viewports['Viewport: 1'].assemblyDisplay.
45         setValues(mesh=OFF, optimizationTasks=ON,
46         geometricRestrictions=ON, stopConditions=ON)
47     session.viewports['Viewport: 1'].assemblyDisplay.
48         meshOptions.setValues(meshTechnique=OFF)
49     session.viewports['Viewport: 1'].assemblyDisplay.
50         setValues(optimizationTasks=OFF,
51         geometricRestrictions=OFF, stopConditions=OFF)
52     #Submits the analysis
53     mdb.jobs['Job-1'].submit(consistencyChecking=OFF)
54     mdb.jobs['Job-1'].waitForCompletion()
55     #Opens the completed analysis

```

```

41 session.mdbData.summary()
42 o3 = session.openOdb(name='C:/Master/AbaqusModels/
    tauing/3boat/Job-1.odb')
43 #Sets a scale for the beam, the view and the legend
44 session.viewports['Viewport: 1'].setValues(
    displayedObject=o3)
45 session.viewports['Viewport: 1'].odbDisplay.
    basicOptions.setValues(renderBeamProfiles=ON,
    beamScaleFactor=10)
46 session.viewports['Viewport: 1'].view.setValues(
    session.views['Front'])
47 session.viewports['Viewport: 1'].odbDisplay.display
    .setValues(plotState=(CONTOURS_ON_DEF, ))
48 session.viewports[session.currentViewportName].
    odbDisplay.setFrame(step='Step-1', frame
    =10000000)
49 session.viewports['Viewport: 1'].
    viewportAnnotationOptions.setValues(legendFont='
    *-verdana-medium-r-normal-*-120-*-p-*-*)')
50 session.viewports['Viewport: 1'].
    viewportAnnotationOptions.setValues(titleFont='
    *-verdana-medium-r-normal-*-100-*-p-*-*)')
51 session.viewports['Viewport: 1'].
    viewportAnnotationOptions.setValues(stateFont='
    *-verdana-medium-r-normal-*-100-*-p-*-*)')
52 #Saves the plot of the von Mises stress, both eps
    and png format
53 session.printToFile(fileName='plot/Mises_'+str(load
    )+'t_425', format=PNG, canvasObjects=(session.
    viewports['Viewport: 1'], ))
54 session.printToFile(fileName='plot/Mises_'+str(load
    )+'t_425', format=EPS, canvasObjects=(session.
    viewports['Viewport: 1'], ))
55 #Sets the view to displacement
56 session.viewports['Viewport: 1'].odbDisplay.
    setPrimaryVariable(variableLabel='U',
    outputPosition=NODAL, refinement=(COMPONENT, 'U2
    '), )
57 #Saving a picture of the plot
58 session.printToFile(fileName='plot/U2_'+str(load)+'
    t_425', format=PNG, canvasObjects=(session.

```

```

    viewports [ 'Viewport: 1' ], ))
59 session.printToFile(fileName='plot/U2_'+str(load)+'
    t_425', format=EPS, canvasObjects=(session.
    viewports [ 'Viewport: 1' ], ))
60 #The plot shows both deformed and undeformed shape
61 session.viewports [ 'Viewport: 1' ].odbDisplay.display
    .setValues(plotState=(CONTOURS_ON_UNDEF,
    CONTOURS_ON_DEF, ))
62 #Saves an image of the plot
63 session.printToFile(fileName='plot/U2_'+str(load)+'
    t_425_undef', format=PNG, canvasObjects=(session
    .viewports [ 'Viewport: 1' ], ))
64 session.printToFile(fileName='plot/U2_'+str(load)+'
    t_425_undef', format=EPS, canvasObjects=(session
    .viewports [ 'Viewport: 1' ], ))
65 print('Analysis with '+str(load)+'t load has
    finished')
66 #Time spent on each analysis
67 endAnalysis=time.time()
68 analysisTime=endAnalysis-startAnalysis
69 file.write('Time consumed for analysis with '+str(
    load)+'t load was '+str(analysisTime)+'s\r\n')
70 #Time spent on all analyses and closing the file
71 end=time.time()
72 totalTime=end-start
73 file.write('Total time for '+str(len(loads))+ ' analyses
    : '+str(totalTime)+'s\r\n')
74 file.close()

```

Appendix B

Analyses with Elastic Wire

This appendix contains two different analyses. In both analyses are there one iteration with rigid wire and one with elastic wire. The stiffness property, EA , for the elastic wire is 1.0×10^8 for both analyses. In the first analysis is this the only varied parameter, while the winching magnitude too is varied in the latter one.

B.1 Elastic/Rigid Wire

The parameters for this analysis is found in Table E.4. The varied parameter between the analyses is the wire stiffness. The first analysis is run with a rigid wire, while the latter is run with an elastic wire with a stiffness of 1.0×10^8 N. As one can see from the plots attached to this appendix the stresses, forces and displacements are much lower than with a rigid wire.

At present phase of the artificial seabed project the properties for the fibre rope is not decided yet. The wire stiffness used in this analysis is chosen to give a proper stiffness. To find a suitable wire stiffness one should use ASAT to run several analysis.

The stiffness used in this analysis is probably to low, due to too large deviations from the rigid wire. In addition to the stiffness one also has to take physical properties as Young's modulus and diameter into account to find a suitable configuration.

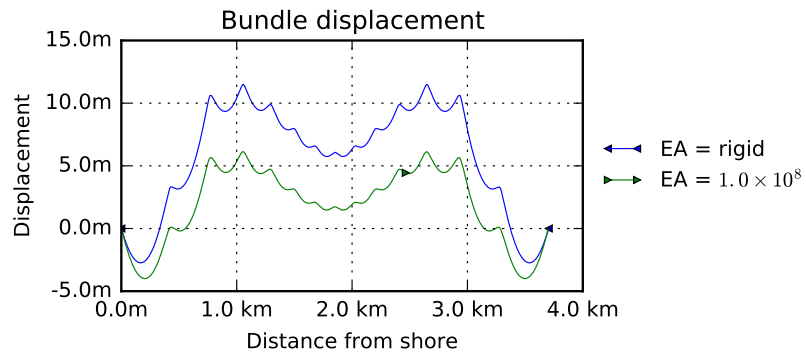


Figure B.1

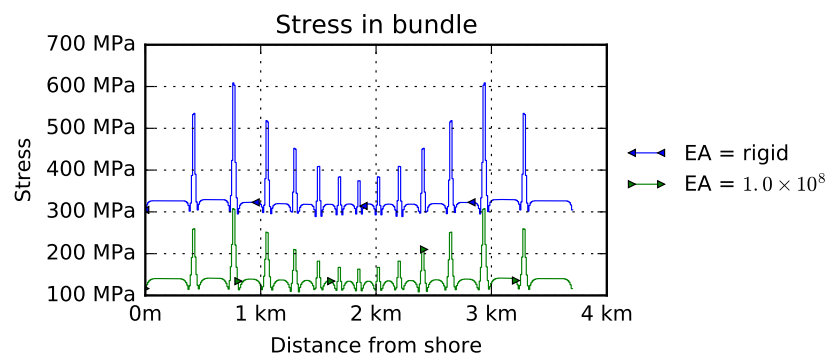


Figure B.2

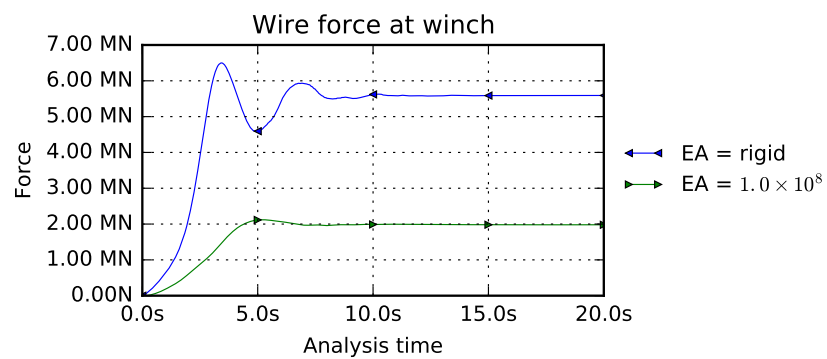


Figure B.3

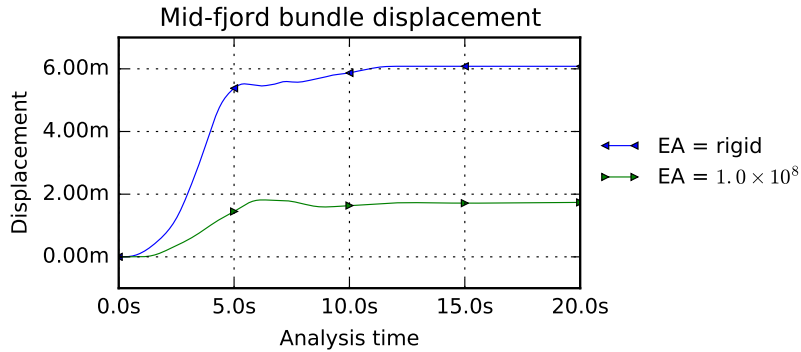


Figure B.4

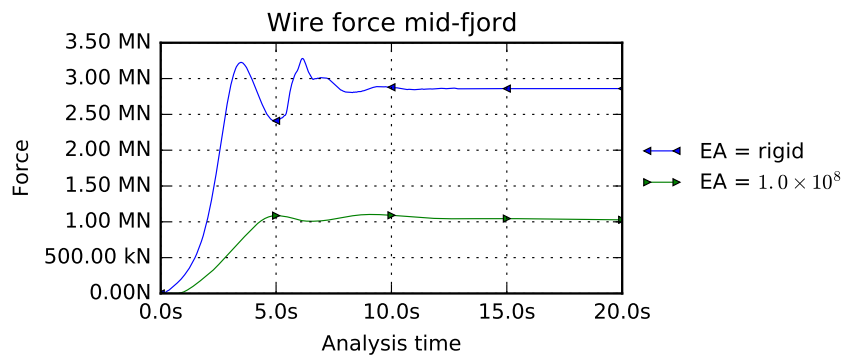


Figure B.5

B.2 Varied Winching Magnitude

In the previous section it is only varied between a rigid and an elastic wire. As one can see from the plots, the deformation and the stresses are lower for the elastic wire, due to the elongation of the wire. For the analyses in this section the winching magnitude is tuned, so the mid-fjord bundle displacement is equal for the two iterations, i.e. there are used different winching magnitudes for the two iterations. Hence, for these analyses there are two varied parameters. The input parameters for this analysis are shown in Table E.5

MARK: The plots consist of results from different analyses and is not possible to reproduce by one single run in ASAT, even though one sets

`doRaiseErrors = 'False'`.

As one can see from the plots, are the final states equal. It look like it is only on line in the plots, but this is because the lines lies upon each other. If one looks at the plots showing the history, one can see that they are a bit different. Due to the elongation of the elastic wire, it takes some longer time before the deformations occurs. But still the curves have a similar shape.

Hence, if one finds the corresponding winching magnitude for an elastic wire, compared to a rigid wire, one can achieve equal geometry for the pre-tensioned bundles.

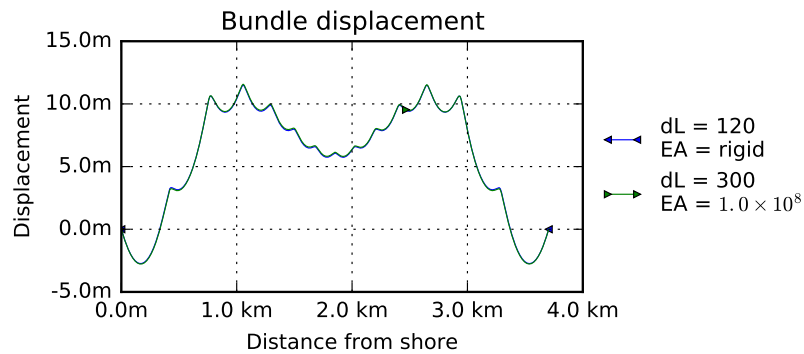


Figure B.6

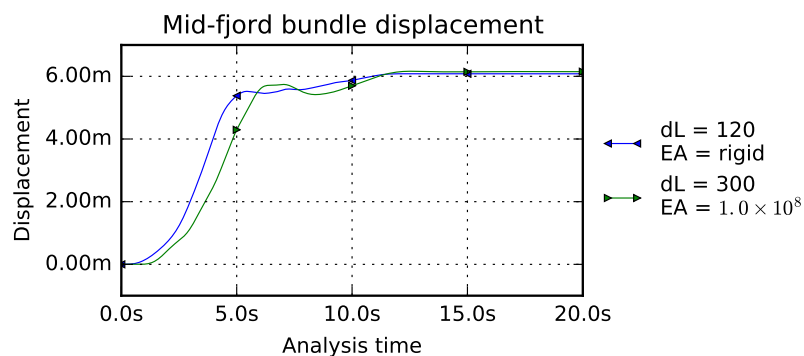


Figure B.7

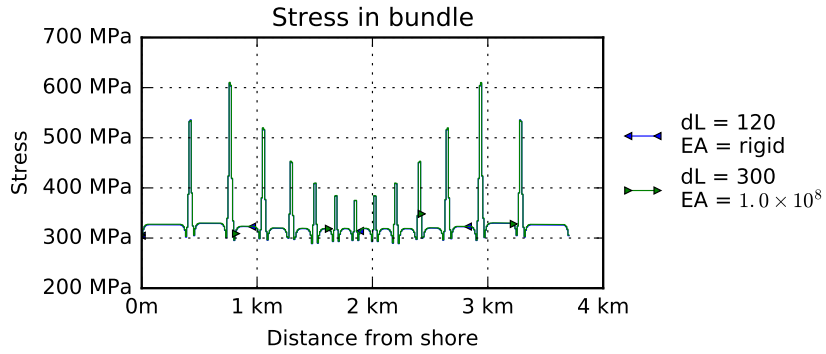


Figure B.8

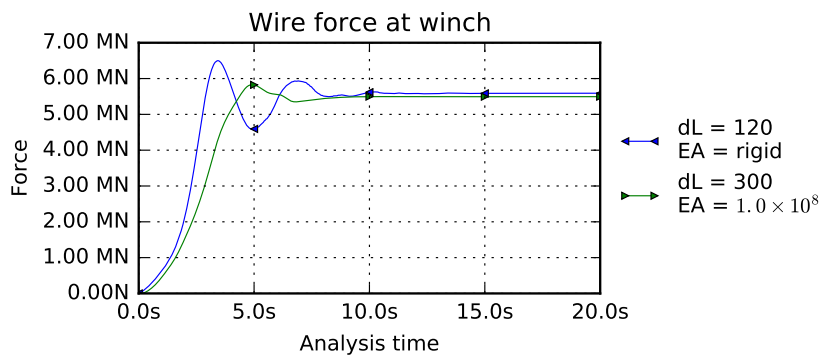


Figure B.9

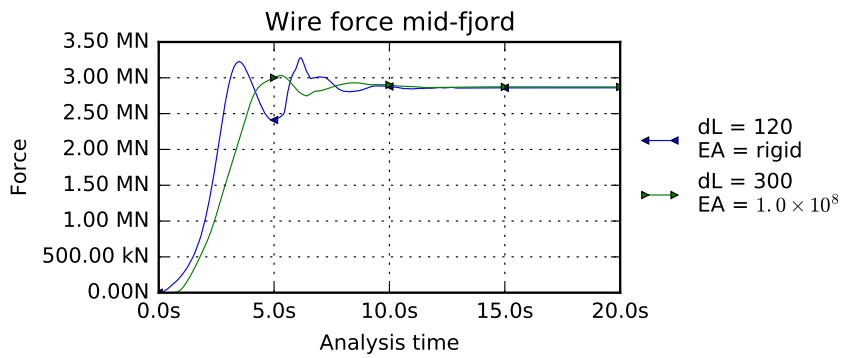


Figure B.10

Appendix C

Additional Plots and Figures

In this chapter more plots and figures are presented. Parts considered as unnecessary in the text, but still useful, are found in this chapter. Plots and figures from all of the different parts of the work are found here.

C.1 New Version of ASAT

C.1.1 Comparison – Old Version

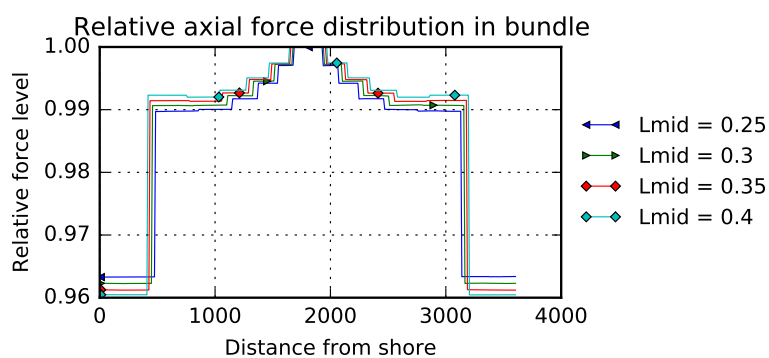


Figure C.1: From old ASAT version

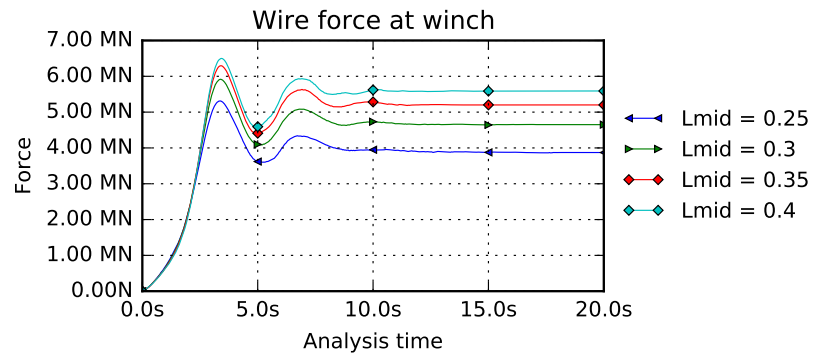


Figure C.2: From old ASAT version

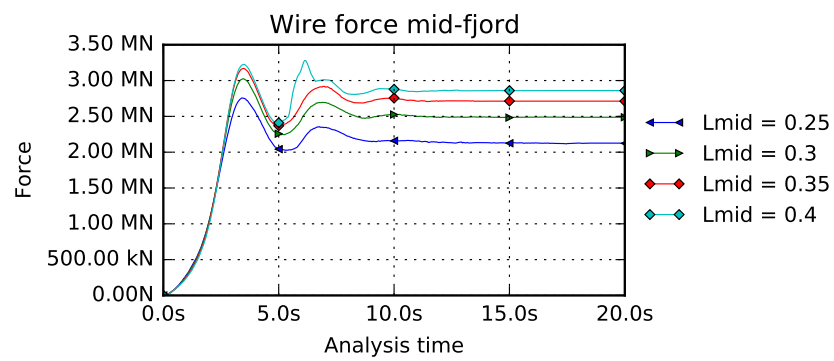


Figure C.3: From old ASAT version

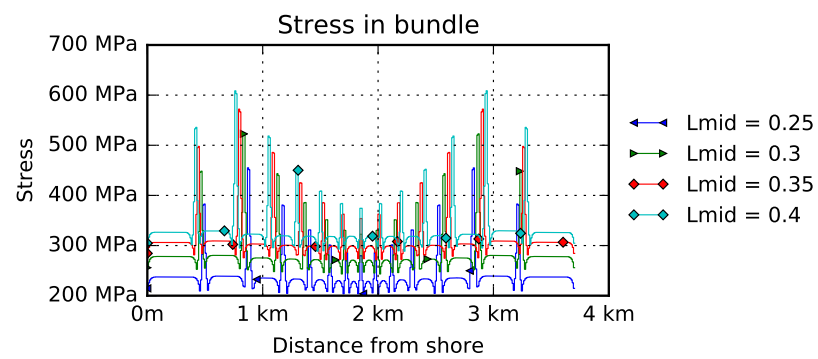


Figure C.4: From old ASAT version

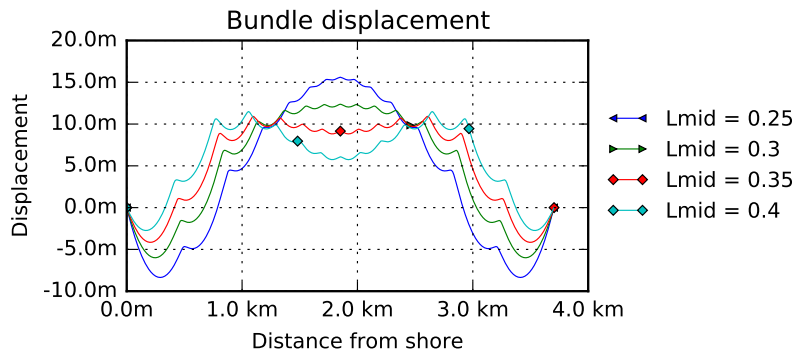


Figure C.5: From old ASAT version

C.1.2 Comparison – New Version

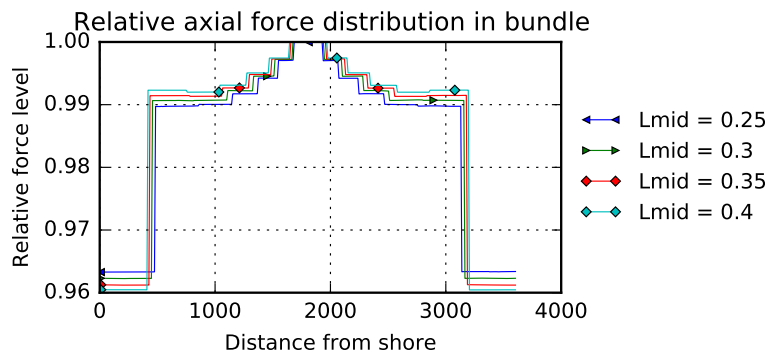


Figure C.6: From new ASAT version

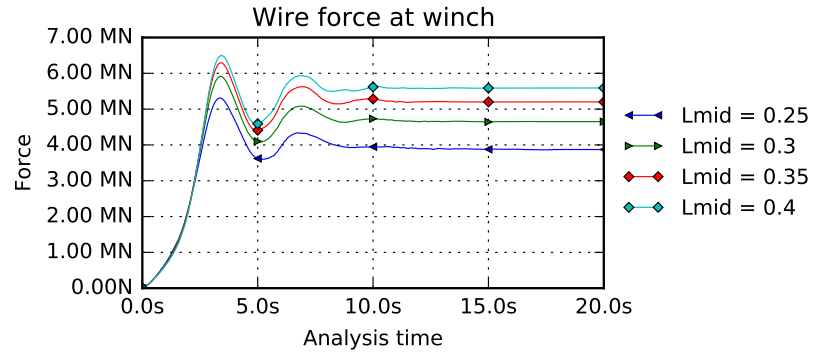


Figure C.7: From new ASAT version

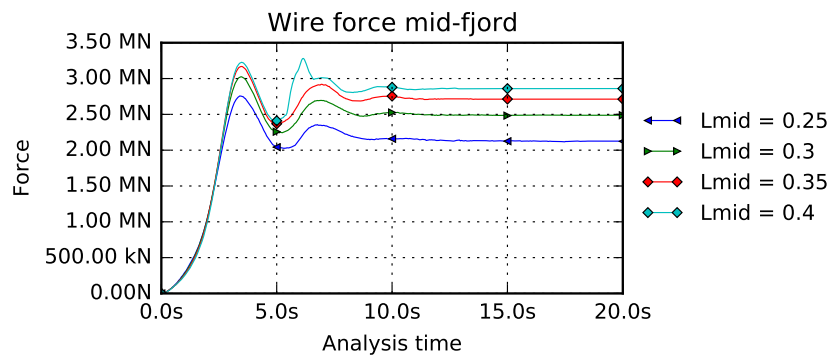


Figure C.8: From new ASAT version

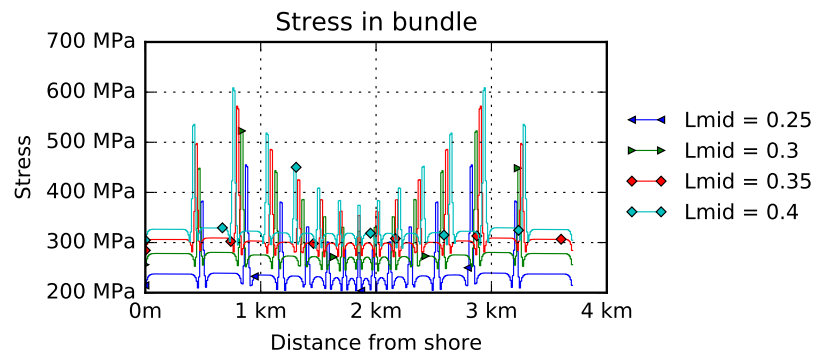


Figure C.9: From new ASAT version

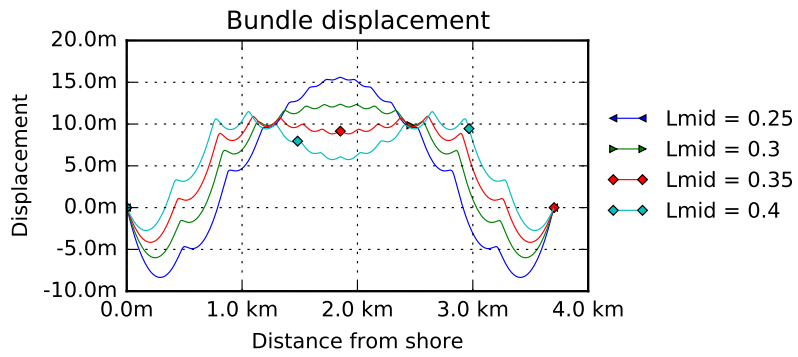


Figure C.10: From new ASAT version

C.1.3 Example of New Version of ASAT

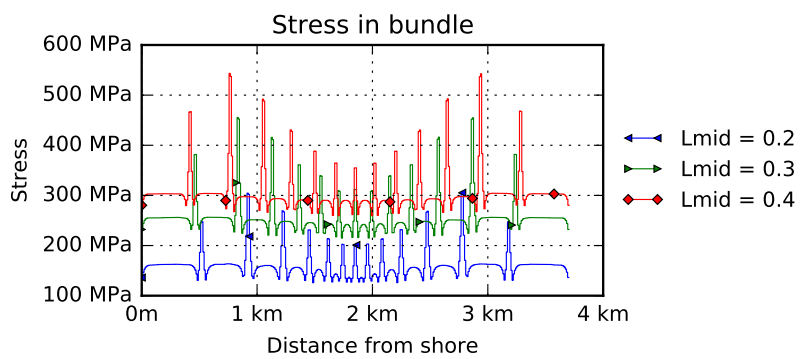


Figure C.11

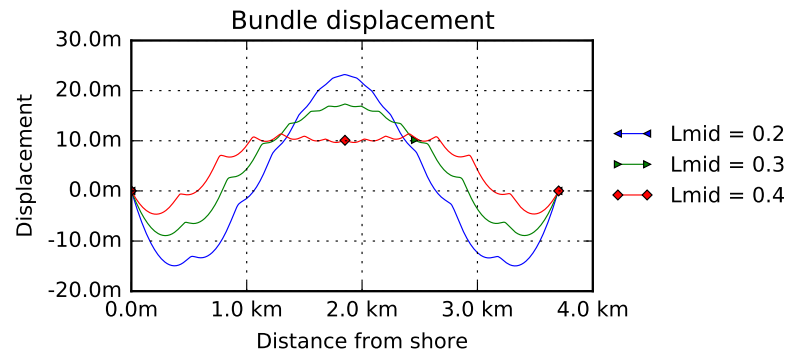


Figure C.12

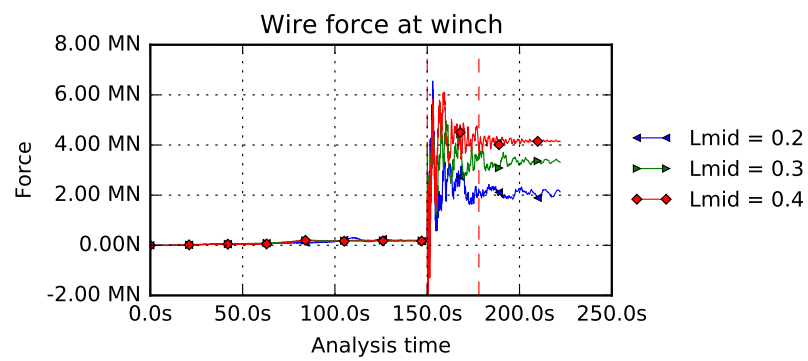


Figure C.13

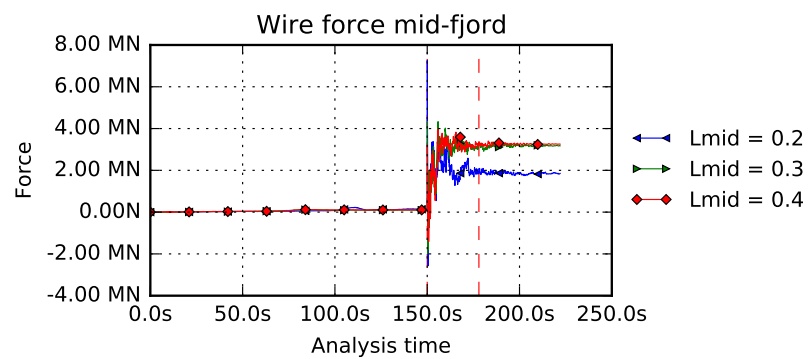


Figure C.14

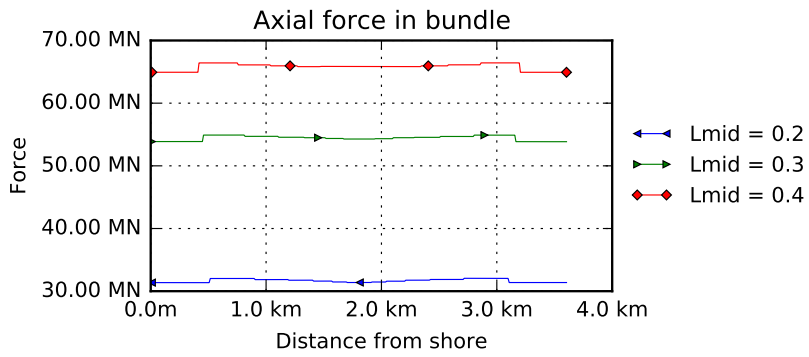


Figure C.15

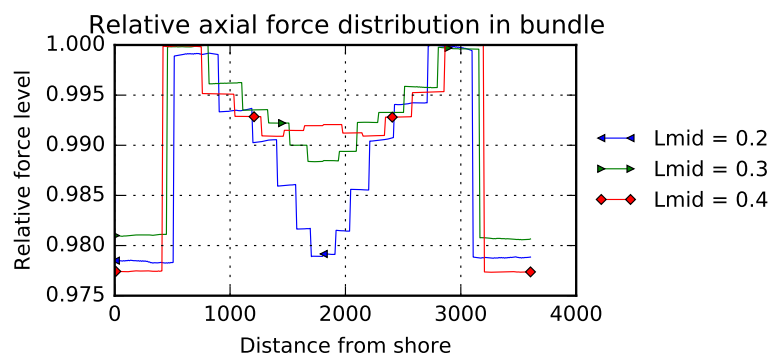


Figure C.16

C.2 Numerical Optimum

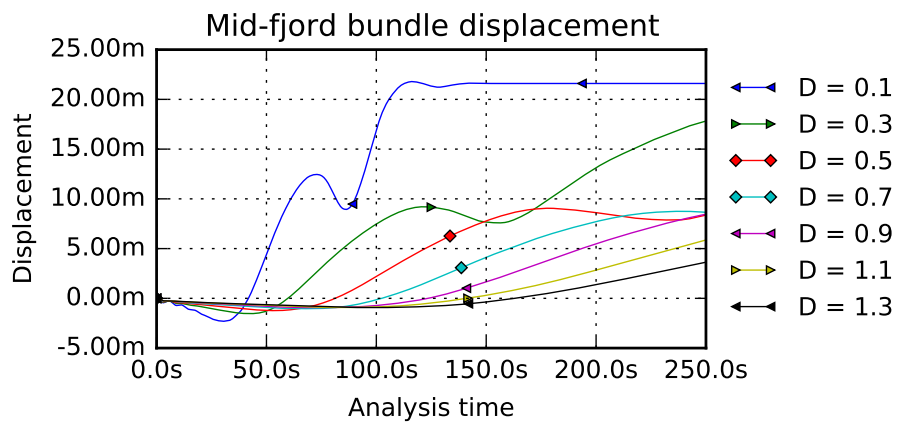


Figure C.17: Equilibrium for different mass damping coefficients

C.3 Water current

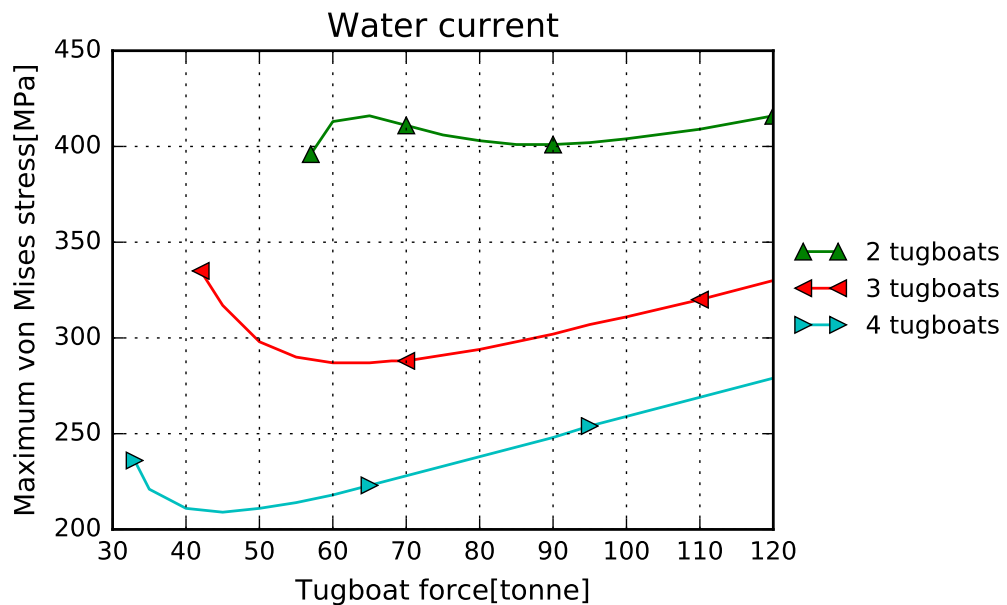


Figure C.18: The most interesting part of Figure 4.10 scaled up

C.4 Buoyancy

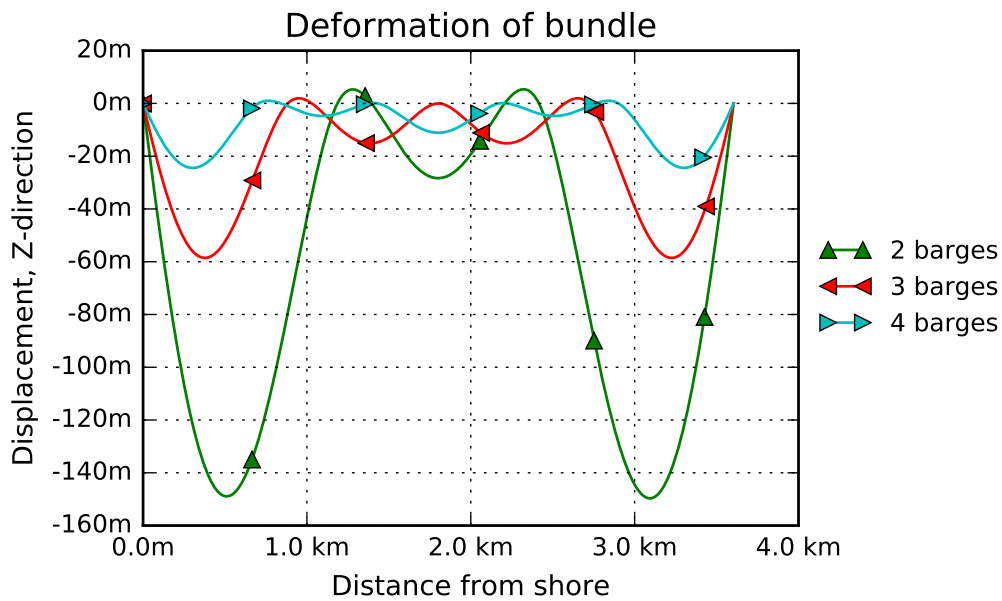


Figure C.19

C.4.1 One barge

Figure C.20 show the deformation for 1 barge with a external towing force. The force that gives zero displacement is 243 kN and is denoted as $1.0F$. Other forces are stated relative to this force.

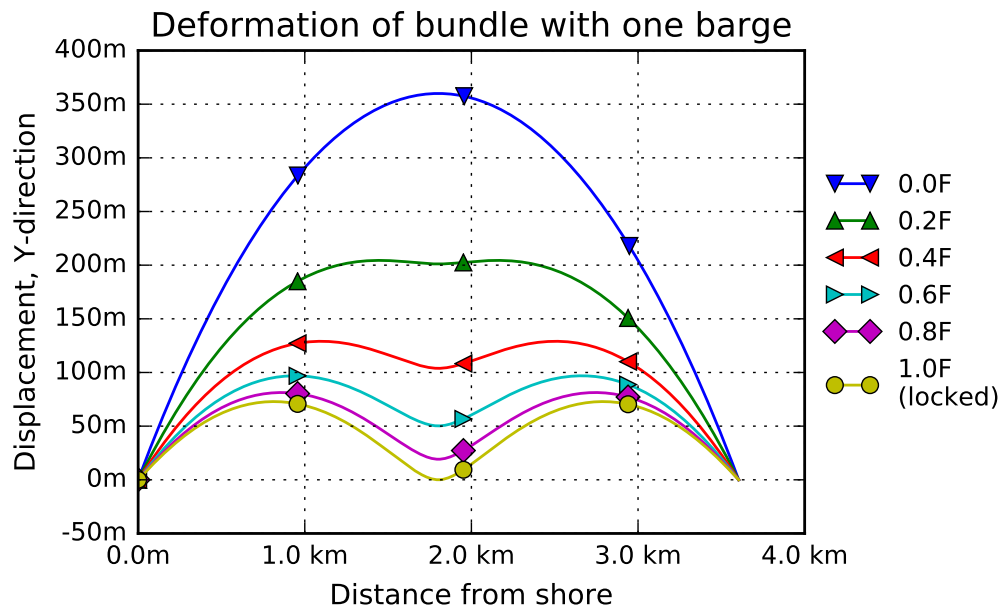


Figure C.20: 1 barge with varying towing force

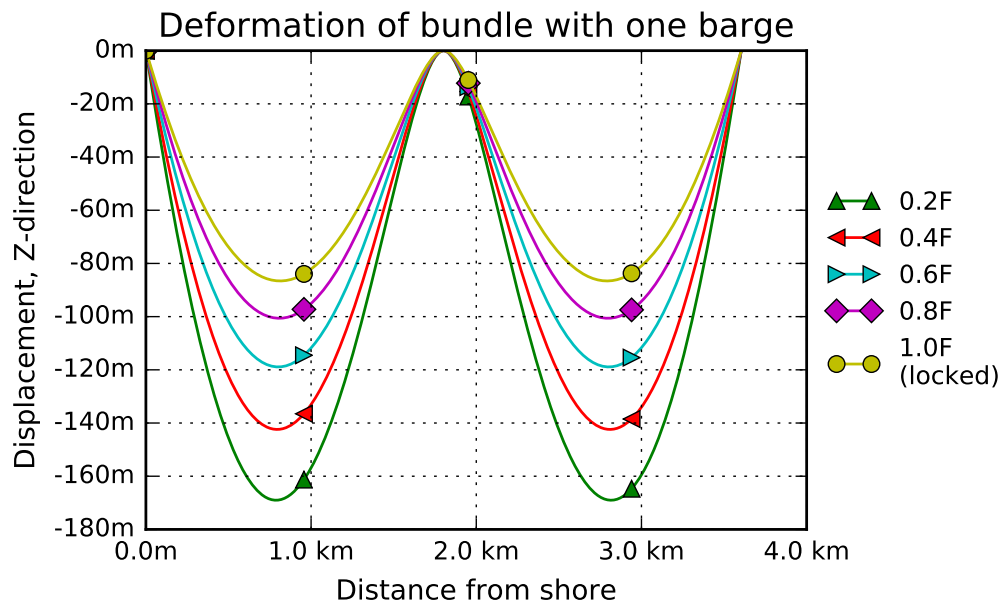


Figure C.21

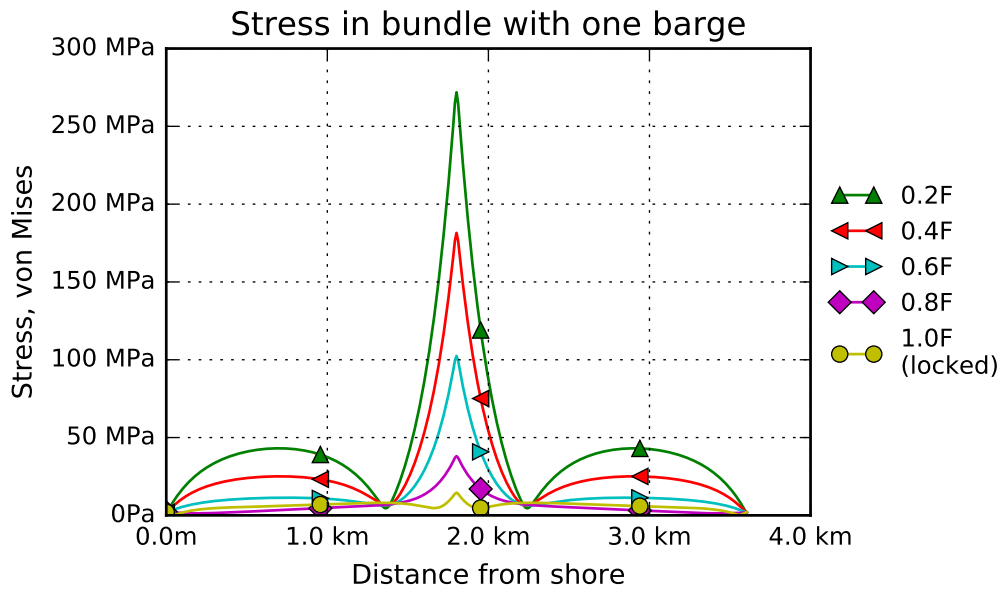


Figure C.22

C.4.2 Two barges

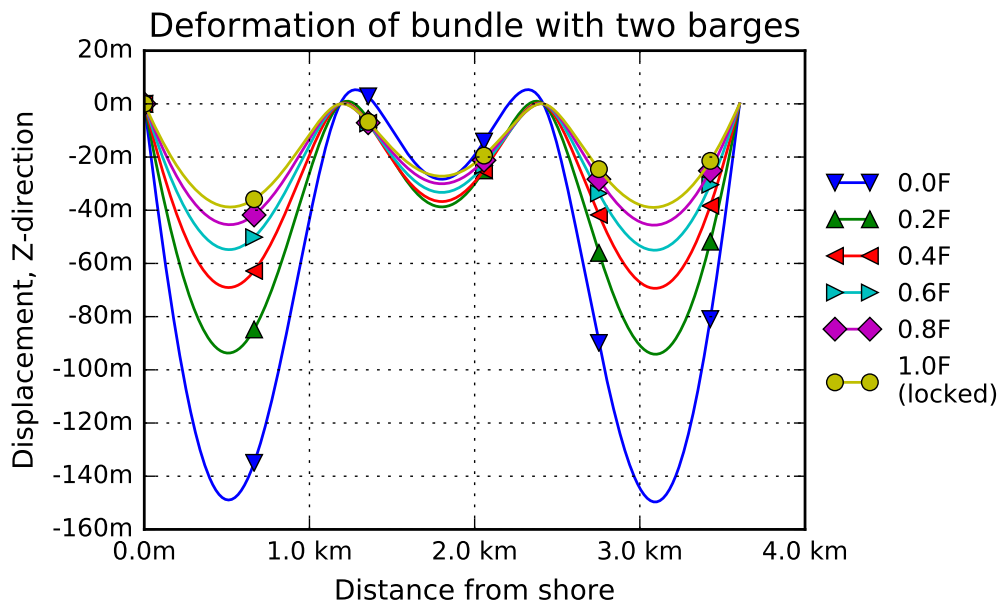


Figure C.23

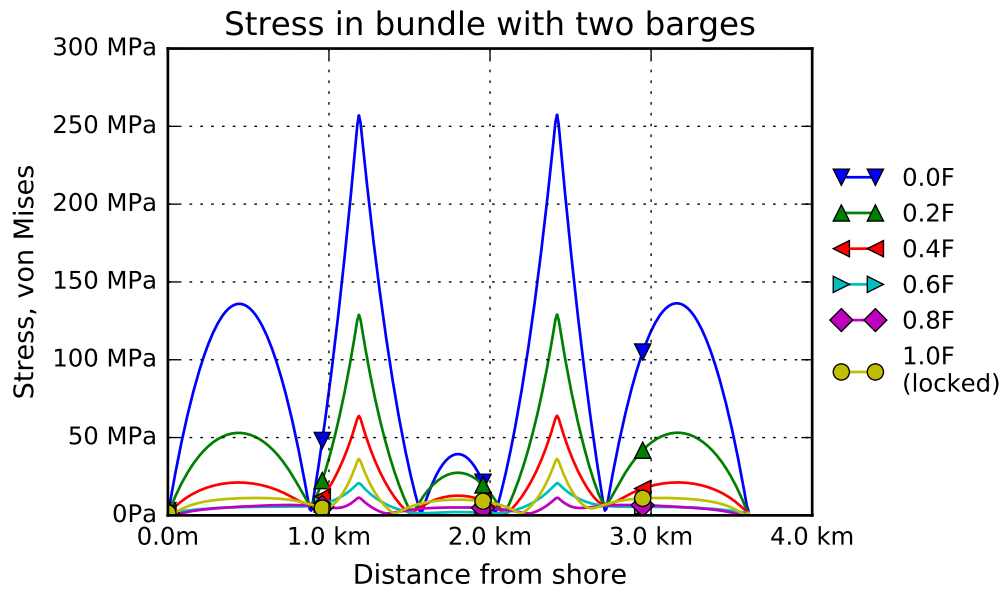


Figure C.24

C.5 Water Current and Buoyancy

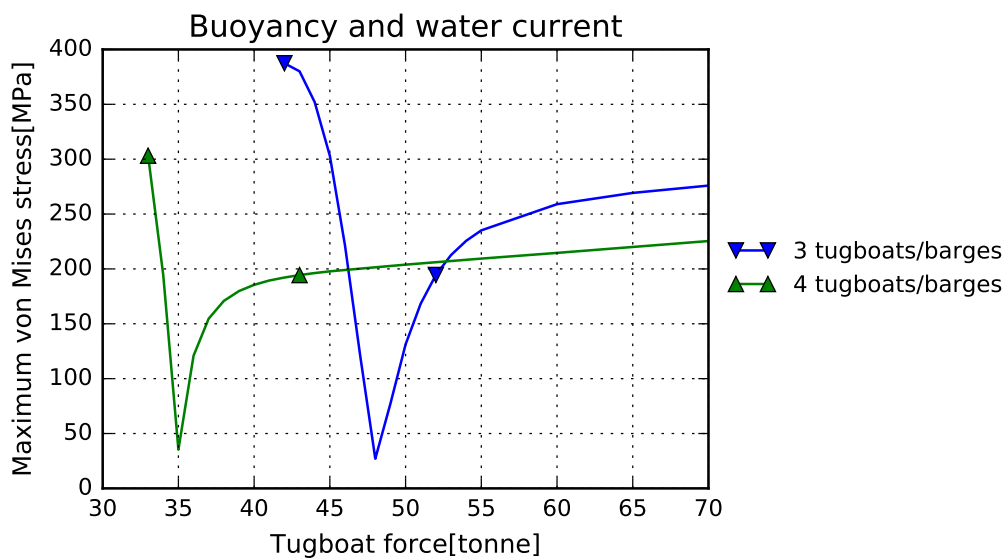


Figure C.25

C.6 Comparison with and without Buoyancy

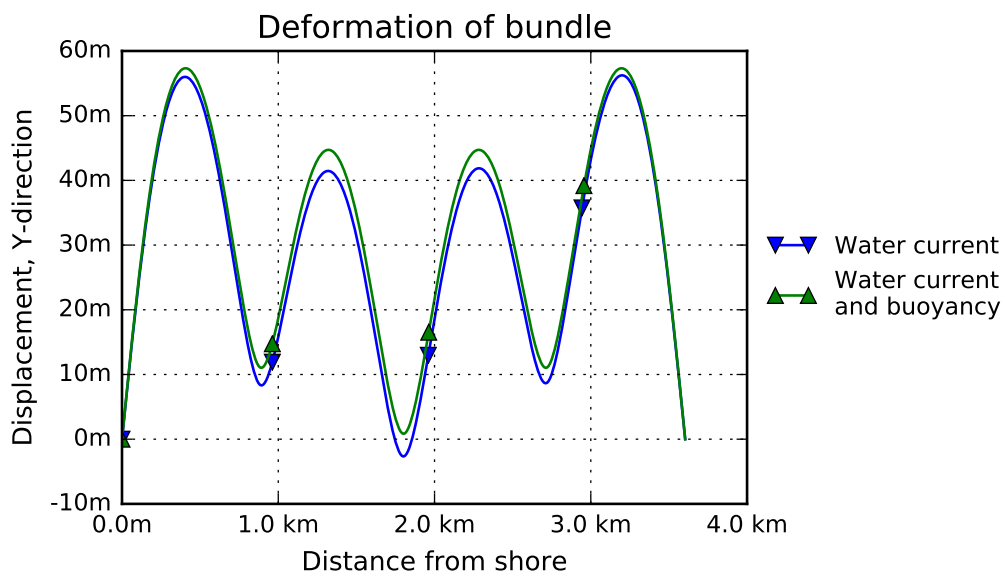


Figure C.26: Tugboat with 55 tonnes towing force. With and without buoyancy and barges

C.7 Plots from Analyses

In the following section images of deformation and stress from the parameter studies are presented. Totally there are run 215 unique analyses, but only a selections of them are shown here.

C.7.1 Water Current

One Tugboat

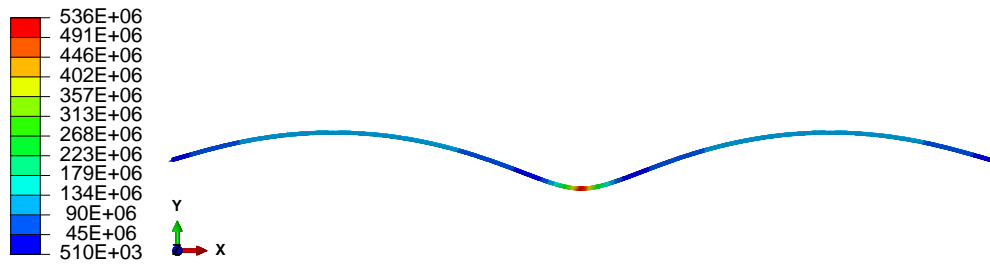


Figure C.27: von Mises stress. Tugboat with 96 tonnes towing force

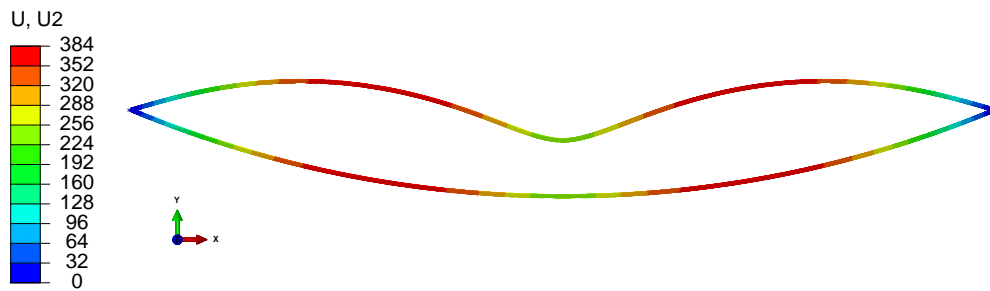


Figure C.28: Y-deformation. Tugboat with 96 tonnes towing force. Deformed and initial shape

Two Tugboats

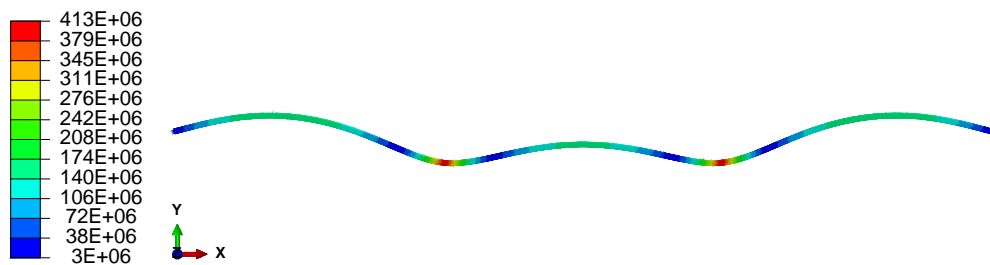


Figure C.29: von Mises stress. Tugboats with 60 tonnes towing force

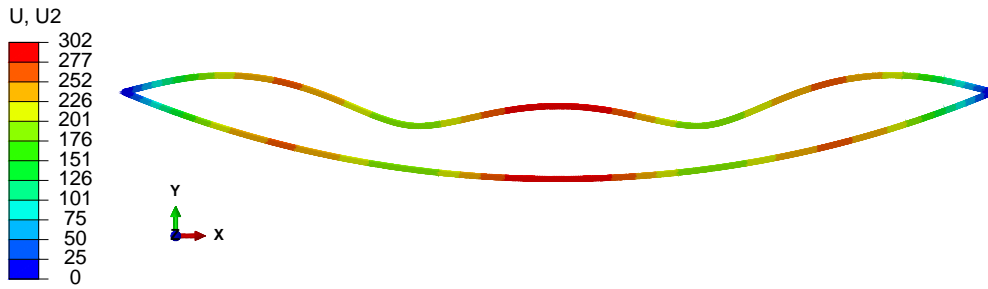


Figure C.30: Y-deformation. Tugboats with 60 tonnes towing force. Deformed and initial shape

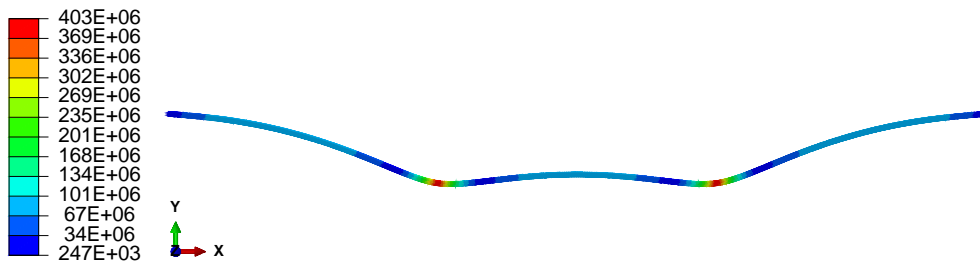


Figure C.31: von Mises stress. Tugboats with 80 tonnes towing force

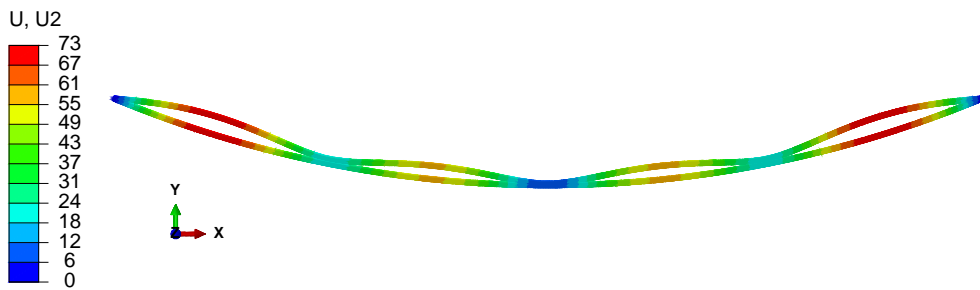


Figure C.32: Y-deformation. Tugboats with 50 tonnes towing force. Deformed and initial shape

Three Tugboats

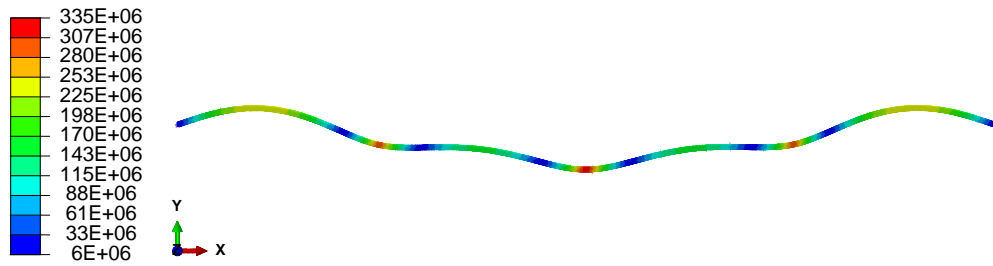


Figure C.33: von Mises stress. Tugboats with 42 tonnes towing force

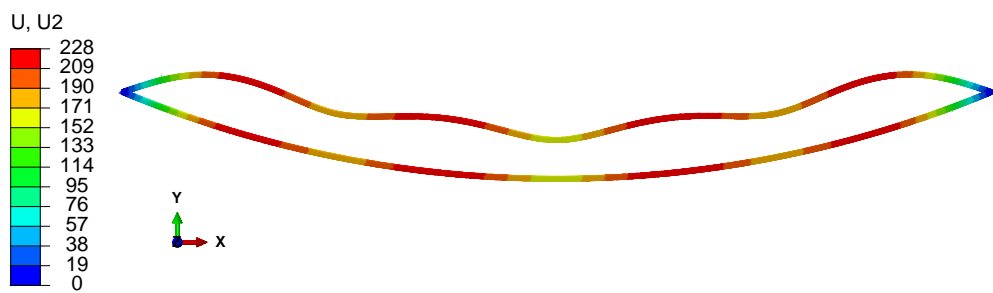


Figure C.34: Y-deformation. Tugboats with 42 tonnes towing force. Deformed and initial shape

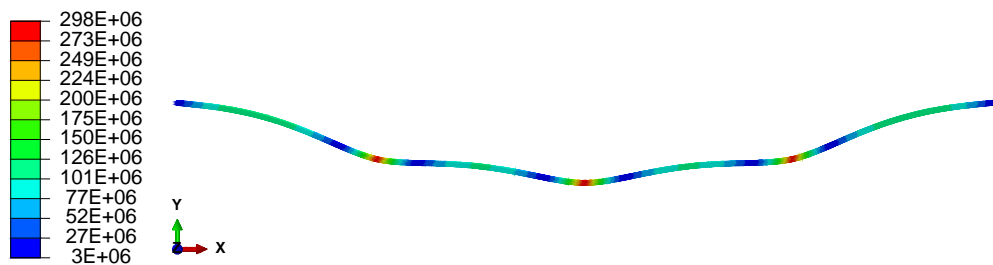


Figure C.35: von Mises stress. Tugboats with 50 tonnes towing force



Figure C.36: Y-deformation. Tugboats with 50 tonnes towing force. Deformed and initial shape

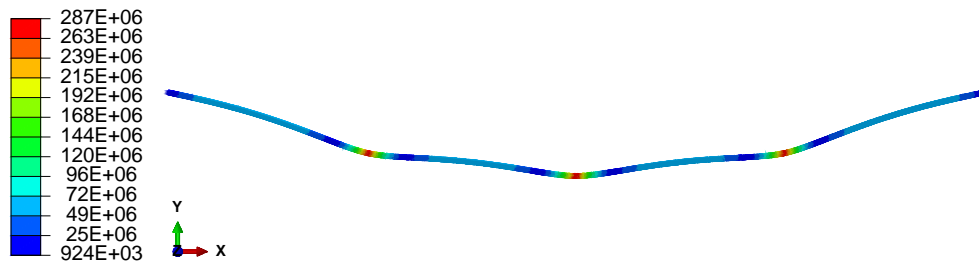


Figure C.37: von Mises stress. Tugboats with 65 tonnes towing force

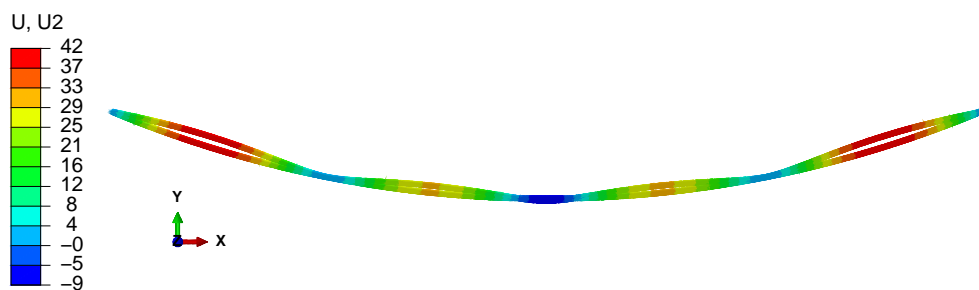


Figure C.38: Y-deformation. Tugboats with 65 tonnes towing force. Deformed and initial shape

Four Tugboats

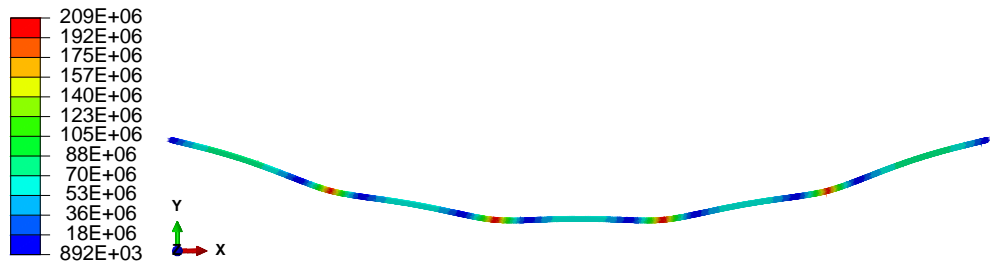


Figure C.39: von Mises stress. Tugboats with 45 tonnes towing force

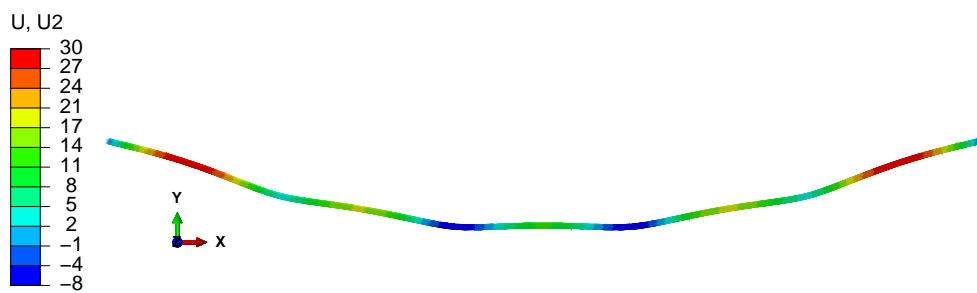


Figure C.40: Y-deformation. Tugboats with 45 tonnes towing force. Deformed shape

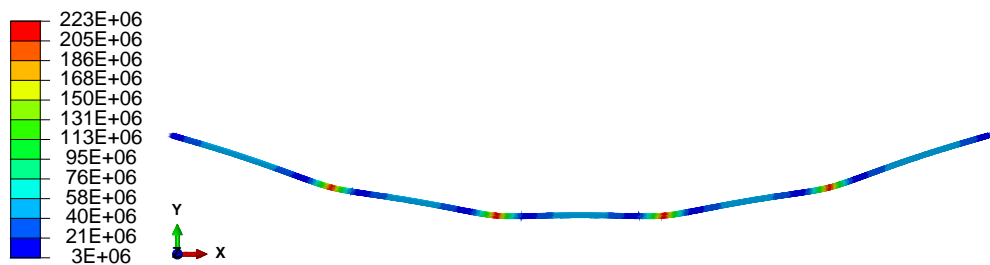


Figure C.41: von Mises stress. Tugboats with 65 tonnes towing force

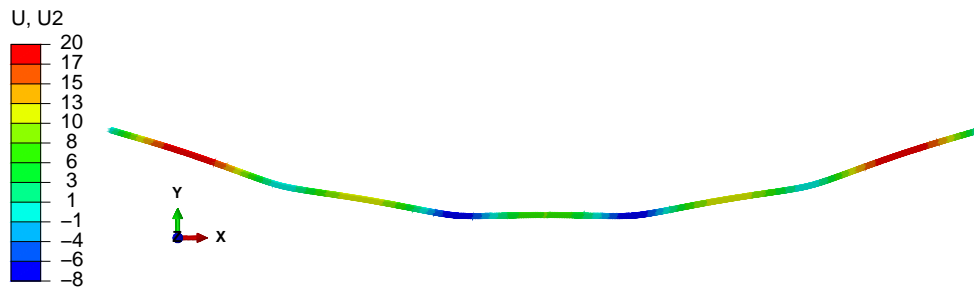


Figure C.42: Y-deformation. Tugboats with 65 tonnes towing force. Deformed shape

C.7.2 Water Current and Buoyancy

Three Tugboats

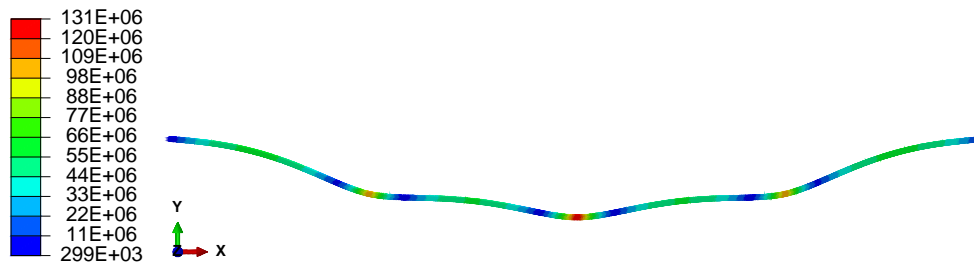


Figure C.43: von Mises stress. Tugboats with 50 tonnes towing force

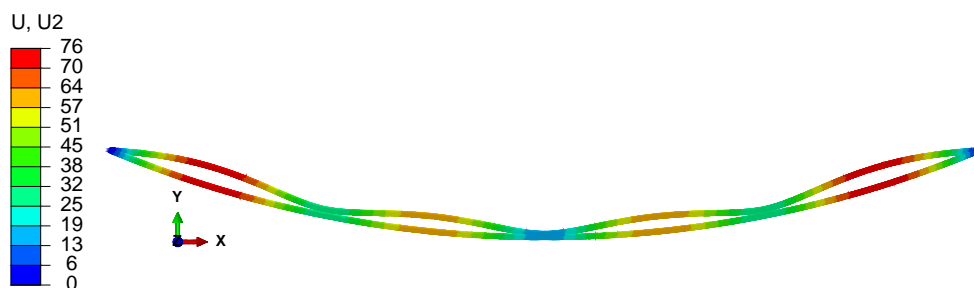


Figure C.44: Y-deformation. Tugboats with 50 tonnes towing force. Deformed and initial shape

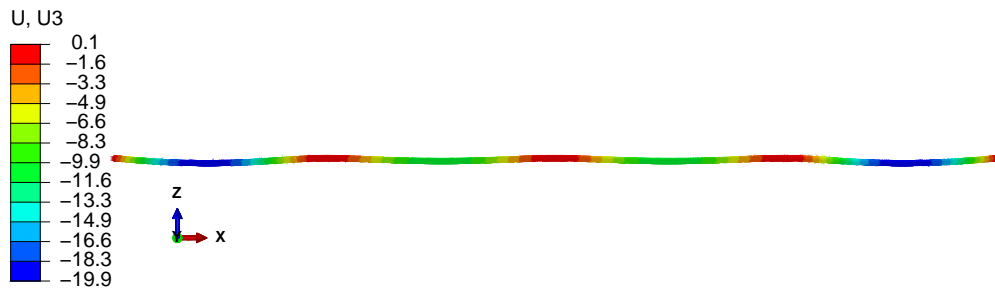


Figure C.45: Z-deformation. Tugboats with 50 tonnes towing force. Deformed shape



Figure C.46: von Mises stress. Tugboats with 60 tonnes towing force



Figure C.47: Y-deformation. Tugboats with 60 tonnes towing force. Deformed and initial shape

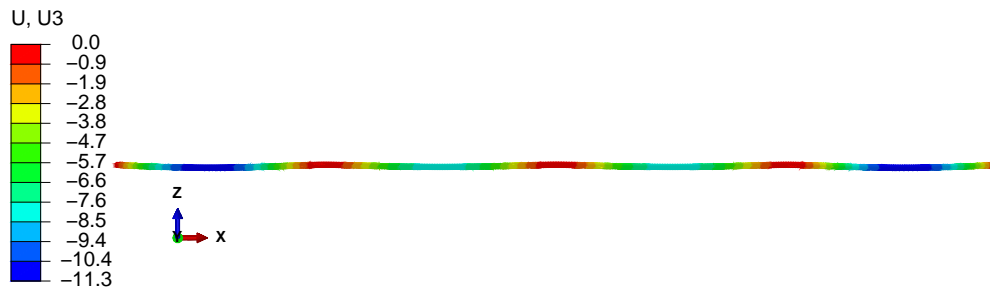


Figure C.48: Z-deformation. Tugboats with 60 tonnes towing force. Deformed shape

Four Tugboats

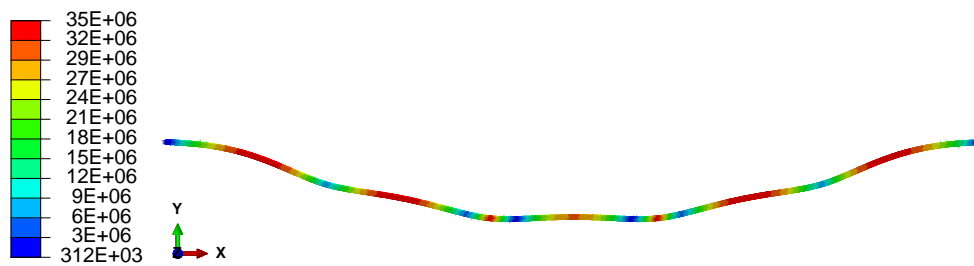


Figure C.49: von Mises stress. Tugboats with 35 tonnes towing force

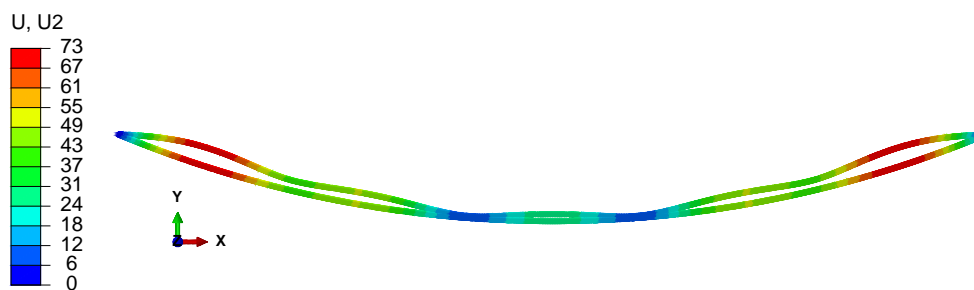


Figure C.50: Y-deformation. Tugboats with 35 tonnes towing force. Deformed and initial shape



Figure C.51: Z-deformation. Tugboats with 35 tonnes towing force. Deformed shape

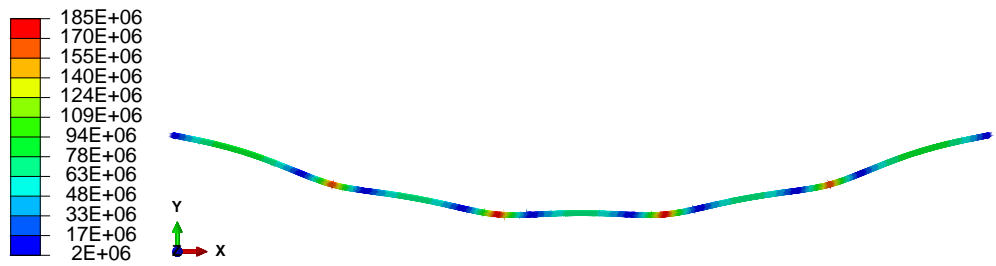


Figure C.52: von Mises stress. Tugboats with 40 tonnes towing force

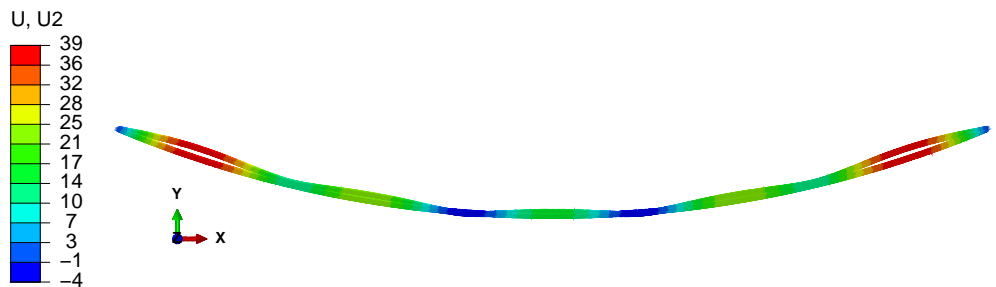


Figure C.53: Y-deformation. Tugboats with 40 tonnes towing force. Deformed and initial shape

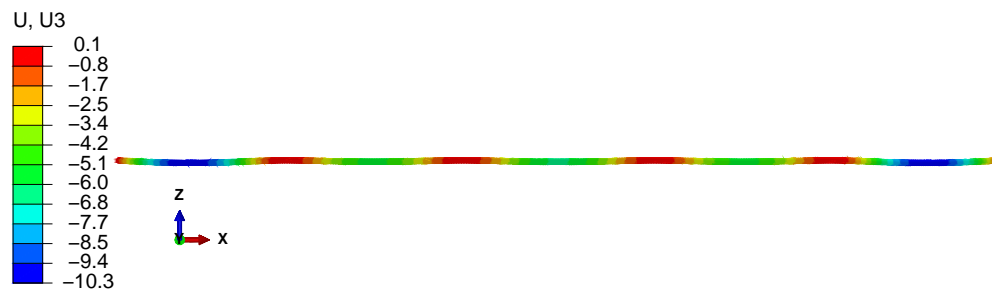


Figure C.54: Z-deformation. Tugboats with 40 tonnes towing force. Deformed shape

Appendix D

Wire Elasticity

On the following pages the calculations to find the possible stiffness for the slipping connector element in Abaqus is shown.

Table D.1: Results from simulations in Abaqus

Analysis	Wire		Rod	
	CTF[N]	Start length[m]	Mises[MPa]	Displacement[10 ⁻³ m]
#1	36 210	0.500	461.0	2.198
#2	19 380	1.000	246.7	1.176
#3	11 260	1.500	143.3	0.6827
#4	8 502	2.000	108.3	0.5155
#5	8 153	2.500	103.8	0.4944
#6	6 812	3.000	86.73	0.4131
#7	5 850	3.500	74.48	0.3547
#8	5 126	4.000	65.27	0.3109

Table D.2: Calculations for the wire based on results from Abaqus

Analysis	Initial length[m]	Displacement[m]	Final length[m]	Strain[10 ⁻³]	EA	Deviation	EA/L	Deviation
#1	0.480	0.0178020	0.4978020	37.09	976 340	0.976	2 034 041	2.034
#2	0.980	0.0188240	0.9988240	19.21	1 008 946	1.009	1 029 536	1.030
#3	1.480	0.0193173	1.4993173	13.05	862 688	0.863	582 897	0.583
#4	1.980	0.0194845	1.9994845	9.84	863 967	0.864	436 347	0.436
#5	2.480	0.0195056	2.4995056	7.87	1 036 597	1.037	417 983	0.418
#6	2.980	0.0195869	2.9995869	6.57	1 036 395	1.036	347 783	0.348
#7	3.480	0.0196891	3.4996453	5.65	1 036 278	1.036	297 781	0.298
#8	3.980	0.0196891	3.9996891	4.95	1 036 181	1.036	260 347	0.260

Table D.3: Calculated data for the pole

Analysis	Strain[10 ⁻³]	Stress[MPa]
#1	2.198	461.58
#2	1.176	246.96
#3	6.827	143.37
#4	5.155	108.26
#5	4.944	103.82
#6	4.131	86.75
#7	3.547	74.49
#8	3.109	65.29

Appendix E

Input parameters to ASAT

To find the numeric optimum for the new version in ASAT, the parameters shown in Table E.1 were used. The parameters not listed here were varied and are stated for each analysis. The final numeric optimum is found in Table 4.1, and represent most of the missing values in this table.

Table E.1: Input parameters for analyses for numeric optimum

Number of iterations	N.A.
Varied parameters: Tb , T , Ta , D , Fb , Fa	
Parameter	Value
t – Winching duration	5.95 sec
Lw – Winch offset from bundle	100 m
$cutMethod$ – Partitioning method	quadratic
$Lmid$ – Weighting of center-span	0.25
nP – Number of partitions	13
Mu – Friction coefficient	0.10
dL – Winching magnitude	120
Le – Element size	10 m
S – Pipe spacing in bundle	0.0 m
$wire$ – Wire type	rigid
Model for analyses	

Table E.2: Input parameters for comparison of new and old version of ASAT

Number of iterations	4
Varied parameter: L_{mid}	$\{0.25, \dots, 0.40\}$
Parameter	Value
Common parameters	
T – Analysis time	20 sec
t – Winching duration	5.95 sec
D – Damping	1.05
L_w – Winch offset from bundle	200 m
$cutMethod$ – Partitioning method	quadratic
L_{mid} – Weighting of center-span	varied
nP – Number of partitions	13
Mu – Friction coefficient	0.10
dL – Winching magnitude	120
Le – Element size	10 m
S – Pipe spacing in bundle	0.0 m
Parameters specific for new version	
Fb – Water current before winching	False
Fa – Water current after winching	False
$wire$ – Wire type	rigid
Model for first iteration	
Model for last iteration	

Table E.3: Input parameters for analysis with new version of ASAT

Number of iterations	3
Varied parameter: L_{mid}	$\{0.20, \dots, 0.40\}$
Parameter	Value
T_b – Analysis time step <i>before</i>	150 sec
T – Analysis time step <i>winching</i>	28 sec
T_a – Analysis time step <i>after</i>	44 sec
t – Winching duration	5.95 sec
D – Damping	0.10
L_w – Winch offset from bundle	200 m
$cutMethod$ – Partitioning method	quadratic
L_{mid} – Weighting of center-span	varied
nP – Number of partitions	13
Mu – Friction coefficient	0.10
dL – Winching magnitude	120
Le – Element size	10 m
S – Pipe spacing in bundle	0.0 m
Fb – Water current before winching	True
$wire$ – Wire type	rigid
Model for first iteration	
Model for last iteration	

Table E.4: Input parameters for analysis with elastic and rigid wire

Number of iterations	2
Varied parameter: <i>wire</i>	{rigid, elastic}
Parameter	Value
T – Analysis time	20 sec
t – Winching duration	5.95 sec
D – Damping	1.05
Lw – Winch offset from bundle	200 m
$cutMethod$ – Partitioning method	quadratic
$Lmid$ – Weighting of center-span	0.40
nP – Number of partitions	13
Mu – Friction coefficient	0.10
dL – Winching magnitude	120
Le – Element size	10 m
S – Pipe spacing in bundle	0.0 m
Fb – Water current before winching	False
Fa – Water current after winching	False
<i>wire</i> – Wire type	varied
EA – Wire stiffness	100 000 000 N

Model for analyses

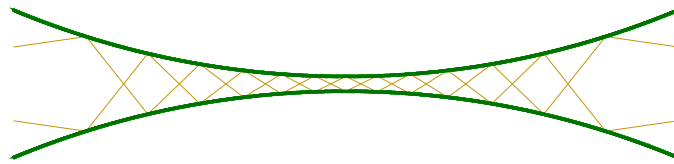


Table E.5: Input parameters for analysis with elastic and rigid wire and varied winching magnitude

Number of iterations	2
Varied parameters: <i>wire</i> <i>dL</i>	{rigid, elastic} {120, 300}
Parameter	Value
<i>T</i> – Analysis time	20 sec
<i>t</i> – Winching duration	5.95 sec
<i>D</i> – Damping	1.05
<i>Lw</i> – Winch offset from bundle	200 m
<i>cutMethod</i> – Partitioning method	quadratic
<i>Lmid</i> – Weighting of center-span	0.40
<i>nP</i> – Number of partitions	13
<i>Mu</i> – Friction coefficient	0.10
<i>dL</i> – Winching magnitude	varied
<i>Le</i> – Element size	10 m
<i>S</i> – Pipe spacing in bundle	0.0 m
<i>Fb</i> – Water current before winching	False
<i>Fa</i> – Water current after winching	False
<i>wire</i> – Wire type	varied
<i>EA</i> – Wire stiffness	100 000 000 N
Model for analyses	
